2013

Defining a Simplified Pharmacophore for Simocyclinone D8 Inhibition of DNA Gyrase

Lauren Gaskell
Virginia Commonwealth University

DEFINING A SIMPLIFIED PHARMACOPHORE FOR SIMOCYCLINONE D8 INHIBITION OF DNA GYRASE

A thesis submitted in partial fulfillment of the requirements for the degree of Master of Science at Virginia Commonwealth University

by

LAUREN M. GASKELL
Bachelor of Science, Clarkson University, Potsdam, New York, 2006

Director: KEITH C. ELLIS
Assistant Professor, Department of Medicinal Chemistry

Virginia Commonwealth University
Richmond, Virginia
January 24, 2013

Acknowledgement

First, I would like to thank VCU and the Department of Medicinal Chemistry. My time at VCU has shown me that with enough sweat, tears and determination, anything is possible.

Through my graduate school experience, my family (both by luck and by choice) and my friends have been incredibly supportive. Thank you.

I would like to thank my committee members, Dr. B. Frank Gupton and Dr. John Hackett. You have both been incredibly instrumental in helping me with my chemistry, my project, and in saving my and Dr. Ellis' sanity.

Other people who have been huge influences on my graduate experience and myself are the members of the Ellis group. Past members Cory Bottone, Dr. Justin Hynekamp, Dr. Sean Vail, Drew Johnson, and Sam Firebaugh, have helped me so much with my early skills and confidence in the lab, and I am so thankful to have had the opportunity to learn from you. Present and visiting members Jenson Verghese, Sudha Kowar, Dr. Thuy Nyguen, Robert Coover, and Matt Baker have spent so much time with me in the lab. We've all helped one another, taught each other, and been together in times of great stress and also in times of celebration. Thank you all for sharing your knowledge and testing mine, allowing me to vent, and for reminding me that my TLC is nearly done. I am so grateful I have been able to share my bench space, my office, and my life with such wonderful people.

I would also like to thank Dr. Aurijit Sarkar. Without his advice, his guidance, his support and friendship, this difficult path would have been even more torturous.

Most importantly, I would like to thank the two people who believed in me even when I didn't. My fiancé, Eric Ziemba, has not always agreed with my decisions regarding graduate school, but has been there for me every step of the way, from celebrating my acceptance to VCU all the way through to the insanity of trying to schedule my defense. I would never have been able to do this without you.

Dr. Keith Ellis has gone above and beyond what is expected of a thesis advisor and mentor. The support, encouragement, and the wealth of knowledge you've given me are things I will always be incredibly grateful for. Without your guidance, patience and your friendship, I never would have made it past the first year, let alone finish.

Table of Contents

Acknowledgement ii

List of Figures v

List of Tables viii

Abstract ix

List of Abbreviations xi

CHAPTER 1: INTRODUCTION 1

1.1: Introduction to the topoisomerase family of enzymes 1

1.2 Types of Topoisomerases 2

1.3 Mechanism of Type II Topoisomerases 5

1.4 Type II Topoisomerases as Antibacterial Targets 7

CHAPTER 2: INTRODUCTION TO SIMOCYCLINONE D8 20

CHAPTER 3: A DECONSTRUCTION-RECONSTRUCTION APPROACH TO DEFINING THE MINIMUM PHARMACOPHORE FOR SIMOCYCLINONE D8 INHIBITION OF DNA-DNA GYRASE BINDING 29

3.1 Synthesis of the coumarin-based deconstruction analogs of SD8 30

3.1.1 Synthesis of the 3-aminocoumarin derivatives 30

3.1.2: Synthesis of the 3-amino-4-hydroxycoumarin derivatives 33

3.1.3 Synthesis of the 3-amino-7-hydroxycoumarin analogs 36

3.1.4 Synthesis of 4,7-Dihydroxycoumarin 40

3.2 Evaluation of the activity of the compounds against DNA gyrase 41

3.2.1 SPR Experiments 42

3.2.2 DNA Gyrase Functional Assay Experiments 47

CHAPTER 4: ATTEMPTS AT SYNTHESIZING 3-AMINO-8-CHLORO-4,7-DIHYDROXYCOUMARIN 48

4.1 Direct Chlorination 48

4.2 Coumarin Formation from Resorcinol 50

4.3: Coumarin Formation from 2,4-Dihydroxybenzaldehyde 51

4.4 Discussion 54

4.5 Future Direction 55

4.6 Summary 55

Experimental Procedures 56

List of References 77

APPENDIX 87

List of Figures

Figure 1. Crystal structure of yeast type II topoisomerase (PDB: 1BGW). 3

Figure 2. The mechanism of type II topoisomerases, from Berger, *et al. Nature,* **1996**, *379*, 225.[9] 5

Figure 3. Structures of examples the four generations of quinolone antibiotics. 9

Figure 4. Crystal structure of topoisomerase IV ParC dimer–DNA complex with bound ciprofloxacin (PDB: 3FOE and 3FOF). 10

Figure 5. Structures of selected examples of the aminocoumarin class of type II topoisomerase inhibitors. 12

Figure 6. Crystal structure of novobiocin bound to the ATP binding domain of ParE (PDB: 1S14). 14

Figure 7. Comparison of the structures of the aminocoumarin Novobiocin, and the endogenous ligand of GyrB, adenosine triphosphate (ATP). 15

Figure 8. Structures of GSK299423 and NXL101, examples of the NBTI class of type II topoisomerase inhibitors. 16

Figure 9. Crystal structure of GSK299423 bound to the GyrA dimer-DNA complex (PDB: 2XCS). 18

Figure 10. Structures of simocyclinone D8 and simocyclinone D4. 20

Figure 11. Crystal structure of both modes of SD8 binding to the GyrA dimer (PDB: 2WL2). 25

Figure 12. Binding of SD8 to DNA gyrase, as proposed by Maxwell, *et al*. Picture from Edwards, *et al*. *Science* **2009,** *326*, 1415. 26

Figure 13. Structures of MDG8N2A and simocyclinone C4. 27

Figure 14. Synthesis of 3-2 31

Figure 15. Synthesis of 3-3 31

Figure 16. Synthesis of 3-4 32

Figure 17. Synthesis of 3-5 32

Figure 18. Synthesis of 3-6 32

Figure 19. Synthesis of 3-7 33

Figure 20. Synthetic scheme of compounds 3-8, 3-9, 3-10, 3-11, and 3-12. 35

Figure 21. Synthesis of 3-13. 36

Figure 22. Synthetic scheme of 3-14, 3-15, 3-16, 3-17, and 3-18. 37

Figure 23. Deprotection of 3-18 to give 3-19. 38

Figure 24. Synthetic scheme of 3-20 and 3-21. 38

Figure 25. Synthetic scheme of 3-22 and 3-23. 39

Figure 26. Synthetic scheme of 3-26. 41

Figure 27. Simocyclinone D8 coumarin pharmacophore as determined by SPR 45

Figure 28. Synthetic scheme of the direct chlorination route. 48

Figure 29. Synthetic products of the Chloramine T reaction. a) 3-amino-8-chloro-4-hydroxy-7-methoxycoumarin, the expected product. b) 3-amino-6,8-dichloro-4-hydroxy-7-methoxycoumarin, the observed over-chlorination product. c) 3-amino-6-chloro-4-hydroxy-7-methoxycoumarin, a by-product. 49

Figure 30. Synthetic scheme for the resorcinol starting material. 50

Figure 31. Observed product from von Peckman reaction. 50

Figure 32. Synthetic route to produce the 8-chloro-4,7-dihydroxycoumarin 3-4 starting with 2,4-dihydroxybenzaldehyde 3-11. 51

Figure 33. Synthetic scheme to make the 8-chloro-4,7-dihydroxycoumarin starting with 2,4-dihydroxyacetophenone. 53

Figure 34. Final product seen from the lactone ring-closing step..... 53

List of Tables

Table 1. Compound inhibition of DNA-DNA gyrase binding interaction by SPR 43

Abstract

DEFINING A SIMPLIFIED PHARMACOPHORE FOR SIMOCYCLINONE D8 INHIBITION OF DNA GYRASE

by

LAUREN M. GASKELL

A thesis submitted in partial fulfillment of the requirements for the degree of Master of Science at Virginia Commonwealth University

Virginia Commonwealth University, 2013

Director: KEITH C. ELLIS
Assistant Professor, Department of Medicinal Chemistry

The type II topoisomerase subfamily of enzymes has been clinically targeted by the widely used, broad-spectrum quinolone class of antibacterials. Due to emerging drug-resistant strains of bacteria, the quinolones' effectiveness is threatened. The natural product simocyclinone D8 (SD8) has shown the ability to inhibit the type II topoisomerase, DNA gyrase, even when mutated to be resistant to the quinolones. In order to determine the pharmacophore required for SD8 binding to DNA gyrase, 16 compounds were synthesized. These compounds were then tested by surface plasmon resonance for their ability to inhibit the DNA – DNA gyrase binding interaction.

It was found that three compounds were able to inhibit the DNA – DNA gyrase binding interaction, while another showed partial inhibition of the interaction. From this data, a minimum pharmacophore was able to be determined. The pharmacophore required a coumarin scaffold bonded to a carboxylic acid group through an approximately 15 Å hydrocarbon linker.

Functional supercoiling assays determined that while the compounds were able to bind the enzyme, the binding did not inhibit DNA gyrase's ability to supercoil DNA.

List of Abbreviations

Å- angstrom

Ac - acetyl

ADP – adenosine diphosphate

atm - atmospheres

ATP – adenosine triphosphate

Bn - benzyl

Boc – *tert*-butoxycarbonyl

ºC – degrees Celsius

cm - centimeter

COOH – carboxylic acid

d - doublet

dd – doublet of doublets

ddd – doublet of doublets of doublets

dec. - decomposed

DNA – deoxyribose nucleic acid

DCM – dichloromethane

DMAP – dimethylaminopyridine

DMF – dimethylformamide

DMSO – dimethylsulfoxide

E. coli – Escherichia coli

EDCI - 1-ethyl-3-(3-dimethyaminopropyl)carbodiimide

EDTA – ethylenediaminetetraacetic acid

Et - ethyl

Fig – figure

fmol - femtomol

g - gram

Gly – glycine

H_2 – hydrogen gas

HCl – hydrochloric acid

HEPES – 4-(2-hydroxyethyl)-1-piperazineethanesulfonic acid

H_2O – water

hr/s – hour/s

IC_{50} – inhibitory concentration of 50%

$InCl_3$ – indium trichloride

IR – infrared spectroscopy

K_2CO_3 – potassium carbonate

kDa – kilodalton

KOH – potassium hydroxide

kV - kilovolts

M – molar

m - multiplet

Me - methyl

MeCN - acetonitrile

MeOH – methanol

MeOD – detuerated methanol

mg – milligrams

MHz - megahertz

mL – milliliter

mM - millimolar

mmol – millimoles

min - minute

mp – melting point

MS – mass spectrometry

μM – micromolar

μL - microliter

NaH – sodium hydride

NBTI – novel bacterial topoisomerase inhibitors

nM – nanomolar

NMR – nuclear magnetic resonance

PDB – protein database

Pd/C – palladium on carbon catalyst

psi – pounds per square inch

R_f – retention factor

RNA – ribonucleic acid

RU – response units

s - singlet

S. aureus – Staphylococcus aureus

SAR – structure-activity relationships

SC4 – simocyclinone C4

SD4 – simocyclinone D4

SD8 – simocyclinone D8

SOS – son of sevenless

SPR – surface plasmon resonance

t - triplet

TEA – triethylamine

TFA – trifluoroacetic acid

THF – tetrahydrofuran

TLC – thin layer chromatography

V - volt

v/v – volume to volume

CHAPTER 1: INTRODUCTION

1.1: Introduction to the topoisomerase family of enzymes

Throughout the life cycle of a cell, its DNA must be transcribed and replicated. The volume of the cell is too small to allow its DNA to be in a free configuration, so DNA is stored in a compact form. The topology of the compacted DNA must be altered in order to allow RNA and DNA polymerases access to the DNA.[1] Strand separation during transcription and replication generates supercoiling of the DNA because its double helical structure does not allow free rotation. Positive supercoiling, or tightening of the double helical structure, forms in front of the replication or transcription fork and negative supercoiling, or loosening of the double helix, occurs behind the fork.[2] If the positive supercoiling is not corrected, it can stall transcription or replication, while negative supercoiling interferes with normal DNA metabolism.

The topoisomerase family of enzymes is responsible for the transition between relaxed and supercoiled states of DNA, as well as removing knots and catenates while maintaining the compact, quaternary structure. Topoisomerases act by cleaving the phosphodiester backbone of DNA by nucleophilic attack by a catalytic tyrosine residue. The catalytic tyrosine is then covalently linked to the phosphate of the DNA, a bond that is easily broken at the end of the topoisomerase catalytic cycle. The action of topoisomerases does not change the sequence of the involved DNA.[1]

1.2 Types of Topoisomerases

In order to perform their various tasks, topoisomerases have evolved into more specialized types that work together in the cell to keep DNA translation and replication running smoothly.[3] Type I topoisomerases were the first topoisomerases discovered.[4] The type I subfamily controls the topological state of DNA by binding to both strands of double stranded DNA but cuts only one strand of the bound DNA. Type I topoisomerases can be further divided into type IA and type IB. Only the relaxation of negative supercoiling is catalyzed by type IA topoisomerases, while both positive and negative supercoiling can be relaxed by type IB. Type IB topoisomerases are the only members of the larger topoisomerase family that bond to DNA at the 5' end of the DNA break through the tyrosine-phosphate bond.[5] All other topoisomerase enzymes make the tyrosine-phosphate bond at the 3' end of the DNA break. An example of a type IB topoisomerase is human DNA topoisomerase I, an enzyme that is clinically targeted by the camptothecin derived family of drugs to combat human cancer. As of yet, there are no therapeutic targets that are members of the type IA topoisomerase family.[1]

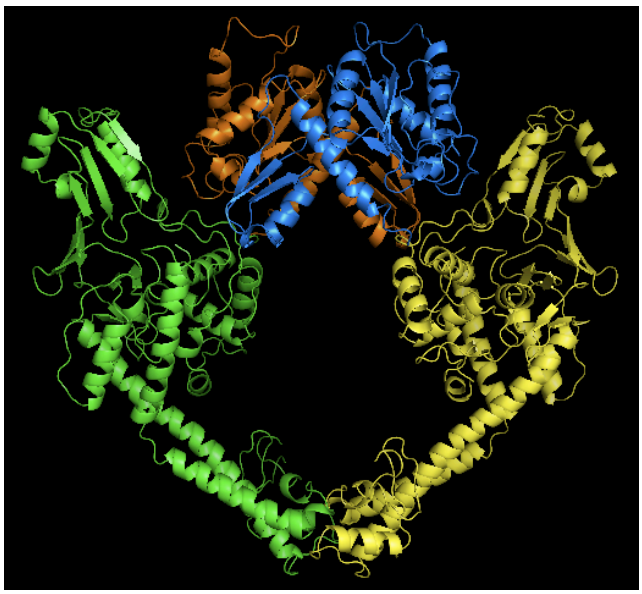

Figure 1. Crystal structure of yeast type II topoisomerase (PDB: 1BGW).

Type II topoisomerases bind double stranded DNA but unlike type I, type II topoisomerases cleave both strands of the DNA. The cleavage points on the two strands occur four base pairs away from one another and the enzymes work by opening a gate between the two strands and passing a segment of double-stranded DNA through.[6] Type II topoisomerases require energy in the form of ATP hydrolysis to ADP.[7] Type I topoisomerases catalyze reactions that are thermodynamically favored and therefore, do not require external energy in the form of ATP. The reactions that are catalyzed by type II topoisomerases also require Mg(II) for rapid enzyme turnover.[8] All type II topoisomerases exist as A_2B_2 heterotetramers, as seen in Figure 1, where two A subunits bind two B subunits to form the holoenzyme. In Figure 1, each of the four subunits is in a different color. The A subunits are in green and yellow, while the fragments of the B subunits are in orange and blue. In type II topoisomerases, the A subunit contains the

catalytic residues responsible for DNA cleavage and religation. The B subunit contains the site where ATP is bound and cleaved for the energy required to drive the reaction.[9] Crystal structures of type II topoisomerases show the enzymes look like a clamp with hinges and jaws.[9] Like type I topoisomerases, type II topoisomerases can be divided into two types, type IIA and type IIB. The division between the types is based on structural and functional differences between the enzymes.

The archetype of the type IIA topoisomerases is bacterial DNA gyrase. DNA gyrase was discovered in 1976[7] and was the first topoisomerase discovered to utilize energy in the form of ATP during catalysis.[3] This enzyme is the only known topoisomerase that is able to generate negative supercoiling as well as relaxing both positive and negative supercoils and acting as a decatenase. The task of generating negative supercoils seems to be DNA gyrase's primary function in the cell.[10] There is one ATPase site in each of the GyrB subunits of the DNA gyrase heterotetramer holoenzyme. The GyrB subunit is 90 kDa and consists of 804 amino acid residues. One catalytic tyrosine residue is at position 120 of each of the GyrA subunits. An arginine residue is also present near the catalytic tyrosine and seems to play a role in catalysis. The Gyr A subunit weighs 97 kDa, and is 875 amino acid residues in length.[9]

The archetype of the type IIB topoisomerases is topoisomerase IV,[11] an enzyme that was discovered in 1990.[12] Topoisomerase IV is believed to be the primary decatenase in the cell. A decatenase unhooks the two daughter plasmids that are generated from DNA replication during bacterial mitosis. [12] Like DNA gyrase, Topoisomerase IV can bind to and relax both positive and negative supercoils. Positive supercoils seem to be topoisomerase IV's preferential DNA topological structure to bind and relax.[13]

topoisomerase IV is a heterotetramer, as required by being a type II topoisomerase. It's A subunit, which is responsible for DNA stand cleavage and religation, is called ParC, and is 84 kDa consisting of 752 amino acids. ParE is topoisomerase IV's B subunit and is responsible for ATP binding and hydrolysis. ParE is 70 kDa and consists of 630 amino acids. Topoisomerase IV and DNA gyrase share a very high level of amino acid homology and about 40% sequence identity.[1]

1.3 Mechanism of Type II Topoisomerases

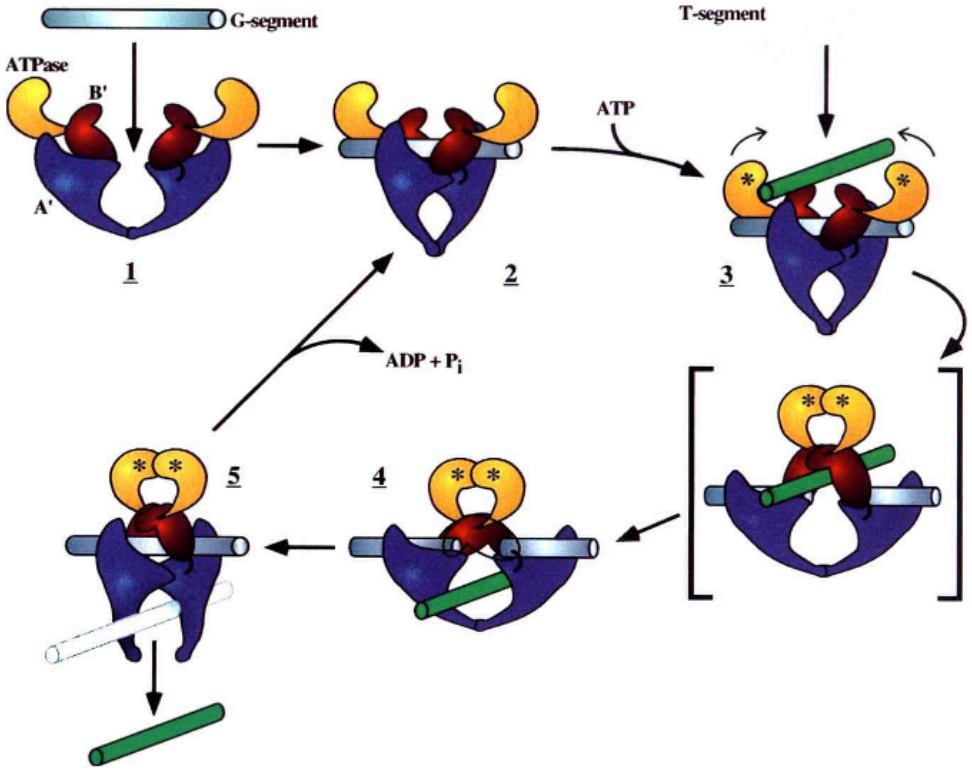

Figure 2. The mechanism of type II topoisomerases.[9]

The mechanism of type II topoisomerases (Figure 2) has yet to be fully deduced, but a "two-gate mechanism" is strongly supported by numerous studies, including crystallography. This "two-gate mechanism" was proposed by Roca and Wang in the early 1990s while studying DNA gyrase and suggests the enzyme itself has two gates, one used for capturing DNA to be translocated and a second used to release the translocated DNA.[14,15] A third gate is formed by the cleaved DNA and thus there are three gates, total, that are opened or closed during the enzyme's catalytic cycle. First is the N-gate, which is comprised of the N-terminus of the GyrB subunit. The second gate is the DNA-gate at the interface of GyrA, GyrB and DNA where DNA cleavage occurs. The last gate is the known as the C-gate at the C-terminus of GyrB.

The first step of the mechanism is the formation of the DNA-gate upon DNA association with the enzyme at the interface of the GyrA and GyrB subunits.[16] About 130 base pairs of DNA wrap in a right-handed supercoil around the enzyme.[17] DNA wrapping around the enzyme allows the T-segment of the DNA, the segment of DNA that will be passed through the cleaved DNA, to align itself at the N-gate, prepared for translocation. The N-gate closes, trapping the T-segment of DNA, upon ATP binding in the GyrB subunit.[18] Once the T-segment is trapped inside the N-Gate, the G-segment of DNA, the segment that forms the DNA-gate, is cleaved. The cleavage sites of the double-stranded DNA occurs four base pairs apart and results in phosphotyrosine bonds covalently attaching the G-segment of DNA to the GyrA subunit of DNA gyrase.[6] At this point in the enzymatic cycle, ATP binding and hydrolysis stimulate the opening of the G-segment to form the DNA gate and the passage of the T-segment through the gate. The subsequent hydrolysis of a second ATP and release of two ADP molecules drives the opening of the N-gate,

reverses the DNA cleavage, and releases the DNA. The exact order and mechanisms of these steps are still unknown. One cycle of supercoiling by DNA gyrase consumes two molecules of ATP, and generates two negative supercoils.[19,10] Mutagenesis experiments have shown that when the ATP binding site is inactivated, DNA gyrase can catalyze the relaxation of negative supercoils by the reverse mechanism.[20] It has been observed that the mechanism of topoisomerase IV is nearly identical to that of DNA gyrase,[9] which should not be surprising when considering the high level of homology between the two enzymes. Topoisomerase IV prefers intermolecular reactions such as decatenation, while DNA gyrase favors translocation of DNA intramolecularly to form supercoils.[21] Despite not being fully elucidated, there is enough known about the mechanism of type II topoisomerases for the subfamily to be a very good target for antimicrobial drugs.

1.4 Type II Topoisomerases as Antibacterial Targets

Bacterial type II topoisomerases have many characteristics that make them excellent targets for antibacterials. The subfamily has proven to be of critical importance in bacterial replication and division. When the enzymatic cycle is halted while DNA is cleaved, DNA cleavage complexes accumulate and induce cell death through signaling pathways. Targeting type II topoisomerases has shown to be non-toxic to eukaryotic enzymes. Clinically used antibacterials have shown 100-fold selectivity for the prokaryotic enzymes over eukaryotic enzymes. Lastly, type II topoisomerase inhibitors tend to target both DNA gyrase and topoisomerase IV due to their high level of homology.[1] In addition to these characteristics, there are multiple instances during the

catalytic cycle that inhibitors can interrupt, such as DNA binding, formation of phosphotyrosyl bonds between DNA and the enzyme, ATP binding and hydrolysis, as well as T-segment translocation.[22]

Based on the inhibitor mechanism of action, type II topoisomerase inhibitors can be divided into two categories: catalytic inhibitors and enzyme poisons. Catalytic inhibitors block the activity of the enzyme. For example, a catalytic inhibitor could block the binding of DNA to the enzyme, binding of ATP to the GyrB subunit, or could block the DNA cleavage action of the catalytic tyrosines. Type II topoisomerase poisons work by halting the enzyme mid-cycle by stabilization of the covalent DNA-enzyme complex.[22] In this instance, the equilibrium would shift to stimulate DNA cleavage and disfavor DNA religation.[23] The type II topoisomerase poisons are regarded, to date, as the most effective drugs that target DNA gyrase and topoisomerase IV. This is due to the fact that upon binding to the enzyme, the drug has the effect of increasing the number of double-stranded DNA-cleavage complexes within the cell. When the concentration of these open-DNA complexes reaches a certain threshold, it activates pathways that promote cellular death and therefore are cytotoxic.[24]

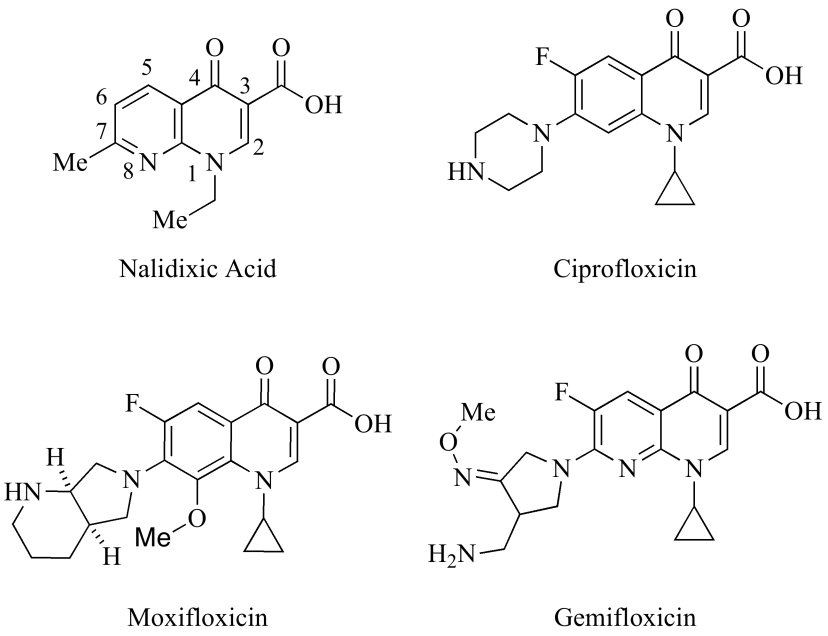

Figure 3. Structures of examples the four generations of quinolone antibiotics.

The most clinically successful class of antibacterials to target type II topoisomerases is the quinolone class of antibiotics (Figure 3). The quinolone class is based on nalidixic acid, an impurity found during the synthesis of the antimalarial chloroquine. Nalidixic acid displayed very good antibiotic activity against *E. coli*, *A. aerobacter*, *Proteus mirabilis*, and *Shigella flexneri*.[25] Nalidixic acid and the derivative oxolinic acid have been used clinically to treat urinary tract infections, but due to their limitation of only being active against Gram-negative bacteria, improvements on the drug were sought. The second generation of quinolone drugs incorporated a piperidine at the 7-position and a fluorine atom at position 6, giving rise to the drugs ciprofloxacin and norfloxacin. These changes between the first and second generations allowed antimicrobial effects to be seen in *Pseudomonas* species as well as some Gram-positive bacteria. Further

changes to the quinolones, such as bulky substitutions at the 7-position, a fluorine atom at the 6-position, and substitution at the 8-position, gave rise to the third generation of the class. Members of the third generation include the antibacterials levofloxacin and moxifloxacin. This generation has greater activity against Gram-positive bacteria, many members of the generation are more specific to topoisomerase IV, and are more useful in combating respiratory infections. In the last decade, the fourth and most recent generation of quinolone drugs was approved. The Food and Drug Administration approved the antibiotic gemifloxacin in 2003. Gemifloxacin has a better potency and a broader spectrum of action than any of the previous generations.[1,26]

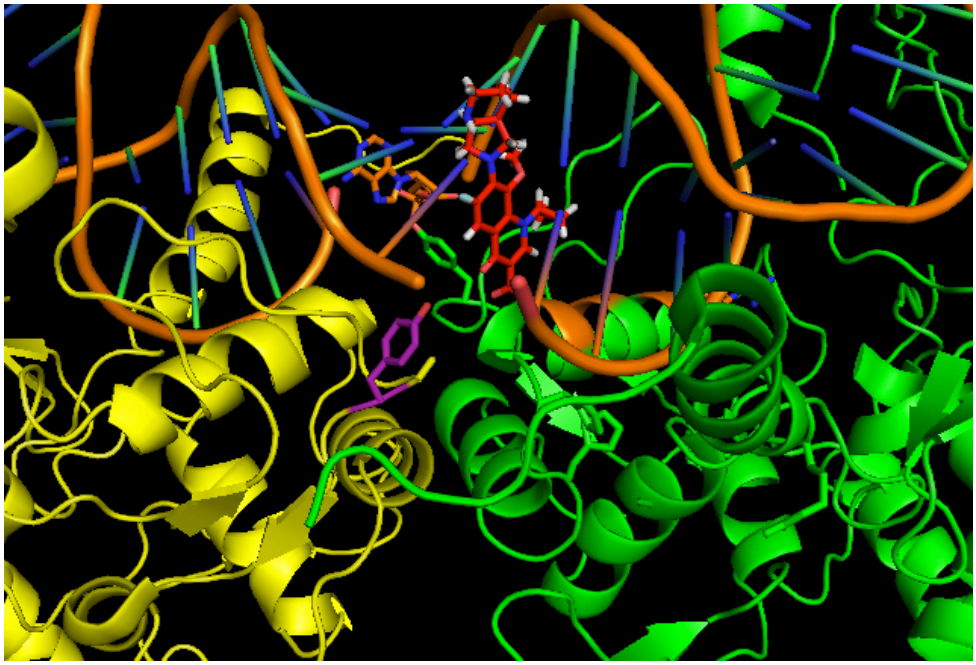

Figure 4. Crystal structure of topoisomerase IV ParC dimer–DNA complex with bound moxifloxacin (PDB: 3FOE and 3FOF).

The quinolone class of drugs acts as type II topoisomerase poisons. They stabilize the cleavage complex step in the enzyme mechanism by targeting and binding to the bound DNA[27] and the GyrA or ParC subunit in DNA gyrase and topoisomerase IV, respectively. X-ray crystal structures have shown the quinolone drug binding occurs at the site of DNA cleavage. The drug molecules intercalate the cut DNA and the rings of the drug stack with the nucleic acids at position +1 and -1 relative to the cuts in the DNA, as seen in Figure 4. The intercalation of the drug stops the enzyme from being able to pull the G-segment of DNA apart prohibiting both T-segment passage and DNA religation.[28] When enough of these cleavage complexes accumulate, the cell activates pathways, which are not fully elucidated, which collectively cause chromosomal fragmentations and cell death.[29]

Bacterial resistance to the quinolone class of drugs is mainly due to amino acid mutations in the DNA-binding regions of both DNA gyrase and topoisomerase IV. These step-wise mutations in the "quinolone resistance-determining region" (positions 67-106 in *E. coli* DNA gyrase) give rise to a binding site that is unable to form binding interactions with the drug. With a binding pocket with a lower affinity for the drug, the enzyme is not as susceptible to the drug's effect.[1] There has also been evidence that mutations are occurring at the mouth of the quinolone-binding site, blocking the site entirely.[30] Other mechanisms of resistance that have been observed are reduced drug uptake, up-regulation of drug efflux pumps, and chemical alteration of the quinolone drug before it reaches its target.[1]

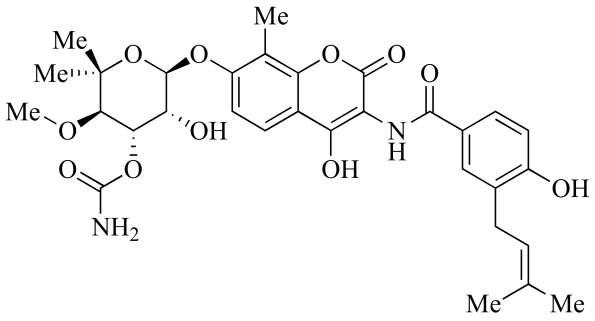

Novobiocin

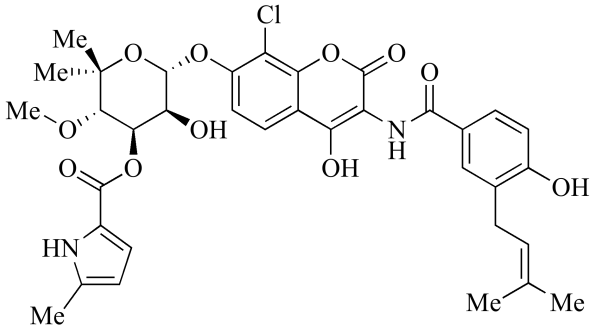

Clorobiocin

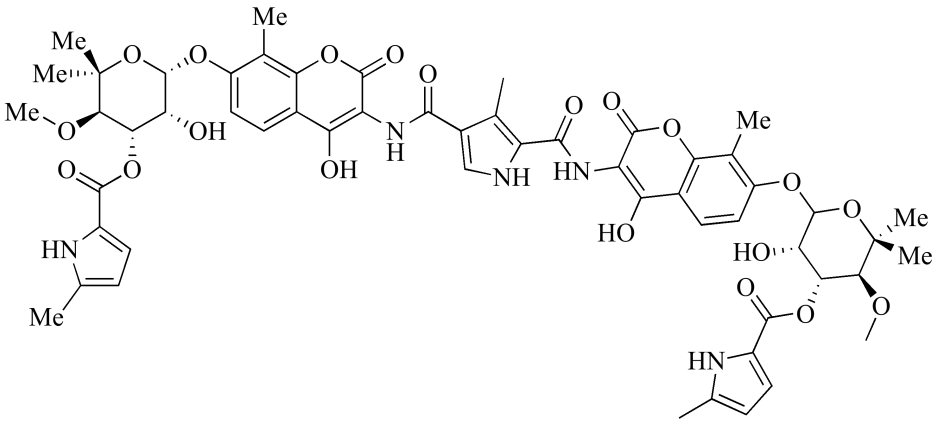

Coumermycin A1

Figure 5. Structures of selected examples of the aminocoumarin class of type II topoisomerase inhibitors.

Type II topoisomerases can be inhibited through drugs that target the ATP binding site on the GyrB or ParE subunit. This class of topoisomerase inhibitors is called the classical aminocoumarins, with examples of this class being novobiocin, clorobiocin, and coumermycin A_1. All members of this class are natural products isolated from *Streptomyces* bacteria and have a shared hallmark structural feature, the 3-amino-4,7-dihydroxycoumarin moiety, found in no other natural product. This group of compounds have been known since the 1950s as nucleic acid synthesis inhibitors, but was found to inhibit DNA gyrase soon after the enzyme was discovered.[7] As seen in Figure 5, one of the most notable differences between clorobiocin and novobiocin is the presence of a chlorine atom at the coumarin's 8-position in place of a methyl group.[31] Despite having no structural similarities with ATP, it has been found that the aminocoumarins inhibit type II topoisomerases by competing for binding with ATP. Crystal structures have shown the aminocoumarins' exact binding site (Figure 6) is not the same as ATP, but overlaps at the binding site of both the adenine ring of ATP and the L-noviosyl sugar of the aminocoumarins, as seen in Figure 7, making the aminocoumarins competitive inhibitors of type II topoisomerases.[32] The binding of novobiocin to topoisomerase IV's ParE ATP binding domain can be seen in Figure 6, with the protein in green and the drug in orange.

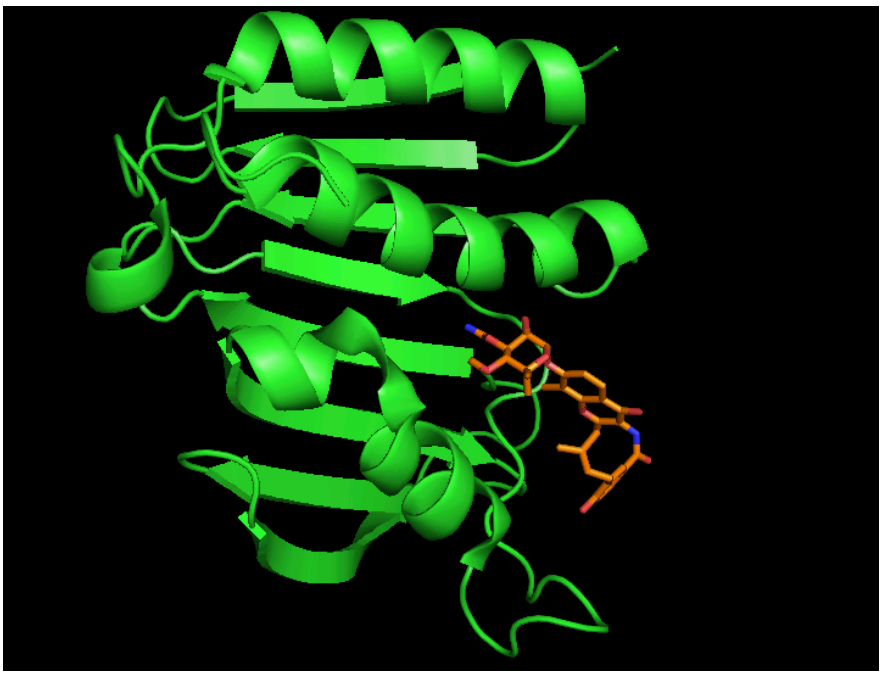

Figure 6. Crystal structure of novobiocin bound to the ATP binding domain of ParE (PDB: 1S14).

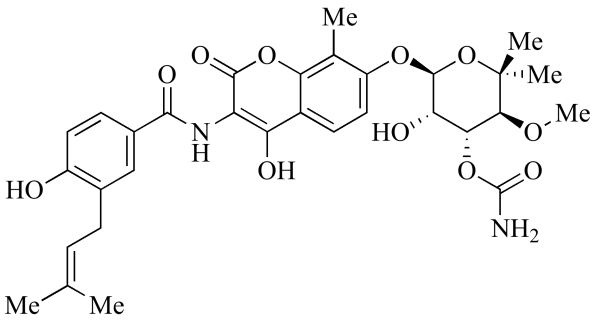

Novobiocin

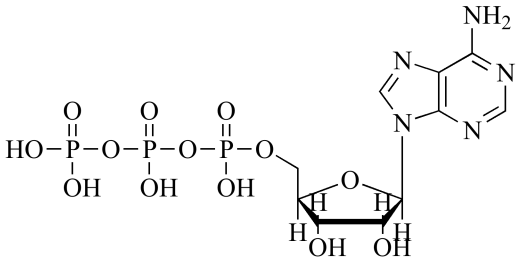

Adenosine Triphosphate (ATP)

Figure 7. Comparison of the structures of the aminocoumarin novobiocin, and the endogenous ligand of GyrB, adenosine triphosphate (ATP).

Despite once being used to treat methicillin resistant Staphylococcus aureus (MRSA) bacterial infections, the aminocoumarins have not seen the clinical success of the quinolones. Aminocoumarin use has been limited by their toxicity to eukaryotic cells as well as their poor solubility and bioavailability.[33] Toxicity of drugs that target an enzyme's ATP site is expected since the structure of the ATP-binding site is highly conserved across many families of enzymes.

Type II topoisomerases can become resistant to the aminocoumarin class of antibiotics by step-wise mutations. The most common naturally occurring mutations are residues that do not make contact with ATP, but are in the aminocoumarin-binding site, such as Arg136, and Gly164, (*E. coli* numbering).[32] A site directed mutagenesis study considered various mutations, both naturally occurring and unnatural, and found that the majority of mutations in the aminocoumarin-binding site gave rise to an enzyme with reduced or no biological activity. This shows that mutation-based resistance is limited since the ATP-site is critical to enzyme function.[34] This class of drugs has proved very useful to probing the ATP-binding site of type II topoisomerases and there are ongoing efforts to make more selective, more bioavailable compounds with greater solubility and less toxicity.[1]

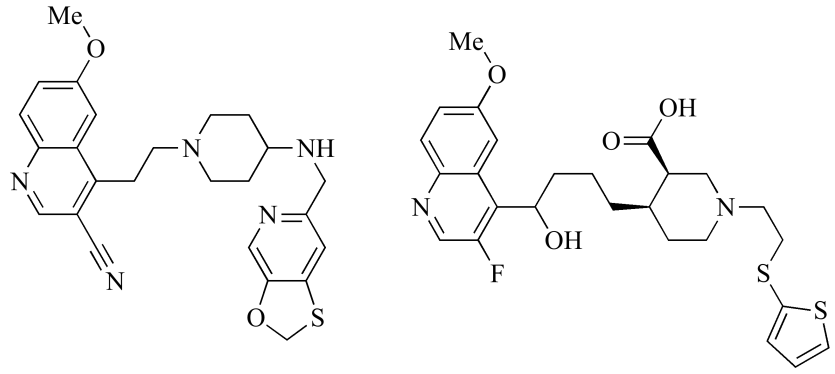

GSK299423 NXL101

Figure 8. Structures of GSK299423 and NXL101, examples of the NBTI class of type II topoisomerase inhibitors.

The third class of antibacterials that target type II topoisomerases are called the novel bacterial topoisomerase inhibitors (NBTIs). This class was pioneered by GlaxoSmithKline, and acts through a different mechanism than the previously discussed antibacterials.[22] The NBTIs act by stabilizing the DNA-enzyme complex before DNA cleavage occurs. A limited amount of single-strand DNA cleavage has been seen with members of the NBTIs, but this does not seem to be main mechanism of action. Members of this class of antibacterials include NXL101 and GSK299423 (Figure 8), synthetic small molecule inhibitors that are structurally different from both the quinolones and the aminocoumarins.[35, 36] While NXL101 has comparable IC_{50} values to ciprofloxacin, its introduction was an improvement over clinically used drugs because NSL101 has the ability to overcome ciprofloxacin resistance.[36] GSK299423, a newer NBTI, is 2000-fold more potent of an inhibitor against *S. aureus* DNA gyrase than ciprofloxacin, with an IC_{50} of 14±5 nM. In the same study, ciprofloxacin's IC_{50} was 31±10 μM.[35]

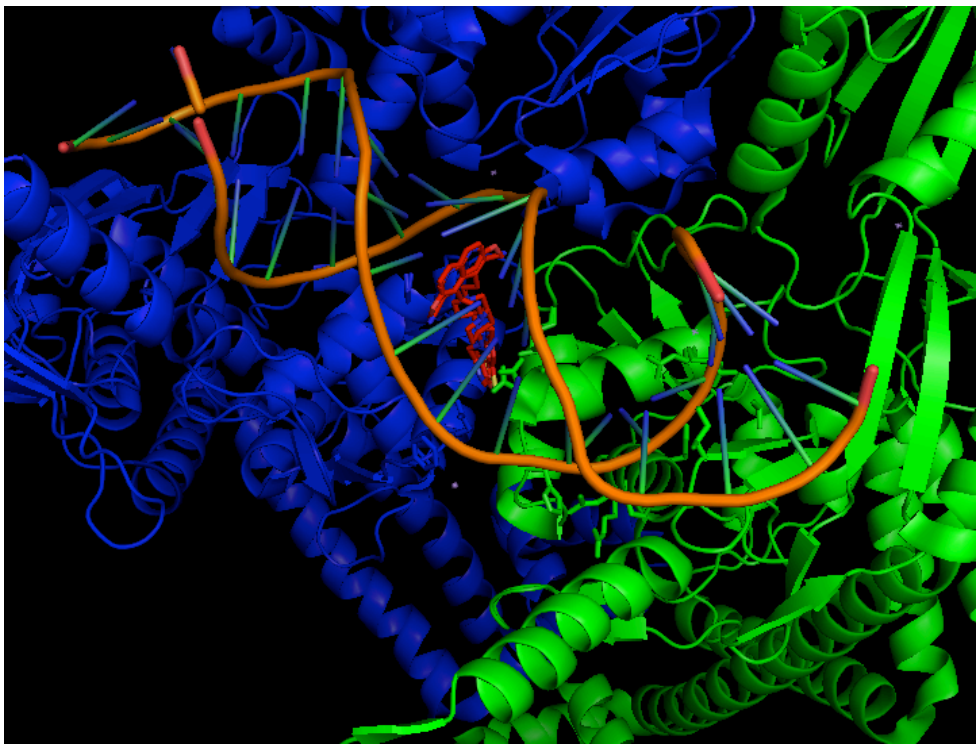

Figure 9. Crystal structure of GSK299423 bound to the GyrA dimer-DNA complex (PDB: 2XCS).

The crystal structure of GSK299423 and the *S. aureus* fusion protein GyrB27-A56 have shown the binding site of this drug is in between the two GyrA subunits, blocking the opening of the G-segment of DNA and subsequent passage of the T-segment.[35] This can easily be seen in Figure 9, where the red drug molecule is intercalating the DNA bound to the blue and green GyrA dimer. The crystal structure of NXL101 and *E. Coli* GyrA also shows NXL101 binding near the binding site of the quinolones, but does not share any amino acid residue contacts with the quinolone class. The solved crystal structures support the experimental findings that the NBTIs maintain antibacterial activity against

strains of bacteria resistant to quinolones.[35,36] The compound NXL101 was in clinical trials, but further development of the drug was halted in 2008.[37]

Each of these three classes of antibacterials has their own limitations. The quinolones have limited use due to increasing resistance seen in the clinic. The competitive ATP inhibitors have selectivity and pharmacokinetic problems, and the NBTIs have yet to have a compound successfully complete clinical trials. These problems with the existing antibacterials that target type II topoisomerases leave much room for improvement.

CHAPTER 2: INTRODUCTION TO SIMOCYCLINONE D8

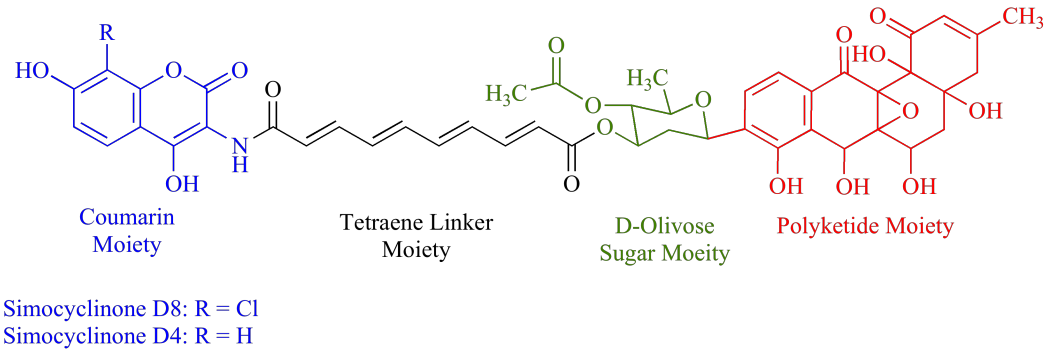

Figure 10. Structures of simocyclinone D8 and simocyclinone D4.

A fourth class of molecules that target type II topoisomerases is the simocyclinone class. Discovered in the year 2000, simocyclinones are natural products isolated from *Streptomyces antibioticus* Tü 6040, a bacterium isolated from a soil sample from Argentina.[38] All members of this class are biosynthetic precursors to the final fermentation product, simocyclinone D8 (SD8).[39] Simocyclinone D8 (Figure 10) is a bivalent ligand with a 3-amino-8-chloro-4,7-dihydroxycoumarin moiety at one end of the linear molecule.[40] Bonded to the amine through an amide bond is a tetraene dicarboxylic acid linker that connects the coumarin to a D-olivose sugar. At the other end of the SD8 molecule is an angucyclic polyketide, which is connected to the D-olivose sugar through a glycosidic linkage. Simocyclinone D4 has the same structure, but does not have the chlorine atom at the coumarin's 8-position. Instead, simocyclinone D4 has a hydrogen atom occupying the 8-position of the coumarin.

The structure of the aminocoumarins and simocyclinones are very similar. Both share a similar coumarin moiety, with clorobiocin and SD8 both containing the same coumarin and SD4 and novobiocin containing the same coumarin. The structures of the simocyclinones and aminocoumarin antibiotics differ markedly at the 7-position of the coumarin. Aminocoumarins are bonded to a L-noviosyl sugar through an ether bond at the 7-position of the coumarin, while simocyclinone D8 has a free hydroxyl group at the 7-position of the coumarin. Despite differences, the structural similarities between the aminocoumarins and the simocyclinones are significant.

The biosynthetic gene cluster for simocyclinone has been sequenced and has shown to share many similarities with the biosynthetic gene clusters for both novobiocin and clorobiocin. One large difference between the gene clusters of the simocyclinones and the aminocoumarin antibiotics is that the aminocoumarin genes have associated transporter proteins and resistance genes. Producing resistance genes is important to bacteria so it does not succumb its own biological weapon. Simocyclinone's gene cluster has the encoded transporter proteins, but does not include any resistance genes. The lack of resistance genes in the simocyclinone gene cluster is interesting, since resistance genes paired with an antibiotic hint at the bacterial target of the antibiotic produced by the organism.[41,42]

First pass screens testing simocyclinone class' antibacterial properties show both simocyclinones D4 and D8 have antibacterial activity against Gram-positive bacteria. No inhibition of Gram-negative bacteria was observed in the initial study. Cytostatic effects on various human cancer cell lines were also observed when cells were treated with simocyclinones D4 and D8.[38]

Due to the simocyclinones' structural similarities to other antibacterials that target type II topoisomerases and preliminary evidence that SD8 functions as an antibiotic, Maxwell's group undertook a study to determine simocyclinone D8's mechanism of action against DNA gyrase isolated from *E. coli*. This study showed SD8 had an IC_{50} of ~100 nM and was a more potent inhibitor of DNA gyrase than either novobiocin or ciprofloxacin, with IC_{50} values of 250 nM and ~700 nM, respectively. Simocyclinone D4 had an IC_{50} of ~ 450 nM. It was determined that SD8 and SD4 did not inhibit using the ATP-competitive mechanism, because its activity was unaffected by changes in ATP concentration. ATP cleavage was also unaffected by the presence of SD8 or SD4, indicating the simocyclinone binding site was not on the GyrB subunit of the enzyme, despite being very structurally similar. Maxwell's group also demonstrated that the simocyclinone-binding site is very near the quinolone-binding site. When a mutant DNA gyrase enzyme, known for being quinolone resistant, was used in place of the wild type enzyme, the IC_{50} of the simocyclinones was higher, but it was not as much of an increase as seen for ciprofloxacin.

The next experiments examined how the simocyclinone class inhibits DNA gyrase. Data showed that the simocyclinones inhibit the catalytic cycle before DNA is cut and may even inhibit DNA from binding to the enzyme all together. This indicates simocyclinones do not have the same mechanism of action as the quinolones despite having similar binding sites. The simocyclinones exhibit tighter binding with the holoenzyme of DNA gyrase than with just GyrA. Binding more tightly to the holoenzyme suggests that the majority of the binding site it contained within the GyrA subunit, the entire simocyclinone-binding site spans both the GyrA and GyrB subunits.

Despite not binding as tightly with the GyrA subunit as the holoenzyme, binding constants showed the SD8 to GyrA binding to be in a 1:1 ratio. Simocyclinone D8 was also tested against other topoisomerases, and was found to inhibit topoisomerase IV and human topoisomerase II, with IC_{50} values of 50 μM and ~5 μM, respectively. The inhibition of human topoisomerase II was stronger than the clinically used chemotherapy agent, etoposide. No SD8 inhibitory effects were seen against human topoisomerase I.[40] Simocyclinone D8 was tested against DNA gyrase from *Staphylococcus aureus*,[43] a Gram-positive bacterium that showed to be highly susceptible to SD8 in the initial antibacterial study.[38] SD8 inhibited the enzyme with an IC_{50} 1.45 μM. Despite needing a larger concentration of the inhibitor than against *E. coli*, SD8 proved to be working by the same mechanism as published by Maxwell, et al.[40] by stopping the binding of DNA to the enzyme. Seeing that most of the type II topoisomerase drugs target both DNA gyrase and Topoisomerase IV, SD8 was tested against Toposiomerase IV from both *S. aureus* and *E. coli*. It was found that SD8 had little effect on the decatenating action of Topoisomerase IV, and it was concluded that topoisomerase IV was not the intended target of SD8. Since SD8 was capable of inhibiting DNA gyrase from *E. coli*, but was not bactericidal to the whole cell, SD8's lack of inhibition must be stemming from another mechanism occurring in the cell. SD8 proved to be a substrate for *E. coli*'s AcrB multi-drug efflux pump. When a mutant strain of *E. coli*, one with no efflux pump, was treated with SD8, the IC_{50} was 5 μM. This showed SD8 was pumped out of the *E. coli* cells before it could bind and have an inhibitory effect on the cell.

Previous genetic studies had not been able to identify the intended target of SD8, so the "SD8 expression profile" was studied by monitoring the changes in gene transcription

when cells were treated with SD8. Upon treatment, the expression profile looked similar to that of novobiocin. There was downregulation of enzymes that removed negative supercoils, and upregulation of GyrA and GyrB genes. There was no SOS signal observed after dosing susceptible cells with SD8, unlike cells that had been treated with norfloxacin, a quinolone antibiotic. The lack of an SOS signal was attributed to SD8's mechanism of action of blocking DNA binding instead of stabilizing the DNA-enzyme cleavage complex. Therefore, cells are not undergoing the same type of programmed cell death that they are with the quinolone drugs, so cell death must be attributed to another mechanism. It was observed the nucleoid in whole cells was larger when treated with SD8, when compared to untreated cells. This indicated unraveling of DNA due to the lack of DNA gyrase's control over DNA morphology. DNA unraveling would lead to cellular death and is postulated to be SD8's bactericidal mechanism.[43]

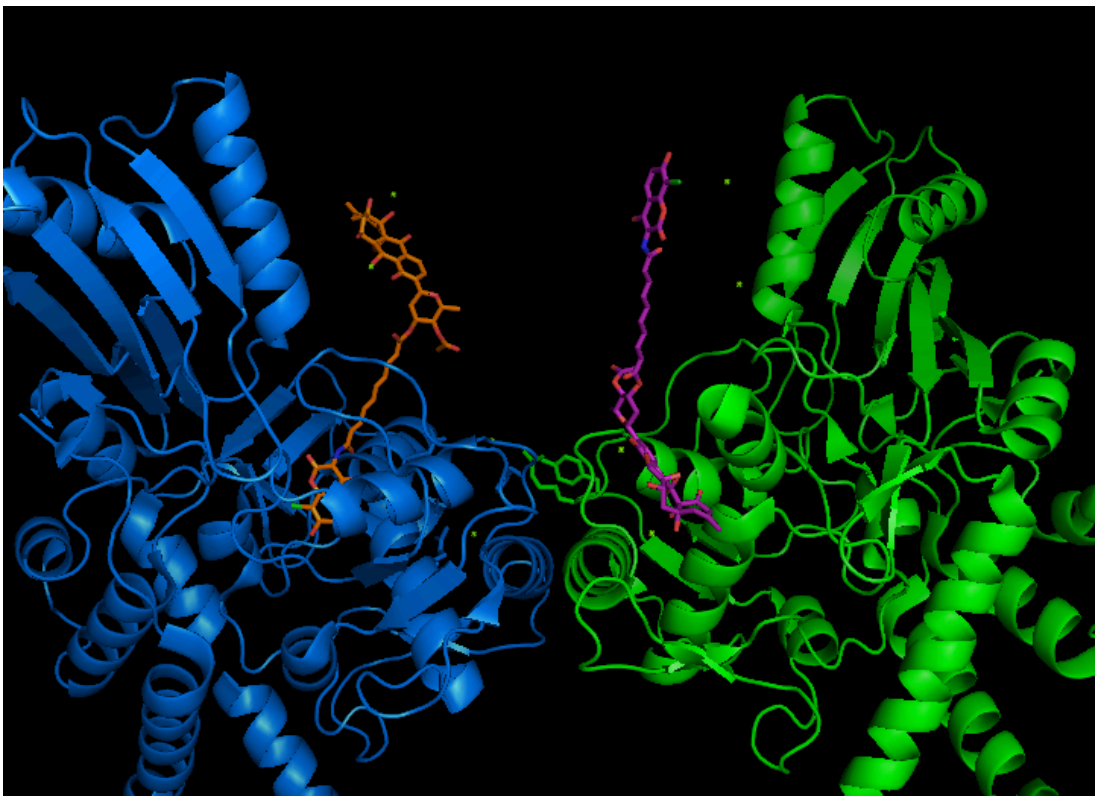

Figure 11. Crystal structure of both modes of SD8 binding to the GyrA dimer (PDB: 2WL2).

A crystal structure of simocyclinone D8 bound to *E. coli* GyrA59, a truncated GyrA subunit, was published in 2009. The structure shows the GyrA59 dimer with two bound SD8 molecules, as the GyrA subunit contains binding sites for the aminocoumarin and the polyketide moieties (Figure 11). Major interactions are seen between the coumarin ring and the enzyme, as well as between the polyketide moiety and the enzyme. Surprisingly, the tetraene diacid linker and D-olivose sugar did not play major roles in the binding, but served only as a tether between the coumarin and polyketide. This study proposed that SD8 binds to DNA gyrase in a "bent over" conformation. In the event that

one molecule of SD8 binds to one heterotetramer holoenzyme of DNA gyrase, the aminocoumarin and the polyketide sections of the molecule bridge the two GyrA subunits.

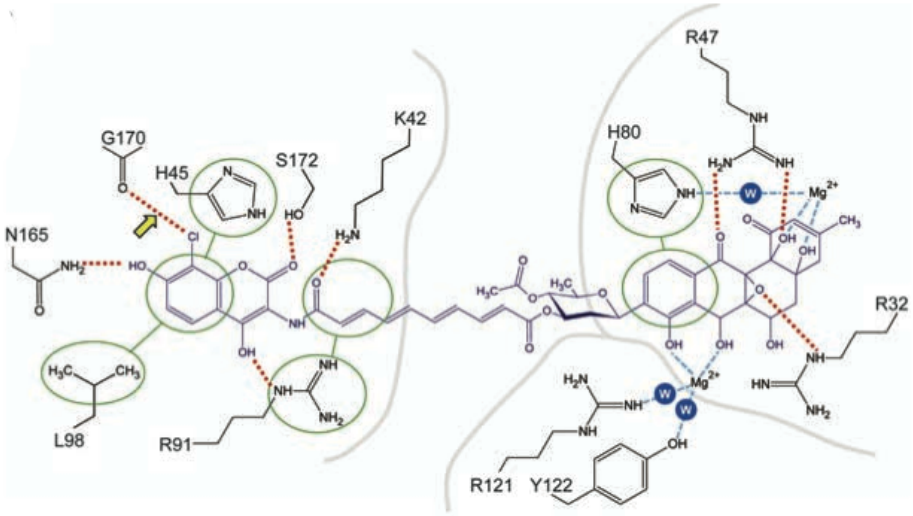

Figure 12. Binding of SD8 to DNA gyrase, as proposed by Maxwell, *et al*.[44]

Binding of SD8 to DNA gyrase involves interactions between at least 14 amino acid residues and the inhibitor molecule, as seen in Figure 12. Some interactions between the enzyme and the polyketide moiety of SD8 involve bonds mediated by both waters (blue circles, labeled "W") and magnesium ions. Other interactions of the polyketide moiety involve π-stacking of His80 to the benzene ring of the moiety, hydrogen bonding of Arg32 to the epoxide, and Arg47 hydrogen bonding to a carbonyl and hydroxyl group on the moiety. Very few interactions were seen between SD8's tetraene linker and the enzyme. The only interactions seen were between Arg91 and Lys42, which pi-stacked and hydrogen bonded with the carbonyl of the amide bond connecting the coumarin to

the linker and the nearest double bond. Arg91 also hydrogen bonded with the hydroxyl at the 4-position of the coumarin. π-Stacking was seen between the benzyl ring of the coumarin, Leu98 and His45. One of the more interesting interactions seen between SD8 and DNA gyrase was the halogen bond between the chlorine of SD8's coumarin ring and the backbone carbonyl of Gly170.

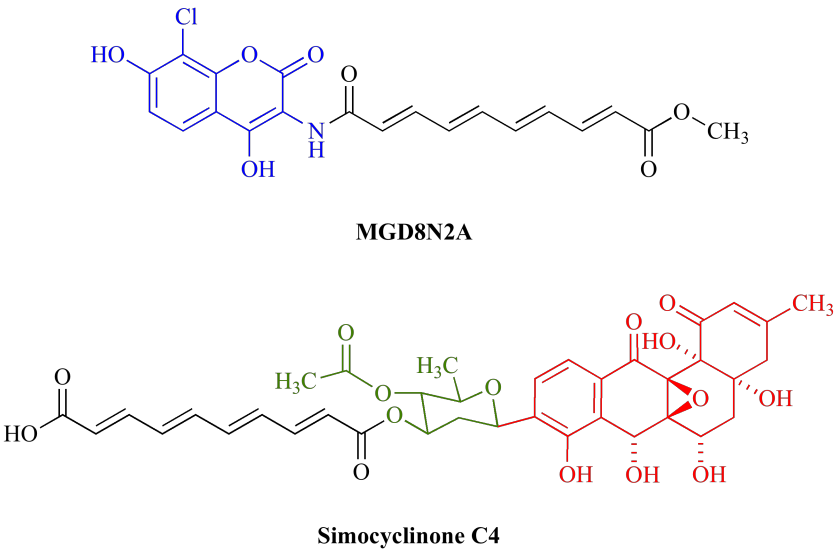

Figure 13. Structures of MDG8N2A and simocyclinone C4.

In order to determine the dependency of each end of simocyclinone D8's binding to *E. coli* DNA gyrase, the IC_{50} values were determined for simocyclinone C4 and MGD8N2A. Simocyclinone C4 (Figure 13) is a biosynthetic intermediate of SD8 lacking the 3-amino-8-chloro-4,7-dihydroxycoumarin. MGD8N2A (Figure 13) is a semi-synthetic compound produced from the saponification of the ester bond connecting the tetraene diacid and D-olivose sugar of SD8, to yield an SD8-like molecule that lacks both the sugar and the polyketide moieties. In this study, the IC_{50} of parent compound SD8

was 0.6 μM, SC4 has an IC_{50} of 70 μM, and MGD8N2A's IC_{50} was 50 μM.[44] This shows that while the fully intact SD8 has the best inhibitory concentration, both ends are capable of binding and inhibiting independently of one another. The coumarin with the tetraene diacid linker proved to be a more potent inhibitor than the polyketide-sugar with the tetraene diacid linker. When these two molecules were mixed together to test the cooperativity of binding, there was no increased binding of either SC4 or MGD8N2A. This could be attributed to steric interaction of the linkers. When this data is taken together, it can be concluded that SD8's binding affinity for DNA gyrase is due to the coumarin and polyketide moieties being linked together.[45] Because each end of SD8 can bind independently, the structure-activity relationship study between both ends of SD8 and DNA gyrase do not need to be done together. Individual studies of each the coumarin and the polyketide can be undertaken.

CHAPTER 3: A DECONSTRUCTION-RECONSTRUCTION APPROACH TO DEFINING THE MINIMUM PHARMACOPHORE FOR SIMOCYCLINONE D8 INHIBITION OF DNA-DNA GYRASE BINDING

Simocyclinone D8's aminocoumarin moiety is one of its more intriguing features. This moiety is shared with the aminocoumarin class of antibiotics and has been widely studied under the context of the antibiotic class. Our main goal was to discern which features of SD8's aminocoumarin and linker contribute to the binding of the molecule to DNA gyrase and the disruption of DNA's binding interaction.

We approached this investigation with the goal of synthesizing coumarin-based deconstruction analogs of SD8 by incorporating a coumarin ring with few substituents. By having a small number of substituents, we could then examine each individual substituent's role in binding to the enzyme. Using this method, we have the ability to determine the pharmacophore, or the minimum coumarin scaffold required for binding to DNA gyrase, and also be able to predict which substituents would be beneficial to binding and what ones would detract from the binding interaction.

To achieve our goal, we concentrated on four coumarins that were either commercially available or easily prepared: 3-amino, 3-amino-4-hydroxy, 3-amino-7-hydroxy, and 4,7-dihydroxy. The main focus of the molecules we synthesized was the coumarin, so the angucyclinone polyketide moiety of SD8 was not attached. It has been shown in binding studies using MGD8N2A, that the coumarin and the linker are able to bind without the polyketide moiety.[44] However, the mechanism of action of MGD8N2A and its potential

ability to disrupt the binding of DNA-to-DNA gyrase has not been explored. The base linker length of ~15 Å was determined by molecular modeling using the crystal structure of Gyrase and SD8 uploaded to the protein data bank by Maxwell, et al. and is the length between the coumarin binding pocket and the mouth of the angucyclinone binding pocket. This length translated to a saturated carbon diacid chain eight carbons in length, not including the carbons in the carboxylic acids. Our goals in this study were to be able to determine not only the basic SAR of the coumarin ring, but to also determine some of the properties of the linker that are necessary for binding, such as charge, steric limitations and the ability to form hydrogen bonds.

3.1 Synthesis of the coumarin-based deconstruction analogs of SD8

3.1.1 Synthesis of the 3-aminocoumarin derivatives

The simplest coumarin we used was 3-aminocoumarin, which was commercially available from Aldrich. Using this coumarin, six compounds were synthesized, ranging in complexity from the coumarin with a fatty acid chain to two coumarins connected through an 8-carbon linker. Since these coumarin compounds were the easiest to synthesize, due to a lack of substituents, they were utilized to explore linker properties. Linker length, charge, and ability to form hydrogen bonds were explored with this set of compounds, as well as the steric limitations around the mouth of the coumarin-binding pocket.

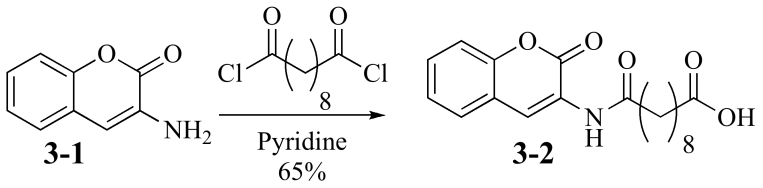

Figure 14. Synthesis of 3-2

The reaction of 3-aminocoumarin with sebacic diacid chloride gave compound **3-2**, in a 65% yield. Pyridine was used as both the solvent and the acid trap. These conditions were selected after attempting the same reaction in tetrahydrofuran using triethyl amine as an acid trap gave poor yield.

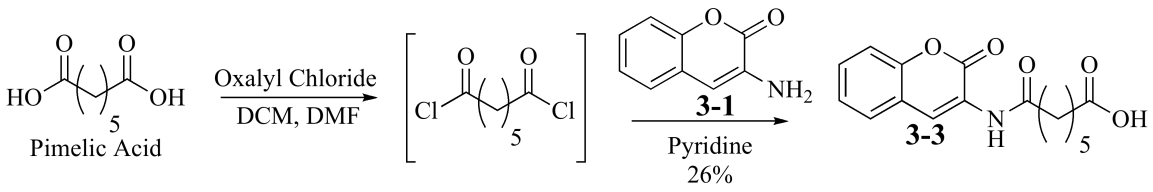

Figure 15. Synthesis of 3-3

The first step in synthesizing **3-3** was generating the diacid chloride of pimelic acid. Pimelic acid was dissolved in dichloromethane, a drop of dimethylformamide was added as a catalyst, followed by oxalyl chloride. Oxalyl chloride was used in place of more commonly used thionyl chloride as we experienced coumarin stability issues when exposed to thionyl chloride. The pimelic diacid chloride was not isolated or characterized, but was concentrated and added to **3-1** in pyridine, dropwise. The two-step reaction gave **3-3**, in a 26% yield. This compound was used to determine if the base linker length of around 15 angstroms was necessary or if a shorter linker would suffice.

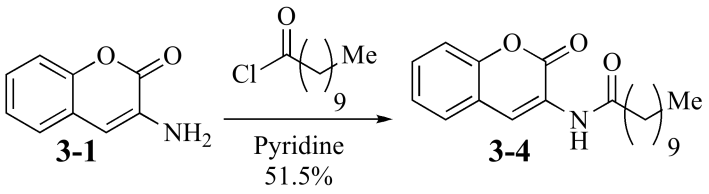

Figure 16. Synthesis of 3-4

The reaction of 3-aminocoumarin with commercially available decanoyl chloride, gave **3-4** in a 51.5% yield. The fatty acid linker allowed us to test if a charged linker aided, hindered, or was neutral when it came to binding.

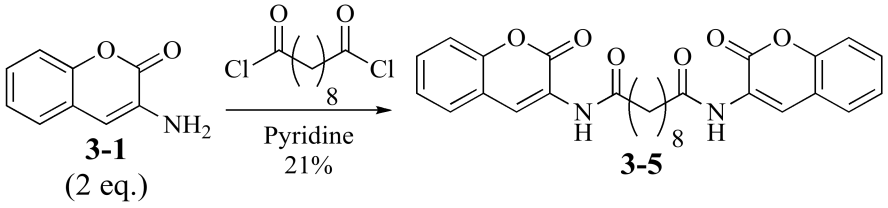

Figure 17. Synthesis of 3-5

Reacting 2 equivalents of **3-1** with one equivalent of sebacic diacid chloride in pyridine gave **3-5**, in 21% yield. Compound **3-5** was designed to access the coumarin binding pockets on both GyrA subunits of the Gyrase holoenzyme.

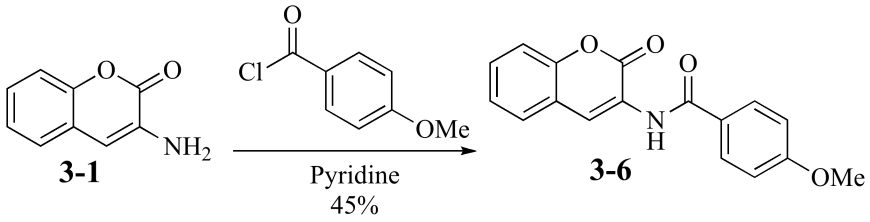

Figure 18. Synthesis of 3-6

Commercially available p-methoxy benzoyl chloride was reacted with **3-1** to give **3-6** in a 45% yield. The p-methoxy benzene was chosen to see if an aliphatic chain was necessary for binding, and also to determine the sterics neighboring the amide bond.

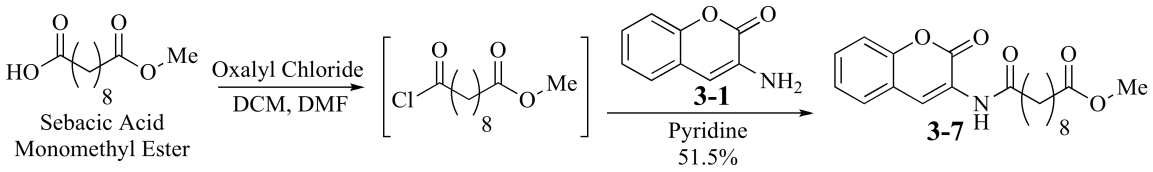

Figure 19. Synthesis of 3-7

Commercially available sebacic acid monomethyl ester was converted to the acid chloride by dissolving the acid in dichloromethane, adding a drop of dimethyl formamide as a catalyst, and using oxalyl chloride as the chlorinating agent. The sebacic acid chloride monomethyl ester was concentrated, but not isolated or characterized before being added dropwise to **3-1** dissolved in pyridine to afford **3-7** in 51.5% yield.

3.1.2: Synthesis of the 3-amino-4-hydroxycoumarin derivatives

The next coumarin we focused on was 3-amino-4-hydroxycoumarin. This coumarin added back one of the hydroxyl substituents on the SD8 coumarin ring. The 3-amino-4-hydroxycoumarin was easily accessible from 4-hydroxy-3-nitrocoumarin through a simple hydrogenation. These compounds were used as tools to explore both the importance of the 4-hydroxyl group as well as the group on the end of the linker. In order to make a direct comparison between the binding of the 3-aminocoumarin, 3-amino-4-hydroxycoumarin, and MGD8N2A, the 3-amino-4-hydroxycoumarin was coupled to the 8-carbon diacid linker. We attempted to synthesize compounds analogous

to each of those with the 3-aminocoumarin, but the 4-carbon of the coumarin ring proved to be nearly as good of a nucleophile as the 3-amine group, with the 4-hydroxyl group acting as a leaving group. It was initially thought the 4-hydroxyl group was acting as the nucleophile, but multiple attempts to saponify the ester failed. These reactions were also attempted using 1-ethyl-3-(3-dimethyaminopropyl)carbodiimide (EDCI) conditions to selectively couple the carboxylic acid and the amine, but the reactions gave extremely poor yields. Due to these issues, synthesis of analogs with the 5-carbon diacid linker, 10-carbon fatty acid chain, the methyl-ester 8-carbon linker, and the p-methoxy benzoic acid were unsuccessful. Aniline and p-hydroxyaniline were installed at the end of the linker as simplified mimetics of the D-olivose sugar. By adding these groups on the end of the linker, we hoped to explore the sterics, charges and electronics of the area surrounding the sugar during SD8 binding to DNA gyrase.

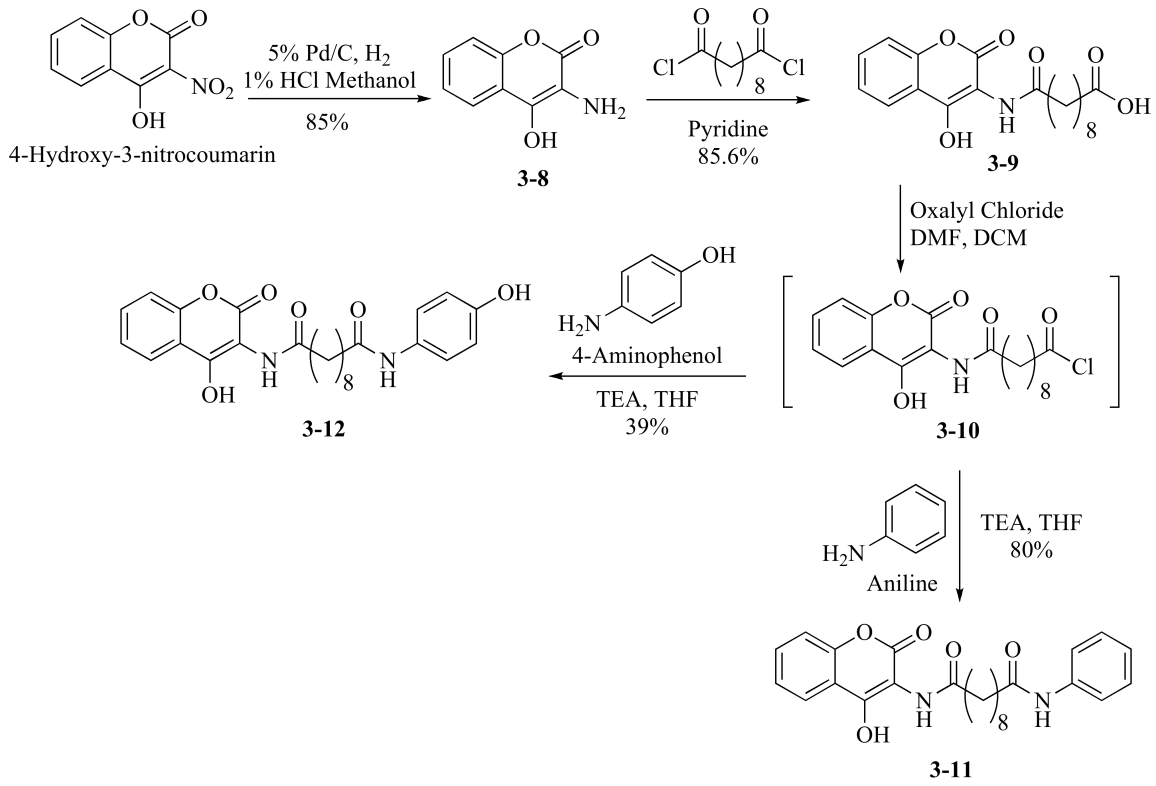

Figure 20. Synthetic scheme of compounds 3-8, 3-9, 3-10, 3-11, and 3-12.

The first step in this synthetic scheme was to reduce the 3-nitro group of 4-hydroxy-3-nitrocoumarinto an amine by catalytic hydrogenation. The hydrogenation was carried out in acidic methanol, using 5% palladium on carbon as the catalyst. This step successfully produced **3-8** in an 85% yield. Compound **3-8** was dissolved in pyridine and sebacic diacid chloride was added dropwise. This reaction produced compound **3-9** in 85.6% yield. To complete the subsequent coupling reactions, the coumarin-linker was dissolved in dichloromethane, a drop of catalytic dimethylformamide was added, and oxalyl chloride was used to give the acid chloride, **3-9**. The acid chloride was not isolated or characterized before being added, dropwise, to solutions of either aniline or 4-

aminophenol. The reaction of the acid chloride with aniline produced **3-11** in 80% yield and the reaction with 4-aminophenol gave **3-12** in 39% yield.

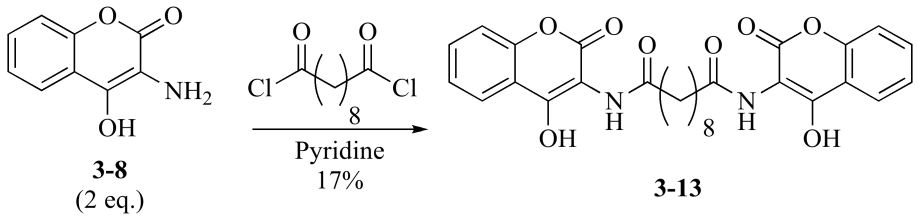

3-8
(2 eq.)

3-13

Figure 21. Synthesis of 3-13.

Two equivalents of **3-8** were dissolved in pyridine and sebacic diacid chloride was added dropwise. Compound **3-13** was produced in 17% yield. Multiple attempts to repeat this reaction gave very poor results.

3.1.3 Synthesis of the 3-amino-7-hydroxycoumarin analogs

The third coumarin we explored was the 3-amino-7-hydroxycoumarin. This coumarin was not as easily accessible as the previous two coumarins. The 3-amino-7-hydroxycoumarin ring was made de novo from 2,4-dihydroxybenzaldehyde and N-acetylgycine. Like with the 3-amino-4-hydroxycoumarin, the 3-amino-7-hydroxycoumarin had some issues with coupling at the amine position. The hydroxyl group in the 7-poistion of the ring donated electrons to the extended π-electron system, making the carbon in the ring's 4-position a very good nucleophile. This nucleophilicity proved problematic as it competed with the 3-amine during the coupling reactions to give rise to compounds with linkers attached at the 3-amine but also at the 4-postion of the

coumarin. We attempted to use an EDCI coupling, like we did with the 3-amine-4-hydroxycoumarin, and like it did with the previous coumarin, gave poor yields, if the reaction made any progress at all.

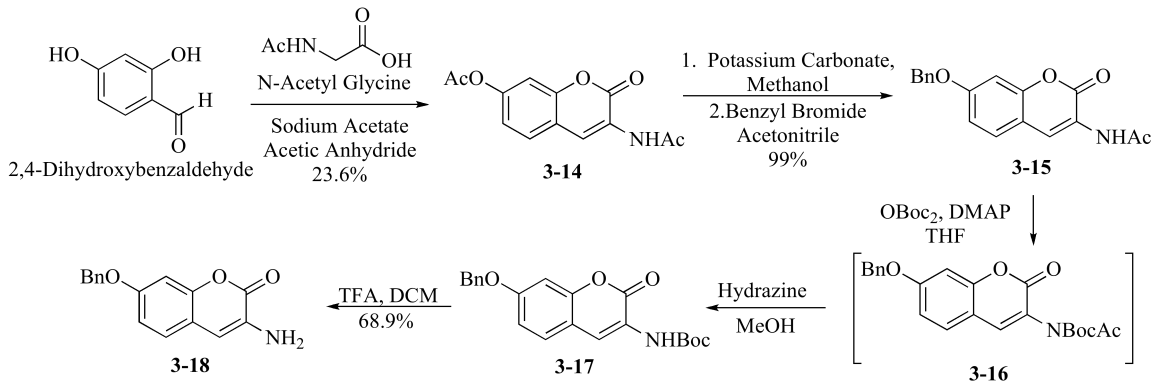

Figure 22. Synthetic scheme of 3-14, 3-15, 3-16, 3-17, and 3-18.

To synthesize the coumarin ring the procedure used by Kudale et al.[46] This procedure dissolved 2,4-dihydroxybenzaldehyde in acetic acid and sodium acetate and N-acetyl glycine were added. This afforded **3-14** as a pale pink solid in 24% yield. The low yield is expected in this reaction. Next, the 7-acetyl protecting group was removed and a benzyl group replaced it in a two-step, one-pot reaction. The acetyl group was cleaved by the addition of potassium carbonate, and the resulting acetate was removed under vacuum with the solvent. Acetonitrile was then used as the solvent for the benzylation. We found if too much potassium carbonate was used, greater than two equivalents, the amine was deprotonated and benzylated. This byproduct could not be carried forward, so the amount of potassium carbonate needed to be below one and a half equivalents. The next series of steps were to generate the free amine from the acetyl-protected amine. The protected amine was secondarily protected with a Boc group. Adding the Boc group to

the amine made the acetate easy to remove using hydrazine. The product from these two steps (compound **3-17**) was not isolated or purified because it was difficult to separate impurities from product through crystallization or flash chromatography. The Boc group was then cleaved using trifluoroacetic acid, giving a yield of 68.9% for the three steps. The resulting 3-amino-7-benzyloxycoumarin was then carried on to coupling and deprotection reactions.

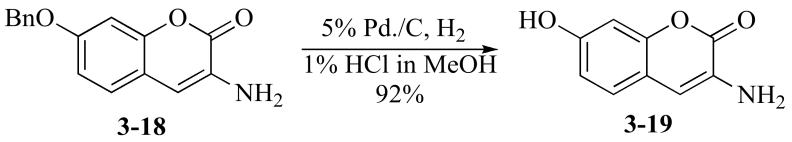

3-18 **3-19**

Figure 23. Deprotection of 3-18 to give 3-19.

We wanted to explore if the coumarin could bind to DNA gyrase without the linker. The benzyl protecting group of **3-18** was removed by hydrogenation in acidic methanol, using palladium on carbon as the catalyst. The hydrogenation reaction gave **3-19** in a 92% yield.

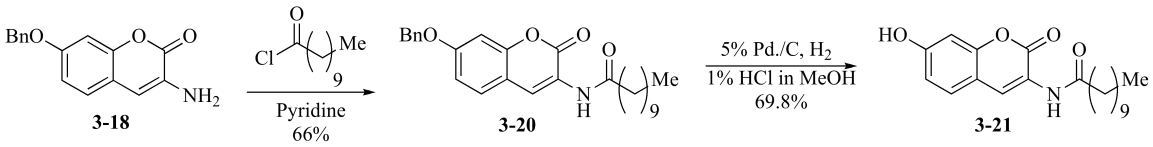

3-18 **3-20** **3-21**

Figure 24. Synthetic scheme of 3-20 and 3-21.

In order to explore the binding of the 3-amino-7-hydroxycoumarin's linker, we coupled decanoyl chloride with **3-18**, to give **3-20** in a 66% yield. The deprotection of the 7-

hydroxyl group was done by hydrogenation carried out in acidic methanol using 5% palladium on carbon as the catalyst. This deprotection step yielded **3-21** in 69.8% yield.

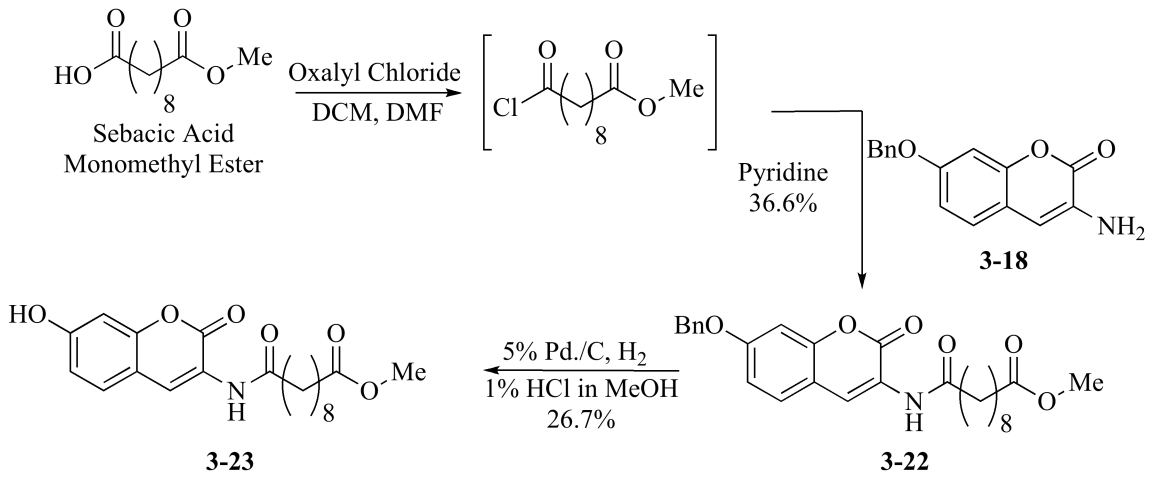

Figure 25. Synthetic scheme of 3-22 and 3-23.

Compound **3-23** was synthesized so we could make a direct comparison with **3-7** to determine the effect of the addition of the 7-hydroxyl to the coumarin ring. To synthesize this compound, sebacic acid monomethyl ester was dissolved in dichloromethane and a catalytic amount of dimethylformamide was added, followed by oxalyl chloride to generate sebacic acid chloride monomethyl ester. The acid chloride was concentrated, but not isolated or characterized before being suspended in more dichloromethane and added dropwise to **3-18** dissolved in pyridine. The coupled product **3-22** was isolated in a 37% yield and was carried through the hydrogenation deprotection to give **3-23** in 27% yield.

3.1.4 Synthesis of 4,7-Dihydroxycoumarin

The last coumarin we explored was the 4,7-dihydroxycoumarin. This coumarin was prepared according to the procedure detailed by Jung et al.[47] We planned to install the amine and couple this coumarin to the linker, but we observed the same issues during the coupling reactions as seen with the 3-amino-4-hydroxycoumarin. This issue was that the carbon in the 4-position of the coumarin acted as a nucleophile and competed with the amine to attack the acid chloride, with the 4-hydroxyl group acting as a leaving group. The final products had linkers at either the amine or the C4 position, or at both positions. When synthesizing coumarin-based deconstruction SD8 analogs proved unsuccessful, we attempted to isolate the 3-amino-4,7-dihydroxycoumarin after the final deprotection steps. Due to the extreme polarity of the coumarin, multiple attempts at isolation were unsuccessful. Ultimately, we decided to synthesize just the 4,7-dihydroxycoumarin and test its ability to bind to DNA gyrase and interrupt the enzyme-DNA binding without the linker or the amine.

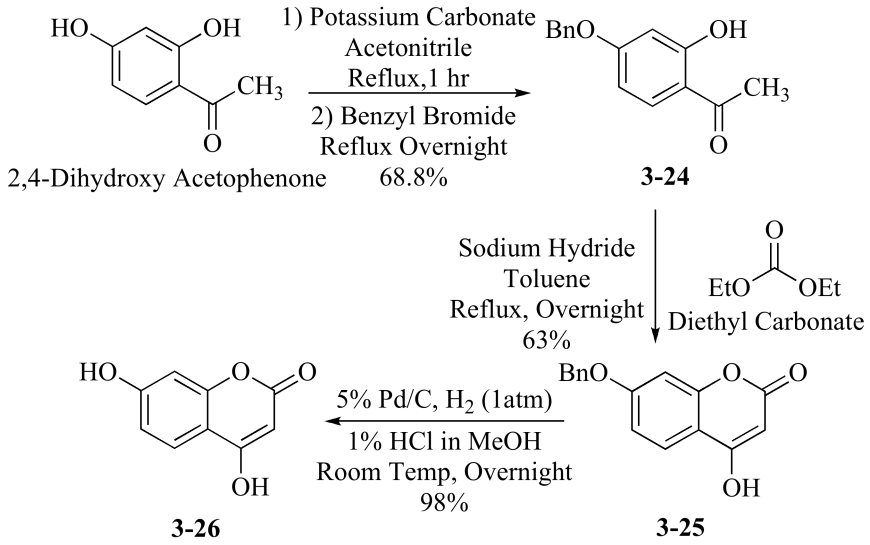

Figure 26. Synthetic scheme of 3-26.

This scheme used 2,4-dihydroxy acetophenone as a starting material. It was first benzyl protected in the 4-position using potassium carbonate and benzyl bromide in acetonitrile. Benzyl protection was selective in 69% yield. Next, the coumarin ring was formed using diethyl carbonate as the carbon source and sodium hydride as the base in 63% yield. Hydrogenation of the benzyl group was carried out in acidic methanol using palladium on carbon as the catalyst. This deprotection step was successful in 98% yield.

3.2 Evaluation of the activity of the compounds against DNA gyrase

The evaluation of the synthesized SD8 analogs' ability to disrupt the DNA-DNA gyrase binding interaction allowed us to determine the SD8 coumarin pharamacophore. The

analogs ability to disrupt the DNA-DNA gyrase binding interaction was evaluated by both surface plasmon resonance (SPR) and by enzyme inhibition studies.

3.2.1 SPR Experiments

SPR studies were used to determine if the compounds were acting by the same mechanism as SD8, by disrupting the binding of DNA-to-DNA gyrase. The experiments were conducted on a BioCore T200 instrument. We immobilized 5'-biotinylated DNA on a streptavidin-functionalized chip. Compounds were tested by first mixing the compound with DNA gyrase. The solution contained 100 nM enzyme and 100 μM compound. The mixture was flowed over the chip and the signal was recorded. If the compound mixed with DNA gyrase did not bind to the enzyme and block the binding of DNA, there was binding between DNA gyrase and the immobilized DNA. When there was binding between DNA gyrase and the immobilized DNA, the response signal increased to between 100 and 150 response units (RU). If the compound mixed with the enzyme bound and blocked its binding to DNA, there was decreased DNA gyrase binding to the DNA immobilized on the chip. When this occurred, there was no change in signal. The purpose of conducting the SPR experiments in this manner was twofold. First, these experiments tested the activity of the compounds, but more importantly, these experiments tested the mechanism of action of the compounds. By pre-incubating the compound with the enzyme, we made sure the mechanism of action of the coumarin compound was due to binding with the enzyme, not from intercalating the DNA. The data gathered from the SPR experiments are presented in Table 1.

Table 1. Compound inhibition of DNA-DNA gyrase binding interaction by SPR

Compound	Inhibition Activity on DNA gyrase by SPR
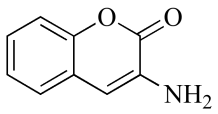 3-1	No activity
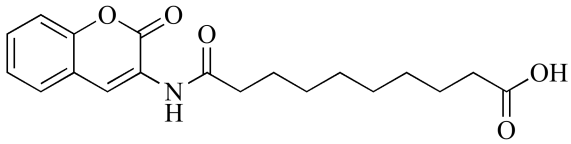 3-2	Inhibited DNA gyrase binding to DNA
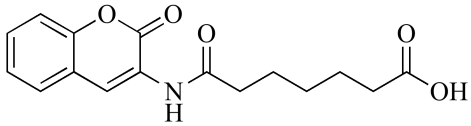 3-3	No activity
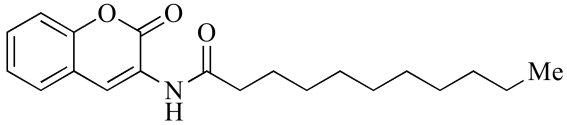 3-4	No activity
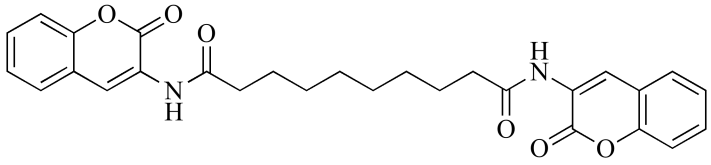 3-5	Increased DNA-DNA gyrase binding interaction
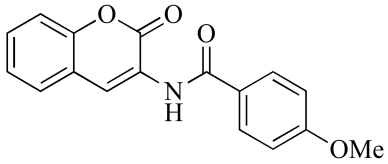 3-6	No activity
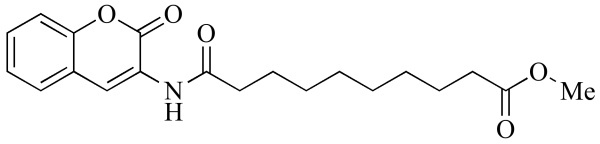 3-7	Partial inhibition of DNA gyrase binding to DNA
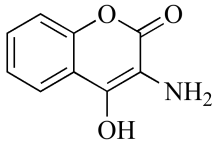 3-8	No activity

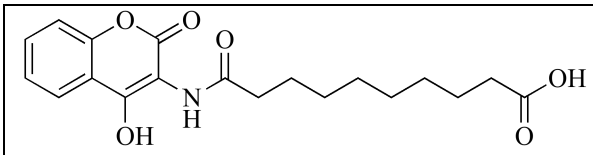 3-9	Inhibited DNA gyrase binding to DNA
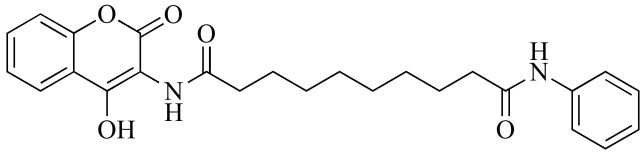 3-11	No activity
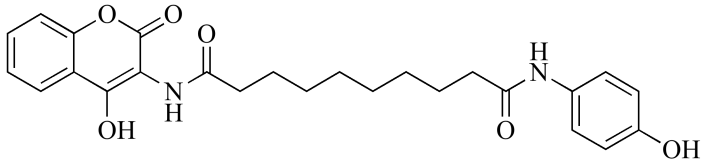 3-12	No activity
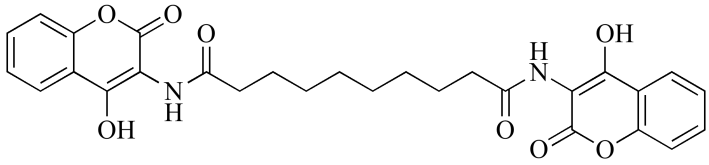 3-13	Increased DNA-DNA gyrase binding interaction
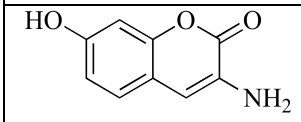 3-19	No activity
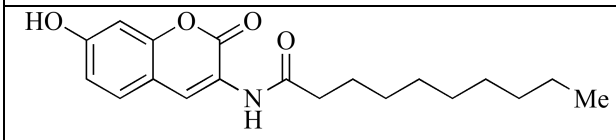 3-21	No activity
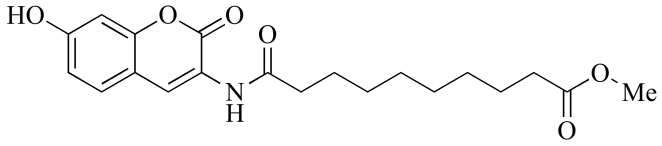 3-23	Inhibited DNA gyrase binding to DNA
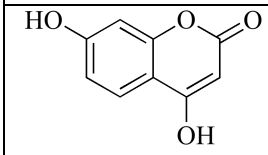 3-26	No activity

Compounds that inhibited the DNA-DNA gyrase binding interaction were **3-2**, **3-7** (partial), **3-9**, and **3-23** (partial). Our results allowed us to make conclusions about the coumarin pharmacophore required for binding to DNA gyrase:

- The compounds' linkers do not need to be conjugated and fully saturated aliphatic chains are tolerated.
- Linkers shorter than 15 Å are not tolerated.
- Substitutions on the coumarin ring are not required for binding, but are tolerated.
- A carboxylic acid group at the end of the linker is required for full inhibition of the DNA-DNA gyrase binding interaction.
- Phenyl or benzyl groups are not tolerated at the end of the linker.
- Benzoyl groups at the coumarin's 3-amine group are not tolerated.

The results show a clear trend that allowed us to define the coumarin-based pharmacophore of SD8's inhibition of the DNA Gyrase-DNA binding interaction (Figure 27). The coumarin-based pharmacophore of SD8 can be defined as a required coumarin ring connected with a carboxylic acid group through an approximately 15 Å, fully substituted linker bonded to the coumarin with an amide bond.

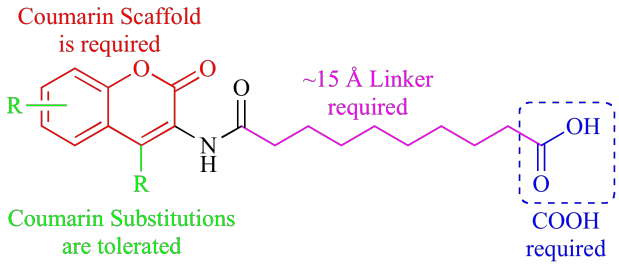

Figure 27. Simocyclinone D8 coumarin pharmacophore as determined by SPR

From this data, rough structure-activity relationships have been elucidated. Compounds **3-1**, **3-8**, and **3-19** have shown that more than just a substituted 3-aminocoumarin ring is necessary for binding. This is not surprising since the coumarins used have few functional groups that can be used to bind to the enzyme. The linker does not need to be rigid or conjugated, as shown by the four compounds that had inhibitory effects. A saturated linker shorter than eight carbons is not tolerated, as shown by **3-3**'s in ability to inhibit the DNA-DNA gyrase binding interaction. The linker also must have a functional group that has the ability to accept a hydrogen bond (**3-4** and **3-21**), but the hydrogen bond donating and accepting carboxylic acid group seems to block the DNA binding interaction better than the methyl ester group. This was illustrated by the partial inhibition of the binding interaction by **3-7** when compared to the total inhibition of DNA-DNA gyrase binding interaction displayed by **3-2**, the analogous compound with the carboxylic acid. Benzyl groups are not tolerated at the end of the linker, as shown by **3-11** and **3-12**. Despite **3-12** having a phenol group at the end of the linker that could accept and donate a hydrogen bond, there was no inhibition of the binding interaction between DNA and DNA gyrase.

Interestingly, the coumarin-linker-coumarin compounds (**3-5** and **3-13**) increased the binding of DNA-to-DNA gyrase. The sensorgrams for **3-5** and **3-13** show that once the mixture of DNA gyrase incubated with compound were flowed into the flow cell, the response signal increased to over 200 RU. The average signal for compounds that did not block DNA from binding to DNA gyrase was between 100 and 150 RU. These compounds were designed to block the DNA-DNA gyrase binding interaction by binding

to both coumarin sites of the DNA gyrase holoenzyme, and bridging the GyrA subunits. How these compounds are increasing the binding interaction is not fully explained by the SPR method.

3.2.2 DNA Gyrase Functional Assay Experiments

Supercoiling assays were conducted by Dr. Hiroshi Hiasa's group at the University of Minnesota. This assay was used to explore if the compounds we synthesized were able to inhibit *E. coli's* DNA gyrase's supercoiling activity. The supercoiling assay specifically examined DNA's ability to supercoil relaxed DNA after being treated with a compound, by electrophoresis through an agarose gel. Relaxed DNA did not travel as far through the gel as supercoiled DNA. Dr. Hiasa's group found that none of the compounds we synthesized were able to inhibit DNA gyrase's supercoiling activity at a concentration of 100 μM. While the compounds were able to bind to the enzyme, the binding is not enough to stop DNA gyrase's catalytic cycle.

CHAPTER 4: ATTEMPTS AT SYNTHESIZING 3-AMINO-8-CHLORO-4,7-DIHYDROXYCOUMARIN

Once the coumarin pharamacophore was defined for SD8's inhibition of the DNA-DNA gyrase binding as containing the coumarin scaffold, an eight-carbon linker, and a terminal carboxylic acid, we decided to further explore the SAR of SD8's chlorocoumarin. The focus of this exploration was to determine the role of chlorine at the 8-position of the coumarin moiety. In order to be able to examine the SAR of that group, we needed to first develop a method in which to synthesis the 3-amino-8-chloro-4,7-dihydroxycoumarin, which has not been prepared previously by organic synthesis. Four approaches were taken to synthesize the 3-amino-8-chloro-4,7-dihydroxycoumarin: direct chlorination of the coumarin ring and coumarin formation from resorcinol, from benzaldehyde, and from acetophenone.

4.1 Direct Chlorination

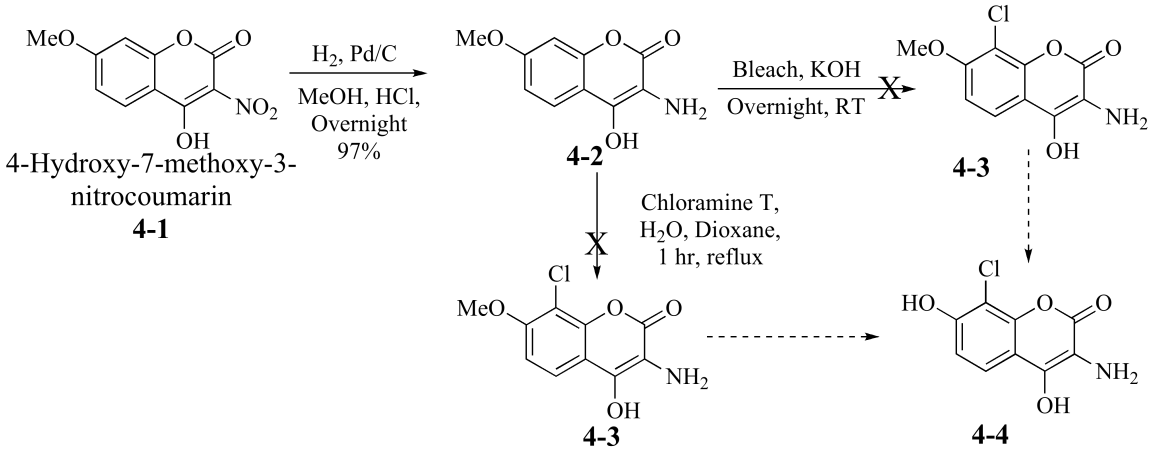

Figure 28. Synthetic scheme of the direct chlorination route.

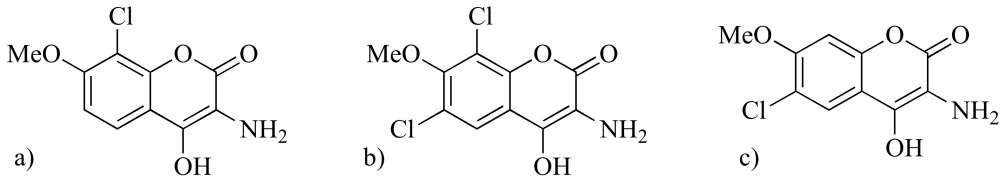

Figure 29. Synthetic products of the Chloramine T reaction. a) 3-amino-8-chloro-4-hydroxy-7-methoxycoumarin, the expected product. b) 3-amino-6,8-dichloro-4-hydroxy-7-methoxycoumarin, the observed over-chlorination product. c) 3-amino-6-chloro-4-hydroxy-7-methoxycoumarin, a by-product.

The direct chlorination route (Figure 28) was the most attractive of the possible routes because it had the least number of steps and started with commercially available 4-hydroxy-7-methoxy-3-nitrocoumarin. The first step was to reduce the nitro to an amine, using hydrogen gas and palladium on carbon as a catalyst.[48] This reduction yielded 97% after overnight reaction and required no further purification. The second step was to install the chlorine at the eight position of the coumarin ring. Two methods of direct chlorination were attempted. The first method was done in an alkaline aqueous solution and used bleach as the chlorinating agent.[49] Chlorination was not observed using these reaction conditions, and there was poor recovery of the starting material. A second method was attempted using Chloramine T as the chlorinating agent and a mixture of water and dioxane as the solvent.[50] This method proved to chlorinate the coumarin with poor regioselectivity, with the six-chlorocoumarin being one of the products. Over-chlorination was seen as well, producing the 3-amino-6,8-di-chloro-4-hydroxy-7-methoxycoumarin (Figure 29). Separation of the 3-amino-8-chloro-4-hydroxy-7-

methoxycoumarin from the byproducts of the reaction was not possible through crystallization or silica gel flash chromatography. The inability to adequately purify the desired product resulted in other synthetic routes being attempted.

4.2 Coumarin Formation from Resorcinol

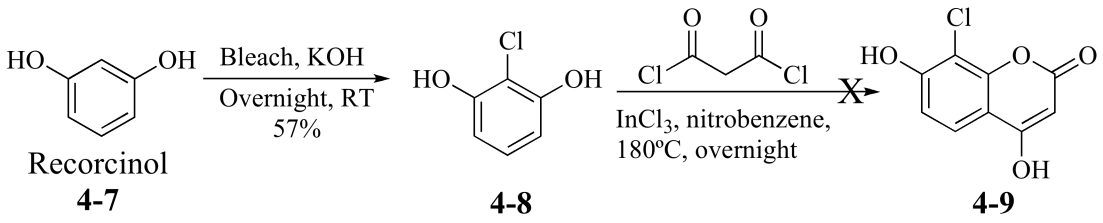

Recorcinol
4-7

4-8

4-9

Figure 30. Synthetic scheme for the resorcinol starting material.

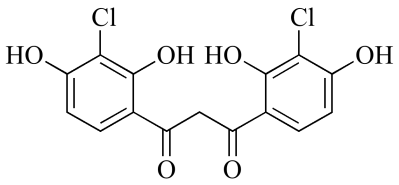

4-10

Figure 31. Observed product from von Peckman reaction.

The second route that attempted to produce 8-chloro-4,7-dihydroxycoumarin, an intermediate in the route to the 3-amino-3-chloro-4,7-dihydroxycoumarin, was the coumarin formation from resorcinol using a von Peckman reaction (Figure 30). Chlorination of resorcinol was the first step in the synthetic scheme. The conditions used cold bleach as the chlorinating agent in an alkaline, aqueous solution,[49] and afforded 57% as an off-white solid, after silica gel flash chromatography. The subsequent step was to

close the coumarin ring in a Von Peckman reaction, using malonyl diacid chloride.[51,52] The first step of the reaction is analogous to a Fridel-Crafts acylation, where the ring acts a nucelophile and attacks one of the acid chloride groups. The closing of the lactone ring then occurs when the phenol group ortho to the actyl group then attacks the other acid chloride group. Unfortunately, this second step did not occur before the Fridel-Crafts reaction occurred again at the second acid chloride yielding the product seen in Figure 31.

4.3: Coumarin Formation from 2,4-Dihydroxybenzaldehyde

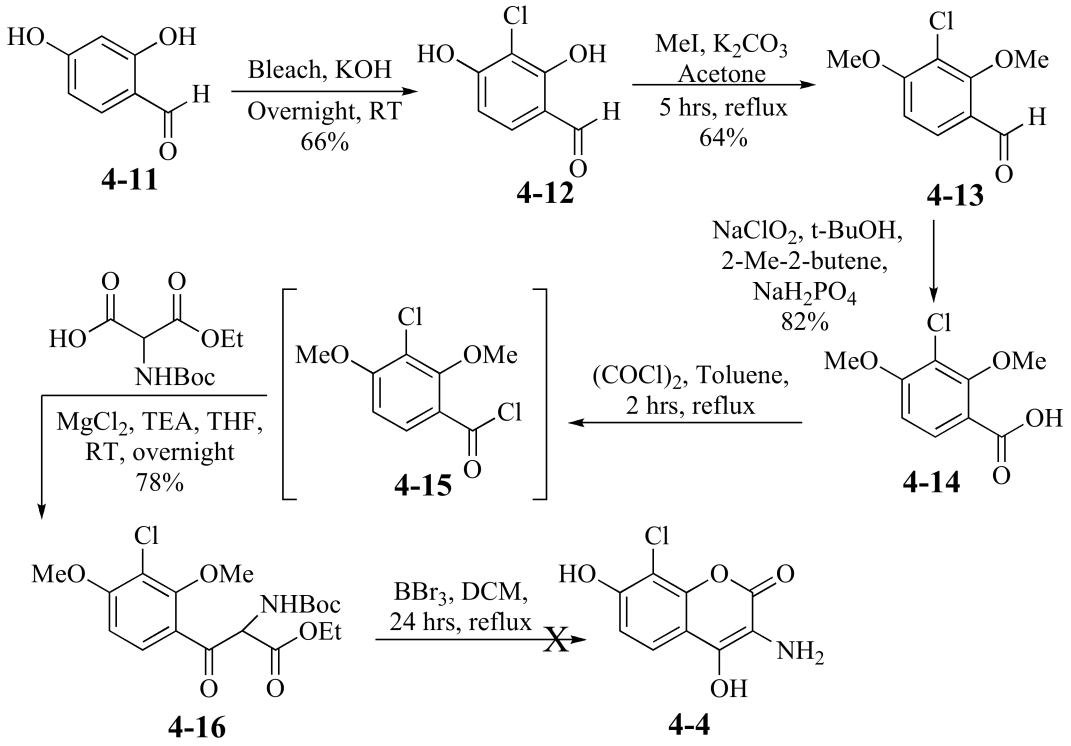

Figure 32. Synthetic route to produce the 8-chloro-4,7-dihydroxycoumarin 3-4 starting with 2,4-dihydroxybenzaldehyde 3-11.

A third synthetic route to obtain the 8-chloro-4,7-dihydroxycoumarin used 2,4-dihydroxybenzaldehyde as the starting material, as seen in Figure 32. The first step is the chlorination using bleach.[49] Chlorination was successful with a yield of 66% of clean product after silica gel flash chromatography purification. Next, the phenol groups were protected with methyl groups, using potassium carbonate as a base and methyl iodide as the methyl group donor. This step proceeded with a yield of just 54%, as there were issues separating the mono-protected benzaldehyde from the di-protected benzaldehyde. Oxidation of the aldehyde group to an acid was done through a Pinnick Oxidation.[52] Product was isolated with an 82% yield. Coupling of the malonic acid occurred through an acid chloride reaction, where the benzoic acid was converted to an acid chloride, and then mixed with a mono-ethyl-protected malonic acid.[53] This coupling reaction had a yield of 78%. The final step in the synthetic route was the closing of the lactone ring of the coumarin, and removing the methyl and BOC protecting groups in one step. This reaction was done using boron tribromide and refluxing for 24 hours.[54] Unfortunately, this reaction did not occur, and no product or starting material could be recovered.

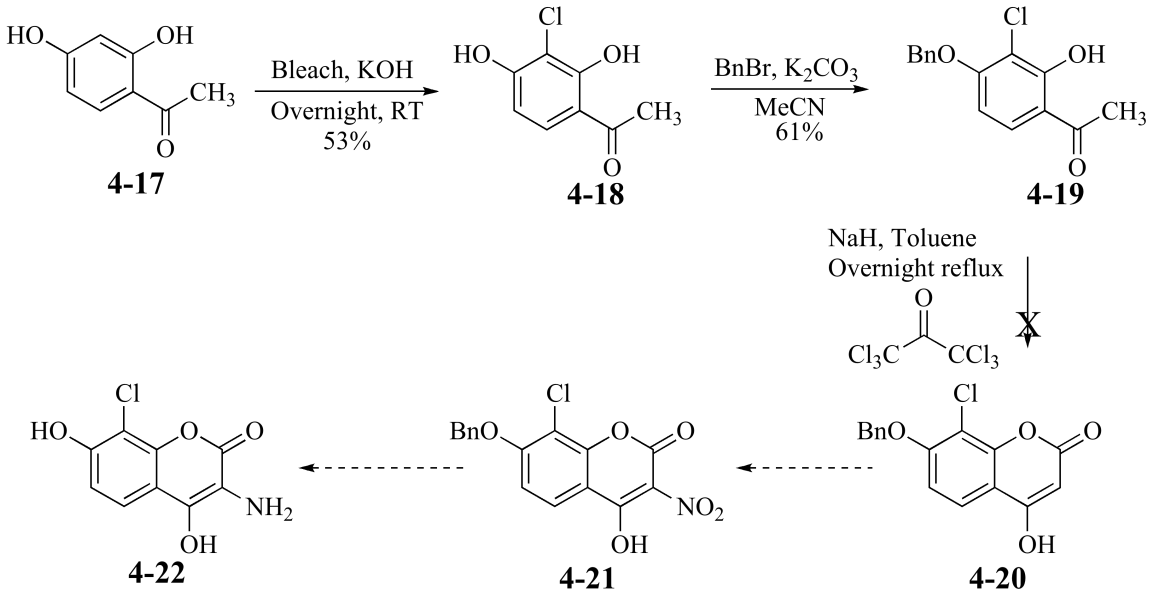

Figure 33. Synthetic scheme to make the 8-chloro-4,7-dihydroxycoumarin starting with 2,4-dihydroxyacetophenone.

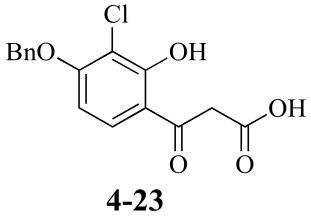

Figure 34. Final product seen from the lactone ring-closing step.

The last attempted synthetic route to synthesize the 8-chloro-4,7-dihydroxycoumarin used 2,4-dihyroxyacetophenone as the starting material Figure 33. Like with the previous two routes, the first step was chlorination.[49] The chlorination of the acetophenone's 3-position was done with bleach and occurred with a 53% yield. Next, a mono-benzyl protection was conducted on the 4-position phenol, using potassium carbonate and benzyl

bromide.[55] The protection was successful with a 61% yield. Closing the lactone ring of the coumarin was attempted using diethylcarbonate as the carbonate source and sodium hydride as the base. When that reaction failed, carbodiimide, a more electron deficient carbonate source, was used,[56] and also failed. Eventually triphosgene was used as the carbonate source. Triphosgene is a safer alternative to carbonyl dichloride, better known as phosgene, a poison gas that has been used as a chemical warfare agent. Despite using an extremely reactive form of carbonyl, this ring-closing step was still unsuccessful. The product recovered was the ß-ketoacid, the intermediate of this two-step reaction (Figure 34). Further attempts to close the ß-ketoacid also failed.

4.4 Discussion

Before attempting these synthetic schemes, it was known that any substituents on the coumarin ring highly affected its electronics due to its extended π-electron system. Once these schemes were attempted and failed repeatedly, we reasoned the lactone ring refused to close due to the electron withdrawing effects of the acetophenone's 3-chlorine substituent. Having the chlorine in the ortho-position pulled electron density out of the 2-phenol, greatly reducing its nucleophilic capabilities. The same electronic effects were seen in the reactions with recorcinol. This reduction in nucleophilicity renders the phenol too weak of a nucleophile to attack a very electron deficient carbon, such as that in triphosgene. We also hypothesized that if we substituted the 2,4-dihydroxy acetophenone with iodine at the 3-position, we would have a greater chance of closing the ring. Iodine is a softer halogen and does not have the extreme electrophilicity or electronegativity of

chlorine. Having iodine in the 3-position may have improved coumarin binding with DNA gyrase since iodine is known to be a better partner in halogen bonding than chlorine. Attempts to iodate the 3-position failed so this theory could not be tested.

4.5 Future Direction

Future work on this project would include:

- Determining additional coumarin structure – activity relationships.
- Exploring the necessity of the amide bond between the coumarin and the linker moieties.
- Exploring different linker structures and geometries.
- Synthesizing compounds with D-olivose sugar at the end of the linker to determine its role in binding and structure - activity relationships.

4.6 Summary

In summary, we've designed and synthesized 12 previously unreported compounds that are SD8 mimetics. Using these and four other compounds, we were able to establish a basic pharmacophore for the coumarin-linker portion of Simocyclinone D8 (SD8) through a surface plasmon resonance (SPR) assay. Bioassay data performed by Dr. Hiasa's group at the University of Minnesota showed none of our compounds inhibited DNA gyrase's ability to induce DNA supercoiling at 100 μM. We also identified at least four pathways that will not lead to the native SD8 coumarin, 3-amino-8-chloro-4,7-dihydroxycoumarin.

Experimental Procedures

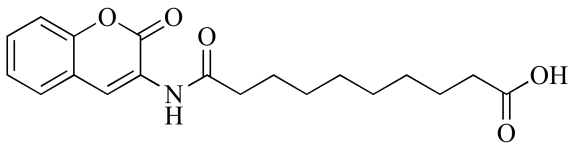

Compound 3-2

Commercially available sebacid diacid chloride (3.4 mmol , 0.915 mL) was dissolved in 15 mL of pyridine. Commercially available 3-aminocoumarin (3.1 mmol, 0.5 g) in 16 mL of pyridine was added dropwise to the acid chloride solution. The reaction was refluxed overnight and then quenched by the addition of water (30 mL) and 6 M hydrochloric acid (3 mL). The product was extracted into an equal volume of ethyl acetate. The organic layer was then separated, washed with 10% copper sulfate solution, and water until the water washes were no longer blue. The organic layer was washed with brine, dried over sodium sulfate, and then concentrated under vacuum. Recovered product was pure by TLC (R_f=0, 30% ethyl acetate in hexanes). This reaction gave a 65% yield as a white solid: mp 153°C dec. IR ν (neat)/cm^{-1} 3329.24, 3076.09, 2923.23, 2853.35; ^{1}H NMR (400 MHz, $CDCl_3$): ∂ =1.24-1.37 (m, 12H), 1.63-1.74 (m, 2H), 2.43 (t, 2H, J=7.6, 7.6), 7.23-7.41 (m, 2H), 7.42-7.46 (m, 1H), 7.50 (dd, 1H, J=1.2, 7.6), 8.05 (s, 1H), 8.70 (s, 1H); ^{13}C NMR (400 MHz, $CDCl_3$): ∂ =25.25, 29.04, 29.70, 37.69, 116.34, 119.93, 123.20, 125.17, 127.78, 129.57, 149.88; HRMS $C_{19}H_{23}NO_5$ Expected: 345.1576, Found: 344.1500.

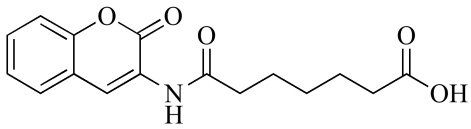

Compound 3-3

Pimelic acid (0.0994g, 0.62 mmol) was dissolved in 0.62 mL dichloromethane. One drop of dimethylformamide was added to the solution before oxalyl chloride (0.337 mL, 3.1 mmol) was added dropwise. The reaction was stirred for one hour at room temperature before the solvent and excess oxalyl chloride was removed by vacuum. The diacid chloride was then redissolved in the necessary amount of dichloromethane. This solution was added dropwise to a mixture of 3-aminocoumarin (0.1 g, 0.62 mmol) and triethyl amine (0.26 mL, 1.9 mmol) dissolved in tetrahydrofuran (2.5 mL, 30.6 mmol). This reaction was refluxed overnight before being quenched by the addition of water (2 mL) and 6M hydrochloric acid (0.5 mL). The product was extracted into dichlormethane, dried over sodium sulfate, and concentrated under vacuum. Purification by MPLC (CombiFlash, 0-100% ethyl acetate in hexanes) gave a white solid: mp 187-190° C, in a 26% yield. IR ν (neat)/cm^{-1} 2470.40, 2861.20, 2925.09 (b), 3324.39; ^{1}H NMR (400 MHz, $CDCl_3$): ∂ =1.48-1.54 (m, 6H), 1.81 (m, 2H), 2.47 (t, 2H, J=7.2, 7.6), 7.28-7.33 (m, 2H), 7.42-7.51 (m, 2H), 8.06 (s, 1H), 8.70 (s, 1H); ^{13}C NMR (400 MHz, $CDCl_3$): ∂ =24.82, 28.58, 37.32, 116.34, 119.89, 123.29, 123.94, 125.17, 127.80, 129.61, 149.89, 158.82, 172.16; HRMS $C_{19}H_{17}NO_5$ Expected: 303.1107, Found: 302.1037.

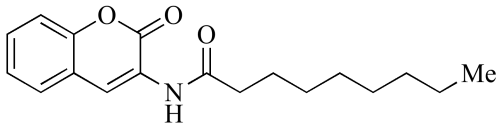

Compound 3-4

Commercially available decanoyl chloride (0.12 mL, 0.68 mmol) was dissolved in pyridine (3.1 mL). To this solution, 3-aminocoumarin (0.110 g, 0.68 mmol) dissolved in pyridine (3.1 mL) was added dropwise. The reaction was refluxed overnight before being quenched by the addition of water (5 mL) and 6 M hydrochloric acid (0.5 mL). The product was extracted into dichloromethane. The organic layer was then washed with 10% copper sulfate solution, followed by water washes until the water was no longer blue-tinted. The organic layer was dried over sodium sulfate and concentrated under vacuum. Purification by MPLC (CombiFlash, 0-100% ethyl acetate in hexanes gradient) gave 0.1158 g product (51.5% yield) as an off white solid: mp 106-107°C. IR ν (neat)/cm^{-1} 2850.48, 2920.80, 3078.91, 3336.64; ^{1}H NMR (400 MHz, $CDCl_3$) ∂ =0.88 (t, 3H, J=6.8, 6.8), 1.27-1.38 (m,14H), 1.73 (m, 2H), 2.43 (t, 2H, J=7.6, 7.6), 7.28-7.33 (m, 2H), 7.44 (m, 1H), 7.5 (dd, 1H, J=1.2, 7.6), 8.04 (s, 1H), 8.70 (s, 1H); ^{13}C NMR (400 MHz, $CDCl_3$) ∂ =14.08, 22.65, 25.36, 29.17, 29.24, 29.32, 29.40, 31.84, 37.80, 116.35, 123.16, 125.17, 127.77, 129.56; HRMS $C_{19}H_{25}NO_3$ Expected: 315.1834, Found: 314.1760.

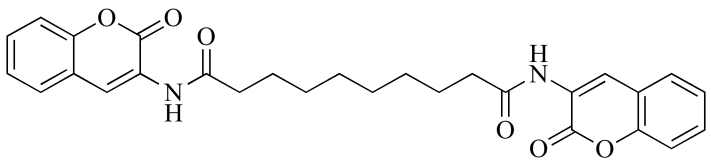

Compound 3-5

3-Aminocoumarin (0.1 g, 0.62 mmol) was dissolved in pyridine (3.1 mL) and heated to reflux. Sebacic acid chloride (0.083 mL, 0.31 mmol) was added dropwise to the solution. The reaction was allowed to reflux overnight before being quenched by the addition of water (3 mL) and a few drops of 6M hydrochloric acid. Dichloromethane was added to extract the product from the aqueous layer. The organic layer was washed with 10% copper sulfate, followed by water washes until the wash was no longer blue. The organic was dried over sodium sulfate and concentrated under vacuum. Purification by MPLC (CombiFlash, 0-100% ethyl acetate in hexanes gradient) gave 31.8 mg (21% yield) of a white solid: mp 213-217°C. R_f=0.05 in 20% ethyl acetate in hexanes. IR ν (neat)/cm^{-1} 2853.28, 2926.80, 3076.77, 3329.31; ^{1}H NMR (400 MHz, $CDCl_3$) ∂ 1.35-1.40 (m, 12H), 1.68-1.75 (m, 4H), 2.43 (t, 4H, J=7.6, 7.2), 7.23-7.33 (m, 4H), 7.42-7.46 (m, 2H), 7.50 (dd, 2H, J=1.2, 7.6), 8.05 (s, 2H), 8.70 (s, 2H); ^{13}C NMR (400 MHz, $CDCl_3$) ∂ =25.24, 29.02, 29.05, 37.68, 116.32, 119.94, 123.16, 124.01, 125.14, 127.75, 129.54, 149.90, 158.83, 172.46; HRMS $C_{28}H_{28}N_2O_6$ Expected: 488.1947, Found: 487.1875.

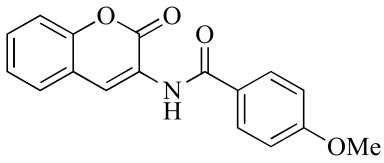

Compound 3-6

3-Aminocoumarin (0.1 g, 0.62 mmol) was dissolved in tetrahydrofuran (2.5 mL). To the solution, triethyl amine (0.26 mL, 1.86 mmol) was added, and the mixture was brought to reflux. Neat p-methoxy benzoyl chloride (0.11 g, 0.62 mmol) was added dropwise, and the reaction was allowed to reflux overnight. The reaction was quenched by the addition of water and a few drops of 6 M hydrochloric acid. Product was extracted into dichloromethane. The organic layer was separated, dried over sodium sulfate, and concentrated under vacuum, giving an off white solid: mp 112-115°C, in a 45% yield. R_f=0.9 in 10% methanol in dichloromethane. IR ν (neat)/cm^{-1} 2832.68, 2932.04, 3007.39, 3361.60; ^{1}H NMR (400 MHz, $CDCl_3$) ∂ =3.82 (s, 3H), 4.31 (s, 1H), 6.33 (s, 1H), 6.90 (d, 2H, J=8.8), 7.17-7.23 (m, 2H), 7.26-7.31 (m, 4H); ^{13}C NMR (400 MHz, $CDCl_3$) ∂ =46.98, 55.32, 105.52, 114.25, 116.06, 121.65, 124.59, 125.10, 125.78. 126.92, 128.68, 129.20, 132.86, 147.99, 159.21, 159.58.

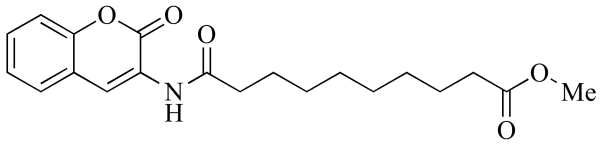

Compound 3-7

Commercially available sebacic acid methyl ester (0.134 g, 0.631 mmol) was dissolved in dichloromethane (0.621 mL). To this solution, one drop of dimethylformamide was

added before oxalyl chloride was added dropwise (0.337 mL, 3.1 mmol). The reaction was allowed to stir one hour at room temperature before the solvent and excess oxalyl chloride was removed by vacuum. The acid chloride was then dissolved in the necessary amount of dichloromethane before being added dropwise to a solution of 3-aminocoumarin (0.1 g, 0.62 mmol) and triethylamine (0.26 mL, 1.8 mmol) in tetrahydrofuran (3.1 mL). This reaction was refluxed overnight before being quenched by the addition of water (3 mL) and a few drops of 6 M hydrochloric acid. The product was extracted into dichloromethane. The organic layer was washed with brine, then dried over sodium sulfate and concentrated under vacuum. Flash silica gel chromatography (20-50% gradient ethyl acetate in hexanes) gave 53.5 mg (24.9% yield) of a white solid: mp 116-117°C. R_f=0.62 1:1 ethyl acetate to hexanes. IR ν (neat)/cm^{-1} 2848.80, 2910.89, 2924.93, 3353.04; ^{1}H NMR (400 MHz, $CDCl_3$) ∂ =1.26-1.40 (m, 8H), 1.62 (m, 2H), 1.73 (m, 2H), 2.30 (t, 2H, J=7.2, 8.0), 2.43 (t, 2H, J=7.2, 7.6), 3.67 (s, 3H), 7.30 (m, 2H), 7.42-7.46 (m, 1H), 7.50 (dd, 1H, J=1.2, 7.6), 8.03 (s, 1H), 8.70 (s, 1H); ^{13}C NMR (400 MHz, $CDCl_3$) ∂ =24.88, 25.27, 29.03, 29.06, 29.08, 34.05, 37.72, 51.37, 116.33, 123.13, 124.01, 125.14, 127.75, 129.54, 172.47, 174.19; HRMS $C_{20}H_{25}NO_5$ Expected: 359.1733, Found: 358.1664.

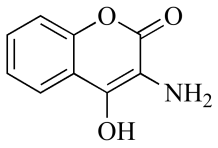

Compound 3-8

4-Hydroxy-3-nitrocoumarin (1 g, 4.8 mmol) was dissolved in 75 mL 1% HCl in methanol. This solution was cooled on ice and purged with nitrogen prior to the addition of 5% palladium on carbon (0.16 g). The reaction vessel was sealed, placed in a Parr shaker hydrogenator, and pressurized with hydrogen to 60 psi. The reaction was monitored by TLC (R_f= 0, 10% methanol in dichloromethane) until it was complete, about 24 hours. The catalyst was filtered off and washed with methanol. The filtrate was concentrated under vacuum to give a light yellow solid: mp 192°C, in a 92% yield. IR ν (neat)/cm^{-1} 2602.02 (w), 2855.92, 2926.51, 3076.80, 3327.77; ^{1}H NMR (400 MHz, DMSO) ∂ 7.32 (dd, 2H, J=7.2, 7.6), 7.56 (ddd, 1H, J=1.2, 7.4, 8.0), 7.96 (d, 1H, J=8.0); ^{13}C NMR (400 MHz, DMSO) ∂ 117.47, 122.46, 125.52, 131.42, 133.32, 135.17, 153.24, 159.54, 180.64; HRMS $C_9H_7NO_2$ Expected: 177.0426, Found: 176.0353.

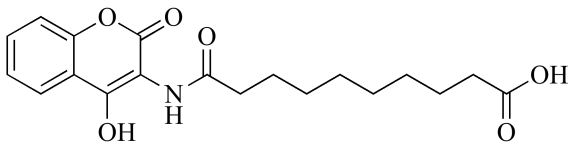

Compound 3-9

4-7 (0.20 g, 0.97 mmol) was dissolved in 10 mL pyridine and heated to reflux. Sebacic diacid chloride (0.26 mL, 0.97 mmol) was added dropwise, and the reaction was allowed to reflux overnight. The reaction was quenched by the addition of water and 1 mL 6 M hydrochloric acid. Product was extracted into dichloromethane and washed with 10% copper sulfate solution. The organic layer was then washed repeatedly with water until

they no longer were blue tinted, next was dried over sodium sulfate and concentrated under vacuum. No purification was necessary. This reaction gave a yield of 85.6% of an off-white solid: mp 85.5-87°C. TLC of product showed smearing from the baseline in 50% acetone in hexanes. IR ν (neat)/cm^{-1} 2850.75, 2918.20 (b); ^{1}H NMR (400 MHz, DMSO) ∂ 1.00-1.49 (m, 12H), 1.81 (m, 2H), 2.99 (t, 2H, J=7.2, 7.6), 7.49 (t, 1H, J= 7.2), 7.62 (d, 1H, J=8.4), 6.67-7.71 (m, 1H), 7.94 (d, 1H, J=1.6), 11.95 (s, 1H); ^{13}C NMR (400 MHz, DMSO) ∂ 26.57, 28.27, 28.81, 28.87, 111.67, 117.64, 121.31, 124.75, 131.39, 152.88, 156.08; HRMS $C_{19}H_{23}NO_6$ Expected: 361.1525, Found: 377.1810 (compound + 1 molecule of water).

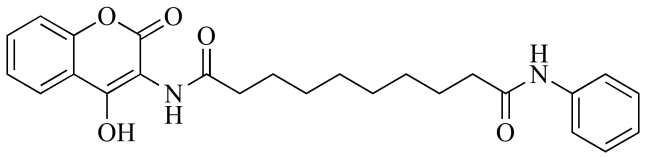

Compound 3-11

4-8 (0.05 g, 0.138 mmol) was dissolved in 0.13 mL dichlormethane. To this solution, a drop of dimethylformamide was added, followed by oxalyl chloride (0.075 mL, 0.69 mmol). The reaction was allowed to stir an hour before the solvent was removed under vacuum. The acid chloride was dissolved in the necessary amount of dichloromethane, and added dropwise to a refluxing solution of aniline (0.014 mL, 0.152 mmol) and triethyl amine (0.058 mL, 0.415 mmol) dissolved in 1 mL tetrahydrofuran. The coupling reaction was allowed to reflux overnight before being quenched by the addition of 1 mL water and few drops 6 M hydrochloric acid. Flash silica gel chromatography (20-100% ethyl acetate in hexanes) gave an off-white solid: mp 123.7-124.8°C, in an 80% yield. IR

ν (neat)/cm^{-1} 2850.11, 2916.59, 3060.42 (w), 3322.75; ^{1}H NMR (400 MHz, DMSO) ∂ 1.25-1.4 (m, 8H), 1.58 (m, 2H), 1.81 (m, 2H), 2.28 (t, 2H, J=7.2), 2.98 (t, 2H, J=7.2), 7.0 (dd, 1H, J=72, 7.6), 7.26 (dd, 2H, J=7.6, 8.4), 7.48 (ddd, 1H, J=0.8, 7.2, 8.0), 7.58 (dd, 3H, J=7.2, 7.6), 7.68 (ddd, 1H, J=1.6, 7.2, 1.2, 7.6), 7.92 (dd, 1H, J=1.6, 8.0), 9.82 (s, 1H); ^{13}C NMR (400 MHz, DMSO) ∂ 25.04, 25.96, 27.42, 28.25, 28.45, 28.54, 36.35, 111.14, 117.16, 121.46, 122.85, 124.00, 125.09, 128.57, 131.71, 139.31, 152.22, 155.02, 155.40, 166.86, 171.20; HRMS $C_{25}H_{28}N_2O_5$ Expected: 436.1998, Found: 435.1924.

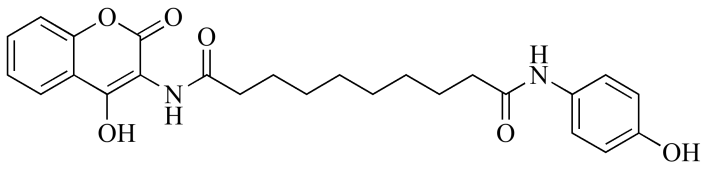

Compound 3-12

4-8 (0.05 g, 0.138 mmol) was dissolved in 0.15 mL dichlormethane. To this solution, a drop of dimethylformamide was added, followed by oxalyl chloride (0.075 mL, 0.69 mmol). The reaction was allowed to stir an hour before the solvent was removed under vacuum. The acid chloride was dissolved in the necessary amount of dichloromethane, and added dropwise to a refluxing solution of 4-aminophenol (0.017 g, 0.15 mmol) and triethyl amine (0.054 mL, 0.39 mmol) dissolved in 0.6 mL tetrahydrofuran. The coupling reaction was allowed to reflux overnight before being quenched by the addition of 1 mL water and few drops 6 M hydrochloric acid. Flash silica gel chromatography (0-10% methanol in dichloromethane) gave an off-white solid: mp 181-184.7°C, in a 39% yield. IR ν (neat)/cm^{-1} 2850.15, 2918.39, 3295.60 (w), 3447.65 (w); ^{1}H NMR (400 MHz, DMSO) ∂ 1.32 (m, 9H), 1.56 (m, 1H), 1.81 (m, 2H), 2.22 (t, 2H, J=7.6), 2.99 (t, 2H,

J=7.6), 6.65 (d, 2H, J=8.8), 7.34 (d, 2H, J=8.8), 7.49 (dd, 1H, J=8.0, 8.8), 7.93 (dd, 1H, J=1.6, 7.6), 9.10 (s, 1H), 9.56 (s, 1H); ^{13}C NMR (400 MHz, DMSO) ∂ 25.17, 25.97, 27.42, 28.26, 28.59, 111.15, 114.92, 117.17, 120.77, 121.48, 125.09, 131.71, 152.23, 155.03, 166.87.

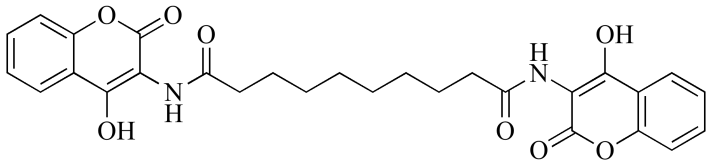

Compound 3-13

4-8 (0.1g, 0.565 mmol) was dissolved in 2.8 mL pyridine and heated to reflux. Sebacic diacid chloride (0.076 mL, 0.282 mmol) was added dropwise and the reaction was allowed to continue overnight. The reaction was quenched by the addition of 3 mL water and 0.5 mL 6 M hydrochloric acid. Product was extracted with dichloromethane. The organic layer was washed with 10% copper sulfate solution, and then water washes until the water was no longer tinted blue. The organic layer was then dried over sodium sulfate and concentrated under vacuum. Flash silica gel chromatography gave a pale yellow solid in a 17% yield. IR ν (neat)/cm^{-1} 2850.06, 2916.86 (s), 3080.12 (w), 3424.25 (b); ^{1}H NMR (400 MHz, DMSO) ∂ 1.22-1.45 (m, 10H), 1.82 (m, 3H), 2.99 (t, 3H, J=8.0), 7.48 (dd, 2H, J= 7.2, 7.6), 7.59 (d, 2H, J=8.4), 7.69 (ddd, 2H, J=1.6, 7.6, 8.0), 7.92 (d, 2H, J=8.0).

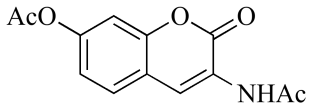

Compound **3-14**

Compound **3-14** was synthesized according to the procedure in Kudale, *et al. Tett. Lett.* **2007**, *29*, 5077.[46] 2,4-Dihydroxybenzaldehyde (10 g, 72.4 mmol) was dissolved in 362 mL acetic anhydride. Sodium acetate (23.76 g, 290 mmol) and N-acetylgycine were added to the solution and the reaction was refluxed overnight. The reaction was quenched by cooling on ice and slowly adding ice-cold water. Precipitate was filter off, and then triturated with ice-cold ethyl acetate to remove impurities. The reaction gave a 23.6% yield of a pale pink solid. ^{1}H NMR (400 MHz, $CDCl_3$) ∂ 2.24 (s, 3H), 2.33 (s, 3H), 7.07 (dd, 1H, J=2.0, 8.4), 7.13 (d, 1H, J=2.0), 7.50 (d, 1H, J=8.4), 8.02 (s, 1H), 8.67 (s, 1H); ^{13} C NMR (400 MHz, $CDCl_3$) ∂ 21.09, 24.71, 110.04, 117.63, 119.12, 122.74, 123.57, 128.36, 150.15, 151.39, 158.49, 168.83, 169.33.

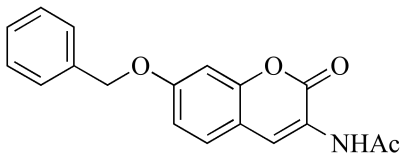

Compound **3-15**

Synthesized according to the procedure in Kudale, *et al. Tett. Lett.* **2007**, *29*, 5077.[46] **3-14** (4 g, 15.3 mmol) was dissolved in 30.5 mL methanol. Potassium carbonate (2.75 g, 20 mmol) was added to the solution and the reaction was allowed to stir 30 minutes. The solvent was then removed by rotary evaporation. The solids were then suspended in 77 mL acetonitrile before the addition of benzyl bromide (2 mL, 16.8 mmol). This second

reaction was refluxed overnight. The reaction was then diluted with water, and neutralized with 6 M HCl. Ethyl actate was then added to precipitate the product. Product was filtered off and rinsed with water and then dried under vacuum to give 4.69 g (99% yield) of a pale yellow solid. ^{1}H NMR (400 MHz, $CDCl_3$) ∂ 2.22 (s, 3H), 5.12 (s, 2H), 6.89 (d, 1H, J=2.0), 6.96 (dd, 1H, J=2.0, 8.4), 7.30-7.44 (m, 6H), 7.95 (s, 1H), 8.63 (s, 1H); ^{13}C NMR (400 MHz, $CDCl_3$) ∂ 24.62, 70.56, 101.89, 113.32, 113.86, 121.69, 123.99, 127.47, 128.33, 128.65, 128.73, 135.95, 151.34, 159.00, 160.35, 169.11.

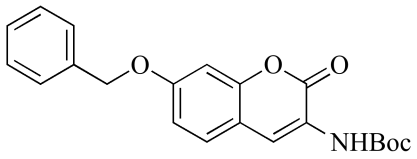

Compound 3-17

Synthesized according to the procedure in Kudale, *et al. Tett. Lett.* **2007**, *29*, 5077.[46] **3-15** (4.5 g, 14.5 mmol) was suspended in 73 mL tetrahydrofuran. To the solution, dimethylamino pyridine (8.89 g, 72.7 mmol) was added followed by di-*tert*-butyl dicarbonate (3.18 g, 14.5 mmol). The reaction was allowed to stir until the yellow suspension became a clear, brown-colored, solution, about 30 minutes. To the solution, hydrazine (3.64 mL, 72.7 mmol) was added, followed by 60 mL methanol. This second reaction was allowed to stir until the reaction became bright orange, about 20 minutes. The solvents were then removed by rotary evaporation, and the solids dissolved in the necessary amount of dichloromethane. The organic solution was washed with 1 M HCl, 10% copper sulfate, saturated sodium bicarbonate, and followed by a brine wash. The organic layer was then dried over sodium sulfate and concentrated under vacuum. ^{1}H

NMR (400 MHz, $CDCl_3$) ∂ 1.53 (s, 9H), 5.11 (s, 2H), 6.89 (d, 1H, J=2.0), 6.92 (dd, 1H, J=2.0, 8.4), 7.38 (m, 6H), 8.23 (s, 1H); ^{13}C NMR (400 MHz, $CDCl_3$) 28.23, 20.87, 70.52, 81.48, 101.81, 113.57, 113.73, 121.17, 122.28, 127.50, 128.12, 128.30, 128.73, 136.04, 150.88, 152.59, 158.86, 159.83.

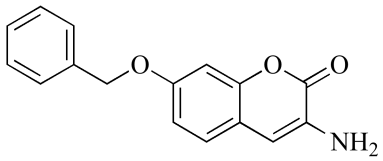

Compound 3-18

Synthesized according to the procedure in Kudale, *et al. Tett. Lett.* **2007**, *29*, 5077.[46] **3-17** (5 g, 13.6 mmol) was dissolved in 68 mL dichloromethane. To the solution, trifluoroacetic acid (20.8 mL, 272 mmol) was added dropwise. The reaction was allowed to stir over night at room temperature. Once TLC confirmed reaction had gone to completion, the mixture was neutralized with saturated sodium bicarbonate. The organic layer was separated from the aqueous, and dried over sodium sulfate. The organic layer was then dried over sodium sulfate and concentrated under vacuum. Flash silica gel chromatography (0-100% ethyl acetate in hexanes gradient) gave product with a 68.9% yield. ^{1}H NMR (400 MHz, $CDCl_3$) ∂ 4.05 (broad s, 2H), 5.09 (s, 2H), 6.69 (s, 1H), 6.89 (m, 2H), 7.19 (d, 1H, J=9.2), 7.31-7.41 (m, 5H); ^{13}C NMR (400 MHz, $CDCl_3$) ∂ 70.47, 101.94, 112.04, 113.30, 114.65, 123.40, 125.82, 127.48, 128.19, 128.69, 136.33.150.27, 158.14.

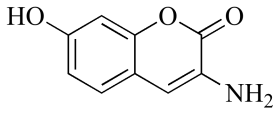

Compound 3-19

3-Amino-7-benzyloxycoumarin 3-18 (0.15 g, 0.561 mmol) was dissolved in 0.56 mL 1% HCl methanol. The solution was cooled on ice and the vessel purged with nitrogen gas before the addition of 5% palladium on carbon (0.0075 g) catalyst. The reaction vessel was placed under vacuum, and then backfilled with 1 atm hydrogen gas. The reaction was monitored by TLC (R_f=0.0, 1:1 ethyl acetate in hexanes). Once TLC indicated no starting material remained, the catalyst was filtered off and rinsed with methanol. The filtrate was concentrated under vacuum to give 92% yield an off white solid: mp 212° C dec. IR ν (neat)/cm^{-1} 2597.88, 2850.52 (b), 3232.68 (b); ^{1}H NMR (400MHz, DMSO) ∂ 6.68 (d, 1H, J=1.6), 6.71 (dd, 1H, J=1.6, 8.4), 7.29 (d, 1H, J=8.4), 8.28 (s, 1H); ^{13}C NMR (400 MHz, DMSO) ∂ 101.91, 112.89, 113.21, 114.22, 126.46, 127.69, 150.09, 157.07, 158.83; HRMS $C_9H_7NO_3$ Expected: 177.0426, Found: 176.0356.

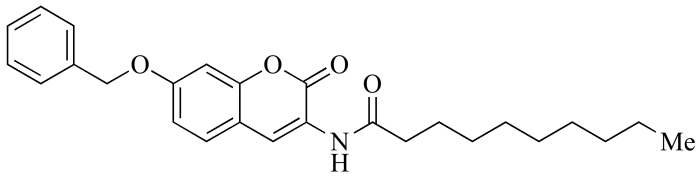

Compound 3-20

Commercially available decanoyl chloride (0.70 mL, 0.4 mmol) was dissolved in 1.75 mL pyrideine and heated. Compound 3-18 was dissolved in 1.75 mL pyridine and added dropwise to the acid chloride solution. The reaction was refluxed overnight before being quenched by the addition of an equal volume of water and 0.5 mL 6M hydrochloric acid.

The product was extracted into dichloromethane and washed with 10% copper sulfate solution, and then water until the water was no longer blue-tinted. The organic was then dried over sodium sulfate and concentrated under vacuum. Flash silica gel chromatography (R_f=0.901 in 1:1 ethyl acetate in hexanes) gave 0.1145 g of an oil (66% yield). IR ν (neat)/cm^{-1} 2852.76, 2923.46, 2952.39 (w), 3037.51 (w), 3316.00; ^{1}H NMR (400 MHz, $CDCl_3$) ∂ 0.88 (t, 36H, J=6.8, 6.8), 1.26 (m, 170H), 1.61 (m, 22H), 2.30 (t, 22H, J=7.2, 7.6), 5.12 (s, 2H), 6.89 (d, 1H, J=2.4), 6.95 (dd, 1H, J=2.4, 8.4), 7.40 (m, 6H), 7.93 (s, 1H), 8.65 (s, 1H); ^{13}C NMR (400MHz, $CDCl_3$) ∂ 14.03, 22.26, 24.95, 25.39, 29.13, 29.21, 29.30, 29.37, 29.66, 30.83, 31.83, 34.11, 37.75, 51.35, 70.56, 101.88, 113.41, 113.83, 121.73, 123.87, 127.47, 128.31, 128.59, 128.72, 174.27, 206.68.

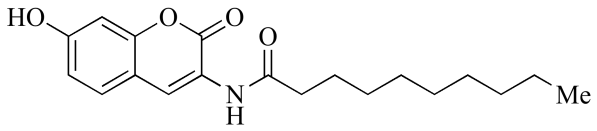

Compound 3-21

Compound 3-20 (0.1 g, 0.230 mmol) was dissolved in 0.3 mL1% HCl methanol. The solution was cooled on ice and the vessel purged with nitrogen gas before the addition of 5% palladium on carbon (0.0005 g) catalyst. The reaction vessel was placed under vacuum, and then backfilled with 1 atm hydrogen gas. The reaction was monitored by TLC (R_f=0.42, 1:1 ethyl acetate in hexanes). Once TLC indicated no starting material remained, the catalyst was filtered off and rinsed with methanol. The filtrate was concentrated under vacuum. Flash silica gel chromatography (0-100% ethyl acetate in hexanes gradient) gave 28.4 mg (70% yield) of off white solid: mp 138.4-142.6°C. IR ν

(neat)/cm^{-1} 2851.98, 2920.44, 3145.96 (b), 3310.21; ^{1}H NMR (400 MHz, $CDCl_3$) ∂ 0.88 (t, 3H, J=6.8, 6.8), 1.27 (m, 6H), 1.71 (t, 1H, J=7.6, 7.6), 2.41 (t, 1H, J=7.6, 7.6), 6.81 (m, 2H), 7.37 (d, 1H, J=9.2), 7.93 (s, 1H), 8.65 (s, 1H); ^{13}C NMR (400 MHz, $CDCl_3$) ∂ 14.04, 22.62, 25.41, 29.16, 29.21, 29.29, 29.38, 31.82, 37.77, 103.06, 113.72, 124.03, 128.95, 157.25, 159.05; HRMS $C_{19}H_{25}NO_4$ Expected: 331.1784, Found: 330.1724.

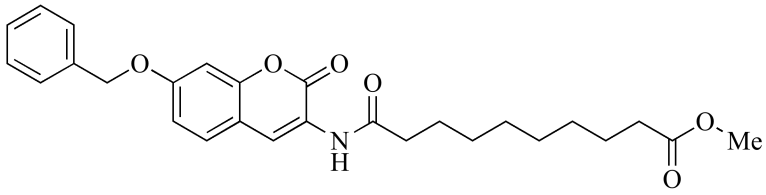

Compound 3-22

Sebacic acid methyl ester (0.0808g, 0.374 mmol) was dissolved in 0.5 mL dichloromethane. A drop of dimethylformamide was added before the addition of oxalyl chloride (0.0016 mL, 1.87 mmol). The reaction was stirred for one hour before the solvent was removed by rotary evaporation. Once the acid chloride was concentrated to an oil, it was dissolved in the necessary amount of dichloromethane before being added dropwise to a solution of 3-18 (0.1 g, 0.374 mmol) and triethylamine (0.156 mL, 1.12 mmol) in 1.5 mL tetrahydrofuran. The coupling reaction was refluxed overnight before being quenched by the addition of 2 mL water and a few drops of 6M HCl. Dichloromethane was used to extract the product. The organic was dried over sodium sulfate and concentrated under vacuum. Flash silica gel chromatography (R_f= 0.676, 1:1 ethyl acetate to hexanes) gave 63.6 mg (66% yield) of white solid: mp 123-126°C. IR ν (neat)/cm^{-1} 2850.75, 2921.49, 3032.86 (w), 3063.75 (w), 3318.49; ^{1}H NMR (400 MHz,

$CDCl_3$) ∂ 1.25-1.40 (m, 8H), 1.62 (m, 2H), 1.72 (m, 2H, 2.30 (t, 2H, J=7.2, 7.6), 2.40 (t, 2H, J=7.6, 7.6), 3.66 (s, 3H), 5.12 (s, 2H), 6.89 (d, 1H, J=2.4), 6.96 (dd, 1H, J=2.4, 8.4), 7.35-7.45 (, 6H), 7.92 (s, 1H), 8.65 (s, 1H).

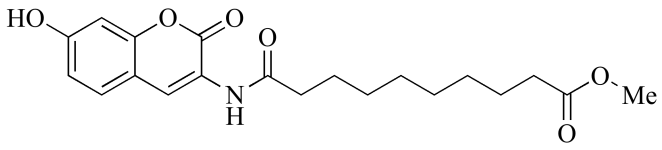

Compound 3-23

Compound 3-22 (0.060 g, 0.129 mmol) was dissolved in 0.3 mL 1% HCl in methanol. The solution was cooled on ice and purged with nitrogen gas prior to the addition of 5% palladium on carbon catalyst (0.010 g). The reaction vessel was placed under vacuum, and then backfilled with 1 atm hydrogen gas. The reaction was monitored by TLC (R_f=0.64, 1:1 ethyl acetate in hexanes). Once TLC indicated no starting material remained, the catalyst was filtered off and rinsed with methanol. The filtrate was concentrated under vacuum. Flash silica gel chromatography (0-100% ethyl acetate in hexanes gradient) gave12.9 mg (26.7% yield) of a white solid: mp 152.0-154.0°C. IR ν (neat)/cm^{-1} 2848.91, 2918.12, 3250.61 (b), 3316.21; ^{1}H NMR (400 MHz, $CDCl_3$) ∂ 1/22-1.41 (m, 8H), 1.62 (m, 2H), 1.70 (m, 2H), 2.30 (t, 2H, J=7.6, 7.6), 3.66 (s, 3H) 6.81 (m, 2H, 7.37 (d, 1H J=8.8), 7.93 (s, 1H) 8.65 (s, 1H); ^{13}C NMR (400 MHz, DMSO) ∂ 24.33, 24.96, 28.31, 28.39, 28.42, 28.47, 33.24, 35.81, 41.30, 51.11, 101.91, 111.37, 120.81, 126.21, 128.92, 151.49, 157.93, 159.45, 172.84, 173.48; HRMS $C_{20}H_{25}NO_6$ Expected: 375.1682, Found: 374.1625.

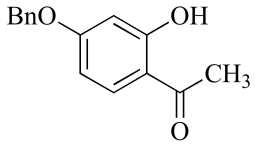

Compound 3-24

Mono protection of the 2,4-dihydroxyacetophenone was carried out according to the procedure in Jung, *et al*. *Eur. J. Med. Chem.* **2003**, *38*, 537.[47] The 2,4-dihydroxyacetophenone starting material (10g, 65.7 mmol) was dissolved in 131 mL acetonitrile. Potassium carbonate (9.99 g, 72.3 mmol) was added to the solution, and the mixture was refluxed for one hour. After one hour, benzyl bromide (7.66 mL, 64.4 mmol) dissolved in 13.4 mL acetonitrile was added dropwise to the mixture. The protection reaction was then refluxed an additional 3 hours before being quenched by the removal of the potassium carbonate. Ethyl acetate was added to the filtrate and was washed with dilute HCl. Silica gel chromatography (20% ethyl acetate in hexanes) gave clean product in a 98.9% yield. ^{1}H NMR (400 MHz, $CDCl_3$) ∂ 2.56 (s, 3H), 5.10 (s, 2H), 6.50 (s, 1H), 6.53 (d, 1H, J=2.48), 7.30-7.47 (m, 5H), 7.64 (d, 1H, J=9.12), 12.73 (s, 1H).

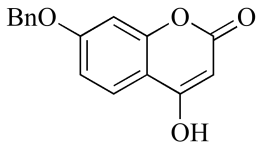

Compound 3-25

Closing of the coumarin ring using the mono-protected acetophenone was carried out according to the procedure in Lei, *et al. Chin. J. Chem.* **2002**, *20*, 1263.[57] Sodium hydride (60% in mineral oil, 0.70 g, 17.5 mmol) was suspended in 30 mL of toluene.

Added to the suspension was 4-benzyloxy-2-hydroxyacetophenone 4-# (1.5 g, 5.9 mmol) dissolved in 15 mL toluene. Once the basic acetophenone mixture stopped bubbling, diethyl carbonate (1.06 mL, 8.8 mmol) in 7.5 mL toluene was added dropwise. The reaction was refluxed overnight before being cooled to 0°C and quenched with water and the necessary 6M HCl to bring the pH to 1. The aqueous solution was washed with ethyl acetate multiple times to extract the product. The combined organic washes were washed with brine and dried over sodium sulfate before being concentrated under vacuum. Flash silica gel chromatography (0-10% methanol in dichloromethane gradient) afforded an off-white solid with a 63% yield.

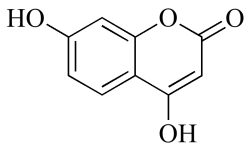

Compound 3-26

7-Benzyloxy-4-hydroxycoumarin **3-25** (0.2g, 0.745mmol) was dissolved in 3 mL methanol. The solution was cooled on ice and the reaction vessel purged with nitrogen gas before the addition of 5% palladium on carbon (0.01 g). The reaction vessel was placed under vacuum, and then backfilled with 1 atm hydrogen gas. The reaction was monitored by TLC (R_f=0.1-0.3 smear in 8% methanol in dichloromethane). Once TLC indicated reaction was complete, the catalyst was filtered off and rinsed with methanol until the filtrate was no longer colored. The filtrate was concentrated under vacuum. Flash silica gel chromatography (0-10% methanol in dichloromethane gradient) gave the white solid: mp 216°C dec., product in 98% yield. IR ν (neat)/cm^{-1} 2599.7 (b, 2852.07,

2920.67, 2952.66 (w); ^{1}H NMR (400 MHz, MeOD) ∂ 5.44 (s, 1H), 6.69 (d, 1H, J=2.0), 7.79 (dd, 1H, J=2.0, 8.4), 7.73 (d, 1H, J=8.4); ^{13}C NMR (400 MHz, MeOD) ∂ 30.73, 103.17, 109.49, 114.11, 125.93, 157.20, 163.67, 167.04, 169.22; HRMS $C_9H_6O_4$ Expected: 178.0266, Found: 177.0193.

SPR Experimental Procedure

Linear, 5' biotinylated DNA was dissolved in SPR buffer (10 mM HEPES pH 7.3, 3 mM EDTA, 0.005% surfactant P20) to give a concentration of 600 nM. The DNA was immobilized on the surface of flow cell two of a streptavidin-coated sensor chip by flowing 50 µL of the solution through at a rate of 10 µL per minute. Flow cells one and two were then capped with 100 µL of a 1 mg/mL solution of biotin in SPR buffer. The BioCore T200 instrument was then primed with SPR buffer containing 1% (v/v) DMSO, and the flow rate was increased to 50 µL/min. To test the compound's ability to inhibit the DNA-DNA gyrase binding interaction, a premixed solution of DNA gyrase (100 nM) with or without compound (100 µM) was injected over flow cells one and two for 7 minutes. After allowing four minutes for dissociation, the surface of the flow cell was regenerated using 1M NaCl in 50 mM NaOH for 30 seconds.

Supercoiling Assay Procedure

Reactions contained 50 mM Tris-HCl (pH of 8.0 at 23ºC), 10 mM $MgCl_2$, 100 mM potassium glutamate, 10 mM dithiothreitol, 50 µg/mL bovine serum albumin, 1 mM ATP, 0.3 µg relaxed DNA, and 10 fmol of *E. coli* DNA gyrase as a tetramer. Each reaction also contained one of the compounds from chapter 3 at a concentration of 100

μm. The reactions were mixed and then heated at 37ºC for 5 minutes before being quenched by the addition of EDTA. Once EDTA was added, the reaction was allowed to incubate for an additional 5 minutes. The reaction products were then analyzed via agarose gel electrophoresis and run through a vertical 1.2% SeaKem ME agarose gel at 2 V/cm. The gel was run for 15 hours in a 50 mM Tris-HCl (pH 7.9 at 23ºC), 40 mM sodium actate, and 1 mM EDTA (TAE buffer). To analyze the gel, it was then stained with ethidium bromide and photographed.

List of References

1. Pommier, Y.; Leo E.; Zhang, H.; Marchand, C. DNA toposiomerases and their poisoning by anticancer and antibacterial drugs. *Chem. Biol. Rev.* **2010,** *17*, 412-424.

2. Liu, L. F.; J. C. Wang. Supercoiling of the DNA template during transcription. *Proc. Natl. Acad. Sci. USA* **1987,** *84*, 7024-7027.

3. Wang, J. C. DNA topoisomerases: Why so many? *J. Biol. Chem.* **1991,** *266*, 6559-6562.

4. Wang, J. C. Interaction between DNA and an *Escherichia coli* protein omega. *J. Mol. Biol.* **1971,** *55*, 523-533.

5. Champoux, J. J.; R. Dulbecco. An activity from mammalian cells that untwists superhelical DNA - a possible swivel for DNA replication. *Proc. Natl. Acad. Sci. USA* **1972,** *69*, 143-146.

6. Liu, L. F.; Liu, C.-C.; Alberts, B. M. Type II toposiomerases: Enzymes that can unknot a topologically knotted DNA molecule via reversible double-stand break. *Cell.* **1980,** *19*, 697-707.

7. Gellert, M.; Mizuuchi, K.; O'Dea, M. H.; Nash, H. A. DNA gyraes: An enzyme that introduces superhelical turns into DNA. *Proc. Natl. Acad. Sci. USA* **1976,** *73*, 3872-3876.

8. Osheroff, N.; Shelton, E. R.; Brutlag, D. L. DNA Topoisomerase II from *Drosphila melanogaster*. *J. Biol. Chem.* **1983,** *258*, 9536-9550.

9. Berger, J. M.; Gamblin, S. J.; Harrison, S. C.; Wang, J. C. Structure and mechanism of DNA topoisomerase II. *Nature* **1996,** *379*, 225-233.

10. Bates, A. D.; Maxwell, A. Energy coupling in type II topoisomerases: Why do they hydrolyze ATP? *Biochemistry* **2007,** *46*, 7929-7933.

11. Bergerat, A.; de Massy, B.; Gadelle, D.; Varoutas, P.-C.; Nicolas, A.; Forterre, P. An atypical topoisomerase II from archaea with implications from meiotic recombination. *Nature* **1997,** *386*, 414-417.

12. Kato, J.-I.; Nishimura, Y.; Imamura, R.; Niki, H.; Hiraga, S.; Suzuki, H. New topoisomerase essential for chromosome segreation in *E. coli*. *Cell* **1990,** *63*, 393-404.

13. Stone, M. D.; Bryant, Z.; Crisona, N. J.; Smith, S. B.; Vologoskil, A.; Bustamante, C.; Cozzarelli, N. R. Chirality sensing by *Esherichia coli* topoisomerase IV

and the mechanism of type II topoisomerases. *Proc. Natl. Acad. Sci. USA* **2003,** *100*, 8654-8659.

14. Roca, J.; Wang, J. C. The capture of a DNA double helix by an ATP-dependent portein clamp: A key step in DNA transport by type II DNA topoisomerases. *Cell* **1992,** *71*, 833-840.

15. Roca, J.; Wang, J. C. DNA transport by a type II DNA topoisomerase: Evidence in favor of a two-gate mechanism. *Cell* **1994,** *77*, 609-616.

16. Cabral, J. H. M.; Jackson, A. P.; Smith, C. V.; Shikotra, N.; Maxwell, A.; Liddington, R. C. Cyrstal structure of the breakage-reunion domain of DNA gyrase. *Nature* **1997,** *388*, 903-908.

17. Orphanides, G.; Maxwell, A. Evidence for a comformational change inthe DNA gyrase-DNA comples from hydroxyl radical footprinting. *Nuc. Acids Res.* **1994,** *22*, 1567-1574.

18. Heddle, J. G.; Mitelheiser, S.; Maxwell, A.; Thomson, N. H. Nucleotide binding to DNA gyrase causes loss of DNA wrap. *J. Mol. Biol.* **2004,** *337*, 597-610.

19. Wigley, D. B.; Davies, G. J.; Dodson, E. J.; Maxwell, A.; Dodson, G. Cyrstal structure of an N-terminal fragment of the DNA gyrase B protein. *Nature* **1991,** *351*, 624-630.

20. Williams, N. A.; Maxwell, A. Probing the two-gate mechanism of DNA gyrase using cysteine cross-linking. *Biochemistry* **1999,** *39*, 13502-13511.

21. Levine, C.; Hiasa, H.; Marians, K. J. DNA gyrase and topoisomerase IV: biochemical activities, physiological roles during chromosome replication, and drug sensitivities. *Biochim. Biophys. Acta* **1998,** *1400*, 29-43.

22. Collin, F.; Karkae, S.; Maxwell, A. Exploiting bacterial DNA gyrase as a drug target: current state and perspectives. *Appl. Microbiol. Biotechnol.* **2011,** *92*, 479-497.

23. Pfeiffer, E. S.; Hiasa, H. Determination of the primary target of a quinolone drug and the effect of quinolone resistance-conferring mutations by measuring quinolone sensitivity based on its mode of action. *Antimicrob. Agents Chemother.* **2007,** *51* (9), 3410-3413.

24. Anderson, V. E.; Osheroff, N. Type II topoisomerases as targets for quinolone antibacterials: Turning Dr. Jekyll into Mr. Hyde. *Curr. Pharm. Des.* **2001,** *7*, 339-355.

25. Lesher, G. Y.; Froelich, E. J.; Gruett, M. D.; Bailey, J. H.; Brundage, R. P. 1,8-Naphthyridine derivatives. A new class of chemotherapeutic agents. *J. Med. Chem.* **1962,** *5*, 1063-1065.

26. Emmerson, A. M.; Jones, A. M. The quinolones: Decades of development and use. *J. Antimirob. Chemother* **2003,** *51* (Suppl. S1), 13-20.

27. Gellert, M.; Mizuuchi, K.; O'Dea, M. H.; Itoh, T.; Tomizawa J.-I. Nalidixic acid resistance: A second genetic character involved in DNA gyrase activity. *Proc. Natl. Acad. Sci. USA* **1977,** *74*, 4772-4776.

28. Laponogov, I.; Sohi, M. K.; Veselkov, D. A.; Pan, X.-S.; Sawhney, R.; Thompson, A. W.; McAuley, K. E.; Fisher, L. M.; Sanderson, M. R. Structural insight into the quinolone-DNA cleavage comples of type IIA topoisomerases. *Nat. Strut. Mol. Biol.* **2009,** *16*, 667-670.

29. Drlica, K.; Hiasa, H.; Kerns, R.; Malik, M.; Mustaev, A.; Zhao, X. Quinolones: Action and resistance upated. *Curr. Med. Chem.* **2009,** *9*, 981-1000.

30. Piton, J.; Petrella, S.; Delarue, M.; André-Leroux, G.; Jarlier, V.; Aubry, A.; Mayer, C. Structural insights into the quinolone resistance mechanism of *Mycobacterium tuberculosis* DNA gyrase. *PLoS ONE* **2010,** *5*, e12245-e12259.

31. Heide, L. The aminocoumarins: biosynthesis and biology. *Nat. Prod. Rep.* **2009,** *26*, 1241-1250.

32. Lewis, R. J.; Singh, O. M. P.; Smith, C. V.; Skarzynski, T.; Maxwell, A.; Wonacott, A. J.; Wigley, D. B. The nature of inihibition of DNA gyrase by the coumarins and the cyclothialidines revealed by X-ray crystallography. *EMBO J.* **1996,** *15*, 1412-1420.

33. Oblak, M.; Kotnik, M.; Solmajer, T. Discovery and devlopment of ATPase inhibitors of DNA gyrase as antibacterial agents. *Curr. Med. Chem.* **2007,** *14*, 2033-2046.

34. Gross, C. H.; Parsons, J. D.; Grossman, T. H.; Charifson, P. S.; Bellon, S.; Jernee, G.; Dwyer, M.; Chambers, S. P.; Markland, W.; Botfield, M.; Raybuck, S. A. Active-site residues of *Escherichia coli* DNA gyrase required in coupling ATP hydrolysis to DNA supercoiling and amino acid substitutions leading to novobiocin resistance. *Antimicrob. Agents Chemother.* **2003,** *47*, 1037-1047.

35. Bax, B. D.; Chan, P. F.; Eggleston, D. S.; Fosberry, A.; Gentry, D. R.; Gorrec. F.; Giordano, I.; Hann, M. M.; Hennessy, A.; Hibbs, M.; Huang, J.; Jones, E.; Jones, J.; Koretke Brown, K.; Lewis, C. J.; May, E. W.; Saunders, M. R.; Singh, O.; Spitsfaden, C. E.; Shen, C.; Shillings, A.; Theobald, A. J.; Wohlkonig, A.; Pearson, N. D.; Gwynn, M. N. Type IIa topoisomerase inhibition by a new class of antibacterial agents. *Nature* **2010,** *466*, 935-938

36. Black, M. T.; Stachyra, T. Platel, D.; Girard, A.-M.; Claudon, M.; Bruneu, J.-M.; Miossec, C. Mechanism of action of the antibiotic NXL101, a novel nonfluoroquinolone inhibitior of bactieral type II topoisomerases. *Antimicrob. Agents Chemother.* **2008,** *52*, 3339-3350.

37. Novexel Discontinues Development of NXL 101. http://www.biospace.com/News/novexel-discontinues-development-of-nxl-101/102001 (accessed September 7, 2012).

38. Schimana, J.; Fiedler, H.-P.; Groth, I.; Sübmuth, R.; Beil, W.; Walker, M.; Zeeck, A. Simocyclinones, novel cytostatic angucyclinone antibiotics producted by *Streptomyces antibioticus* Tü 6040. I. Taxonomy, fermentation, isolation and biological activities. *J. Antibiot.* **2000,** *53* (8), 779-777.

39. Theobald, U.; Schimana, J.; Fiedler, H.-P. Microbial growth and production kinetics of *Streptomyces antibioticus* Tü 6040. *Antonie van Leeuwenhoek* **2000,** *78*, 307-303.

40. Flatman, R. H. Howells, A. J.; Heide, L.; Fiedler, H.-P.; Maxwell, A. Simocyclinone D8, an inhibitor of DNA Gyrase with a novel mode of action. *Antimicrob. Agents Chemother.* **2005,** *49* , 1093-1100.

41. Trefzer, A.; Pelzer, S.; Schimana, J.; Stockert, S.; Bihlmaier, C.; Fiedler, H.-P.; Welzel, K.; Vente, A.; Bechthold, A. Biosynthetic gene cluster of simocyclinone, a natural multihybrid antibiotic. *Antimicrob. Agents Chemother.* **2002,** *46*, 1174-1182.

42. Galm, U.; Schimana, J.; Fiedler, H.-P.; Schmidt, J.; Li, S.-M.; Heide, L. Cloning and analysis of the simocyclinone biosynthetic gene cluster and *Streptomyces antibioticus* Tü 6040. *Arch. Microbiol.* **2002,** *178*, 102-114.

43. Oppegard, L. M.; Hamann, B. L.; Streck, K. R.; Ellis, K. C.; Fiedler, H.-P.;, Khodursky, A. B.; Hiasa, H. In vivo and in vitro patterns of the activity of simocyclinone D8, an angucyclinone antibiotic from *Streptomyces antibioticus*. *Antimicrob. Agents Chemother.* **2009,** *53*, 2110-2119.

44. Edwards, M. J.; Flatman, R. H.; Mitchenall, L. A.; Stevenson, C. E. M.; Le, T. K. K.; Clarke, T. A.; McKay, A. R.; Fiedler, H.-P.; Buttner, M. J.; Lawson, D. M.; Maxwell, A. A crystal structure of the bifunctional antibiotic simocyclinone D8, bound the DNA Gyrase. *Science* **2009,** *326*, 1415-1418.

45. Edwards, M. J.; Williams, M. A.; Maxwell, A.; McKay, A. R. Mass Spectrometry Reveals that the antibiotic simocyclinone D8 binds to DNA Gyrase in a "bent-over" conformation: evidence of ositive cooperaivity in binding. *Biochemistry* **2011,** *50*, 3432-3440.

46. Kudale, A. A.; Kendall, J.; Warford, C. C.; Wilkins, N. D.; Bodwell, G. J. Hydrolysis-free synthesis of 3-aminocoumarins. *Tet. Lett.* **2007,** *48*, 5077-5080.

47. Jung, S.-H.; Cho, S.-H.; Dang, T. H.; Lee, J.-H.; Ju, J.-H.; Kim, M.-K.; Lee, S.-H.; Ryu, J.-C.; Kim, Y. Structural requirement of isoflavones for the inhibitory activity of interleukin-5. *Eur. J. Med. Chem.* **2003,** *38*, 537-545.

48. Brady, I.; Leane, D.; Huges, H. P.; Forster, R. J.; Keyes, T. E. Electronic propterties of Ru(II) complexes bound to a biphenolate bridge with low lying π^* orbitals. *Dalton Trans.* **2004,** *2*, 334-341.

49. Bui, E.; Bayle, J. P.; Perez, F.; Liebert, L.; Courtieu, J. Synthése de complexes nématiques du cuivre á partir de ligands substitués par des halogénes. *Liquid Crystals* **1990,** *8*, 513-526.

50. Curini, M.; Epifano, F.; Maltese, F.; Marcotullio, M. C.; Tubaro, A.; Altinier, G.; Gonzales, S. P.; Rodriguez, J. C. Synthesis and anti-inflammatory activity of natural and semisynthetic geranloxycoumarins. *Bioorg. Med. Chem. Lett.* **2004,** *14*, 2241-2243.

51. Tsantrizos, Y. S.; Bailey, M. D.; Dilodeau, F.; Carson, R. J.; Fader, L.; Halmos, T.; Kawai, S.; Landry, S.; Laplante, S.; Simoneau, B. Preparation of 2-(quinolin-2-yl)acetic acid derivatives as inhibitors of human immunodeficiency virus replication. Germany, WO 2009062289, April 22, 2009.

52. Kürti, L.; Cazkó, B. *Strategic Applications of Names Reactions in Organic Synthesis*. Elsevier Academic Press: New York, 2005.

53. Tan, J. S.; Ciufolini, M. A. Total synthesis of topopyrones B and D. *Org. Lett.* **2006,** *8*, 4771-4774.

54. Dubuffet, T.; Loutz, A.; Lavielle, G. An efficient larger scale synthesis of coumarins by a dealkylative boron-mediated ring closure of 3-(ortho-methoxyaryl)propenoic esters. *Syn. Comm.* **1999,** *29*, 929-936.

55. Carlton, D. L.; Collin-Smith, L. J.; Daniels, A. J.; Deaton, D. N.; Goetz, A. S.; Laudeman, C. P.; Littleson, T. R.; Musso, D. L.; Morgan, R. J. O.; Szewcyk, J. R.; Zhang, C. Disocvery of small molecular agonists for the bombesin receptor subtype 3 (BRS-3) based on an omeprazole lead. *Bioorg. Med. Chem. Lett.* **2008,** *18*, 5451-5455.

56. Pandey, G.; Muralikrishna, C.; Bhalerao, U. T. Mushroom tyrosinase-catalyzed synthesis of coumestans, benzofuran derivatives, and related heterocyclic compounds. *Tetrahedron* **1989,** *45*, 6867-6874.

57. Lei, J.-G.; Lin, G.-Q. The first total synthesis of 4,4'-diisofraxidin. *Chin. J. Chem.* **2002,** *20*, 1263-1267.

APPENDIX

NMR Spectra

Compound 3-2

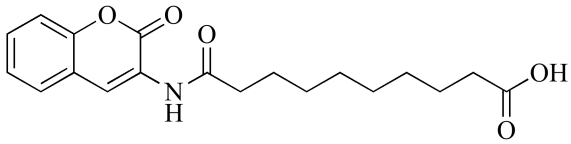

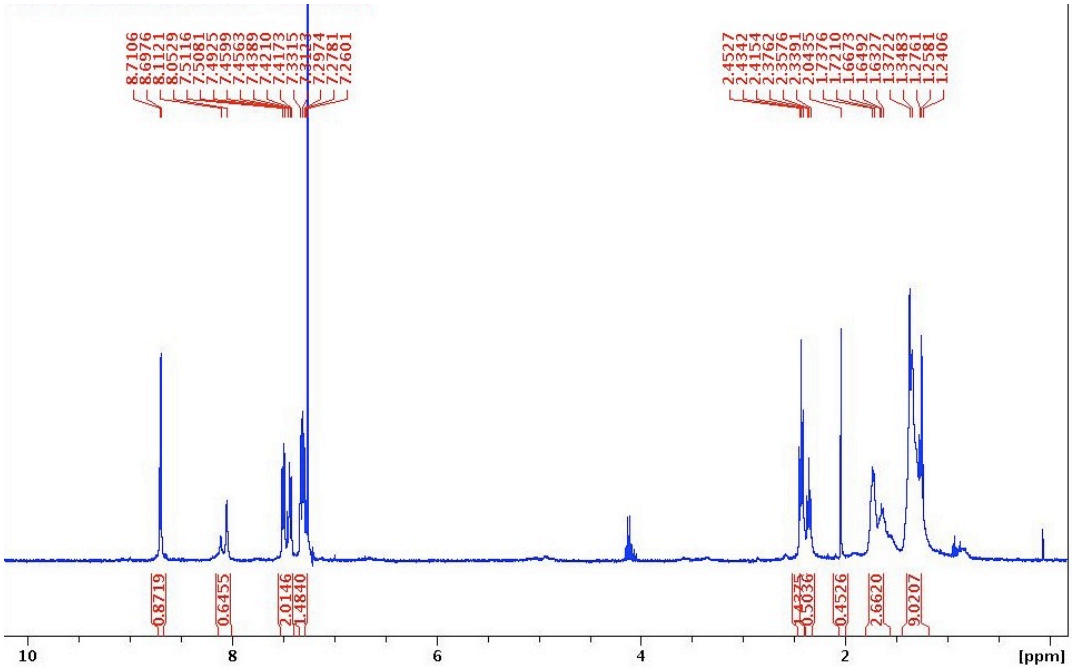

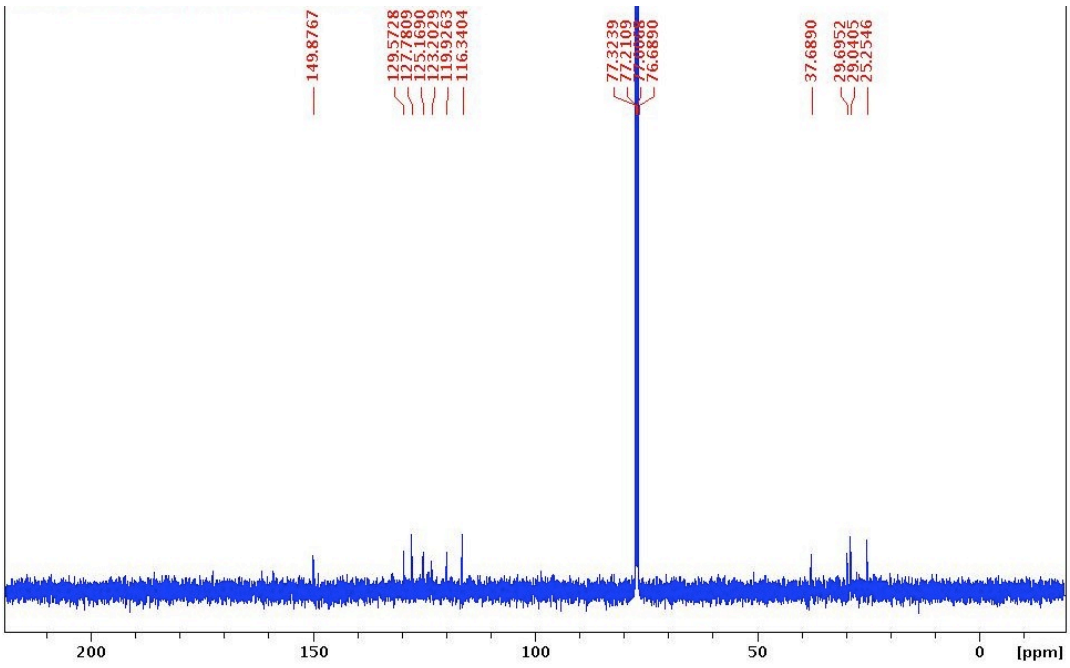
149.8767
129.5728
127.7609
127.1890
123.1029
119.9263
116.3404
77.3239
77.2109
77.0978
76.6890
37.6890
29.6952
29.0405
25.2546
200
150
100
50
0
[ppm]

Compound 3-3

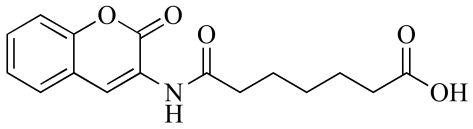
O
O
O
O
N
H
OH

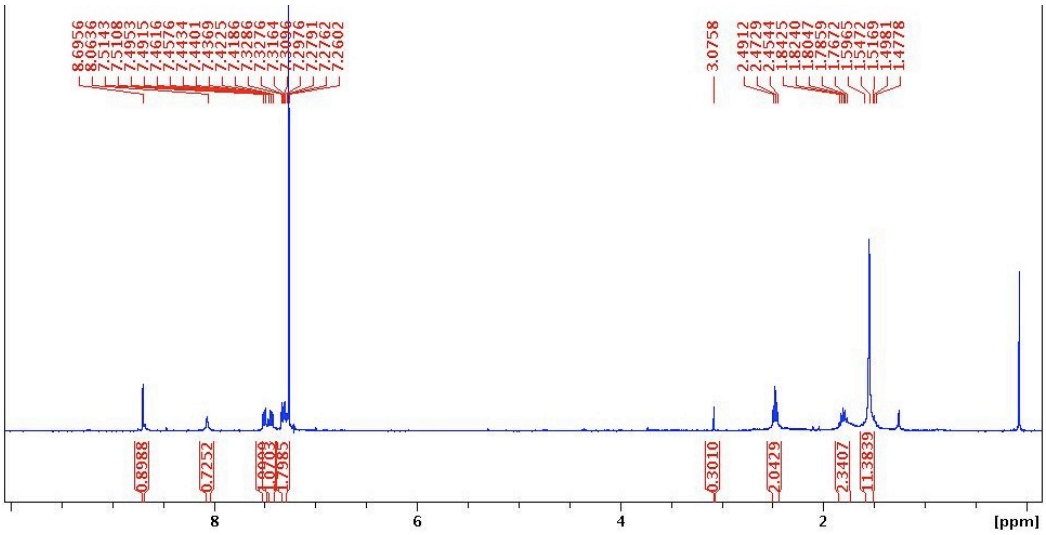
8.6956
8.0636
7.5143
7.5108
7.4953
7.4915
7.4616
7.4576
7.4434
7.4401
7.4369
7.4225
7.4186
7.3286
7.3276
7.3164
7.3096
7.2976
7.2791
7.2762
7.2602
3.0758
2.4912
2.4719
2.4544
2.4375
1.8240
1.8047
1.7859
1.7672
1.5965
1.5472
1.5169
1.4981
1.4778
0.8988
0.7252
0.3010
2.0429
2.3407
11.3839
8
6
4
2
[ppm]

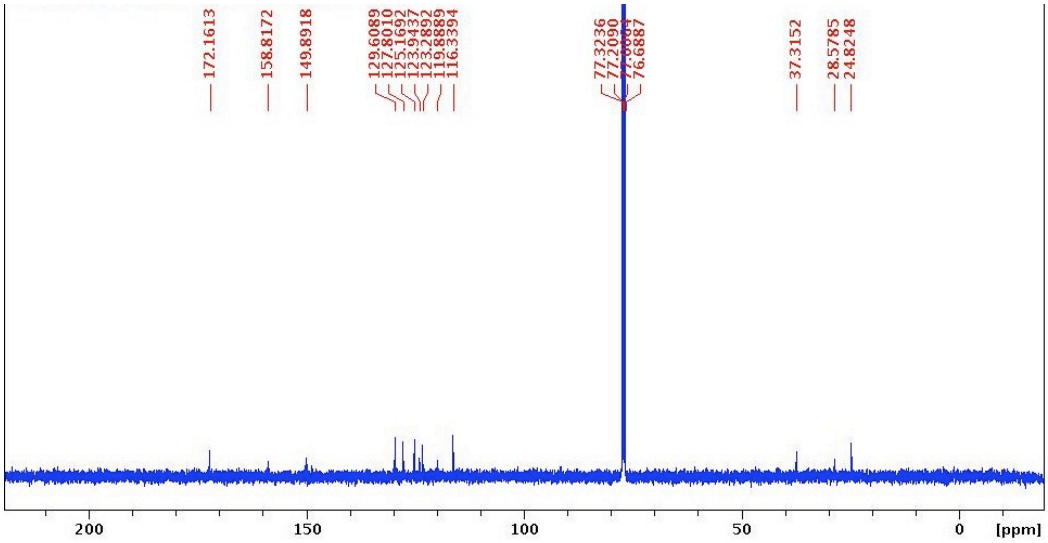
172.1613
158.8172
149.8918
129.6089
127.8010
125.1692
123.9437
123.2892
119.8889
116.3394
77.3236
77.2090
76.6887
37.3152
28.5785
24.8248
200
150
100
50
0
[ppm]

Compound 3-4

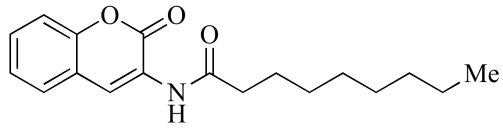
O
O
O
N
H
Me

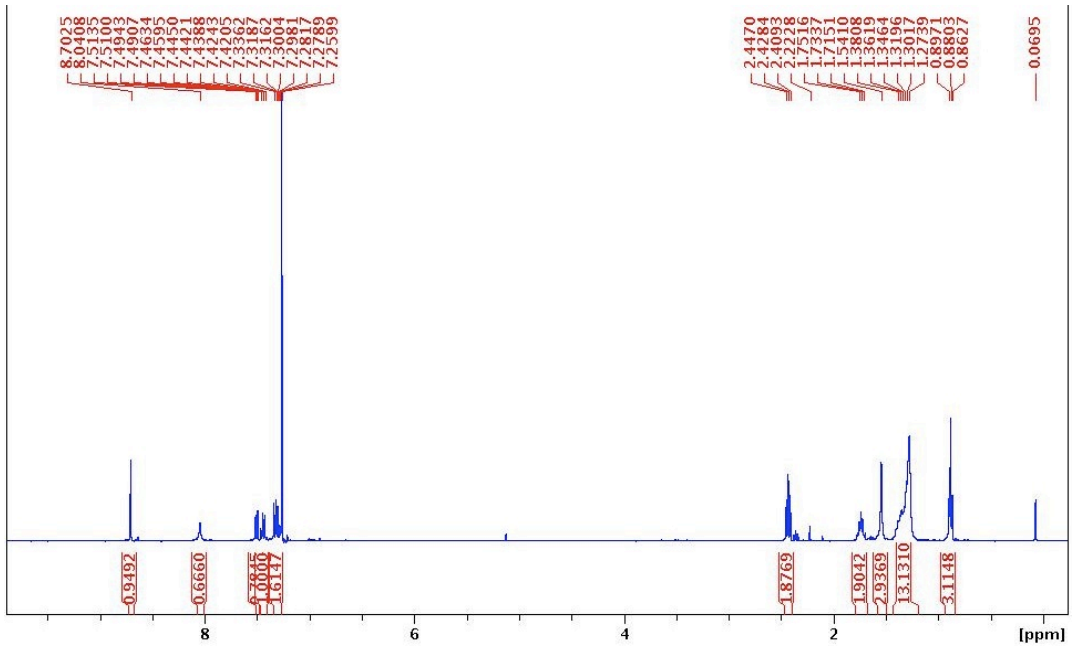
8.7025
8.0408
7.5135
7.5100
7.4943
7.4907
7.4634
7.4595
7.4450
7.4421
7.4388
7.4243
7.4205
7.3262
7.3187
7.3162
7.3004
7.2981
7.2817
7.2789
7.2599
2.4470
2.4284
2.4093
2.2228
1.7516
1.7337
1.7151
1.5410
1.3808
1.3619
1.3196
1.3017
1.2739
0.8971
0.8803
0.8627
0.0695
0.9492
0.6660
0.7845
1.0000
1.6147
1.8769
1.9042
2.9369
13.1310
3.1148
8
6
4
2
[ppm]

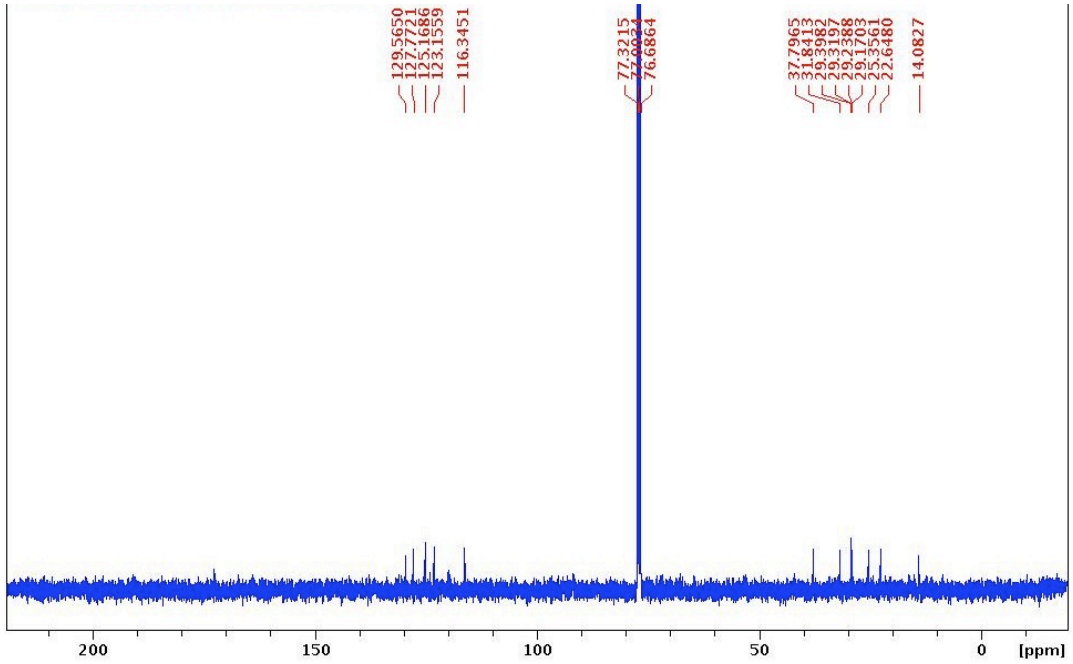
129.5650
127.7721
125.1686
123.1559
116.3451
77.3215
77.0074
76.6864
37.7965
31.8413
29.3982
29.3197
29.2388
29.1703
25.3561
22.6480
14.0827
200
150
100
50
0
[ppm]

Compound 3-5

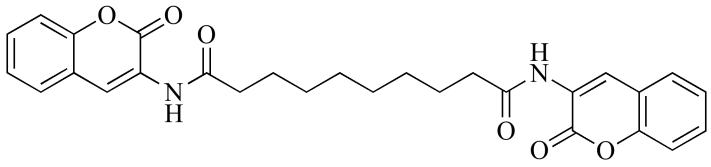

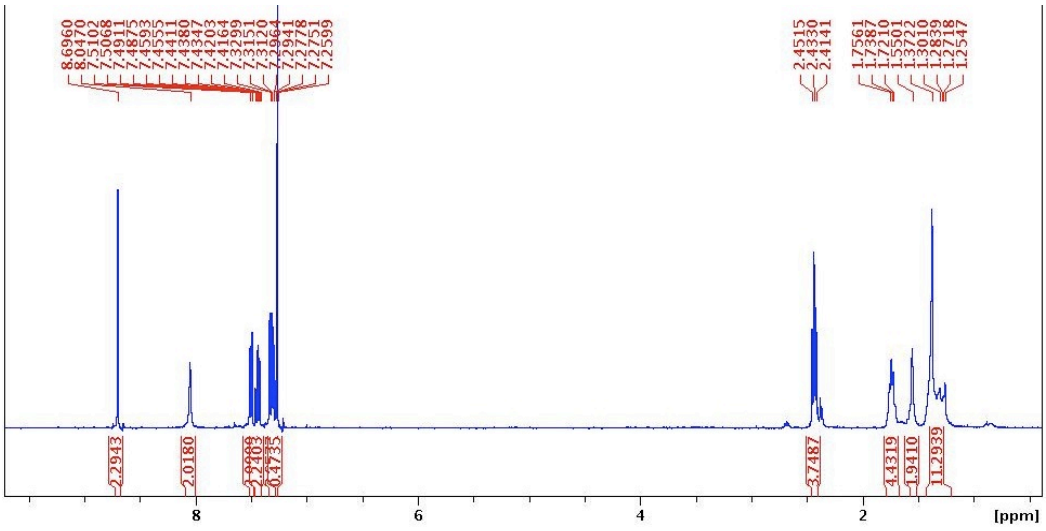
8.6960
8.0470
7.5102
7.5068
7.4911
7.4875
7.4593
7.4555
7.4411
7.4380
7.4347
7.4203
7.4164
7.3299
7.3151
7.3120
7.2964
7.2941
7.2778
7.2751
7.2599
2.4515
2.4330
2.4141
1.7561
1.7387
1.7210
1.3701
1.3572
1.3021
1.2839
1.2718
1.2547
2.2943
2.0180
3.7487
4.4319
1.9410
11.2939
8
6
4
2
[ppm]

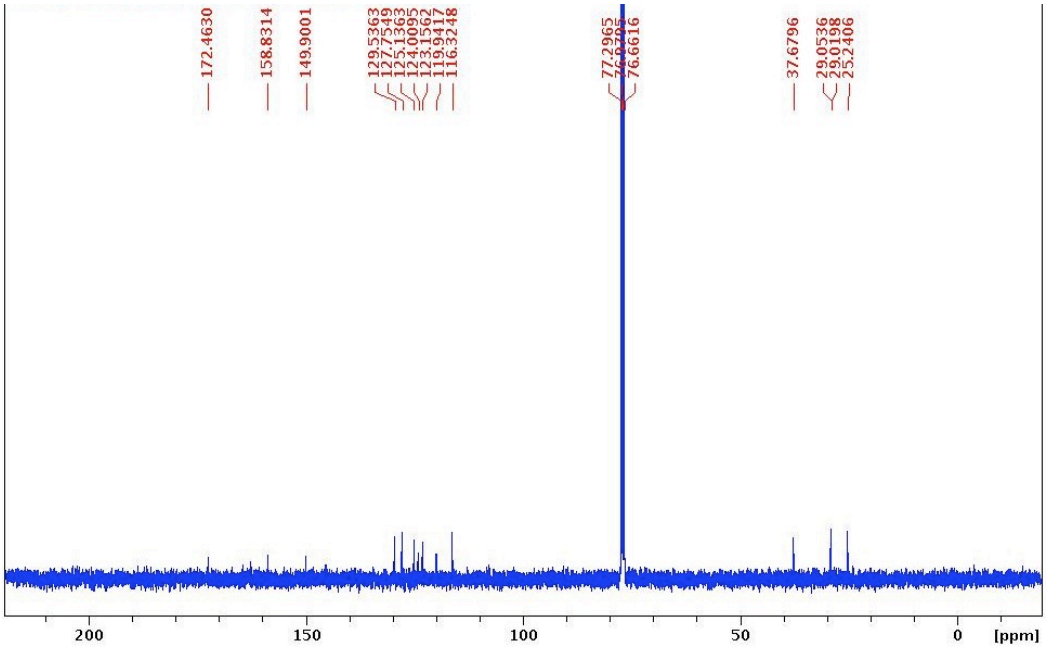
172.4630
158.8314
149.9001
129.5363
127.7549
125.1363
124.0095
123.1562
119.9417
116.3248
77.2965
76.6616
37.6796
29.0536
29.0198
25.2406
200
150
100
50
0
[ppm]

Compound 3-6

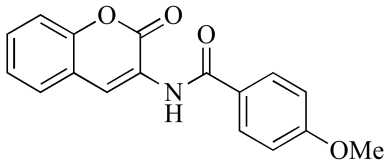
O
O
O
N
H
OMe

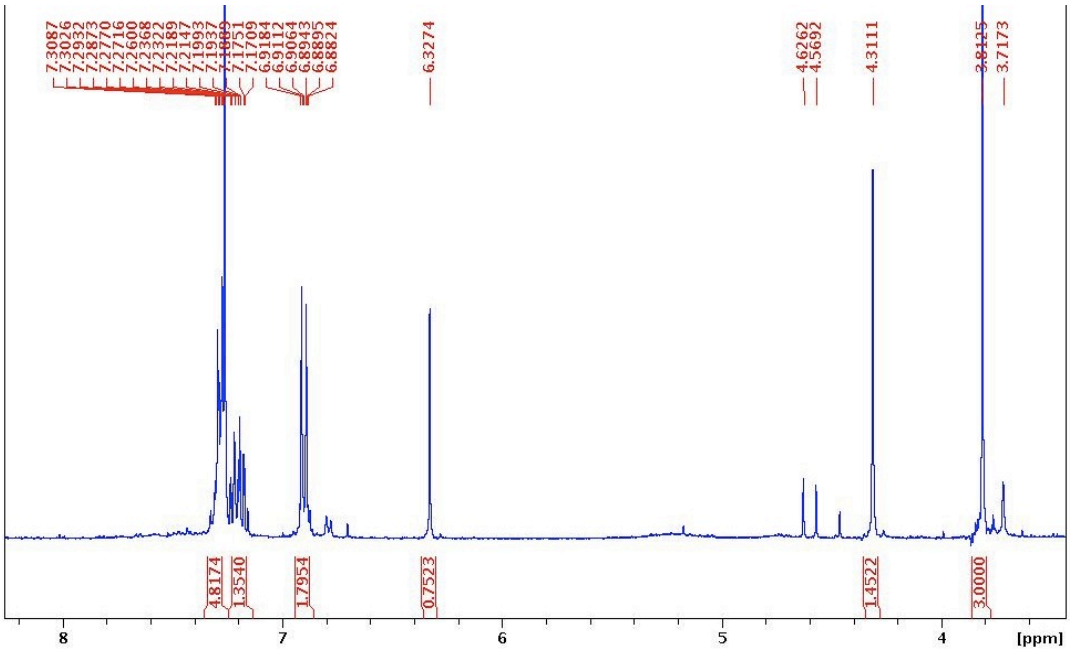
7.3087
7.3026
7.2932
7.2873
7.2770
7.2716
7.2600
7.2368
7.2322
7.2189
7.2147
7.1993
7.1937
7.1751
7.1709
6.9184
6.9117
6.9064
6.8943
6.8895
6.8824
6.3274
4.6262
4.5692
4.3111
3.8125
3.7173
4.8174
1.3540
1.7954
0.7523
1.4522
3.0000
8
7
6
5
4
[ppm]

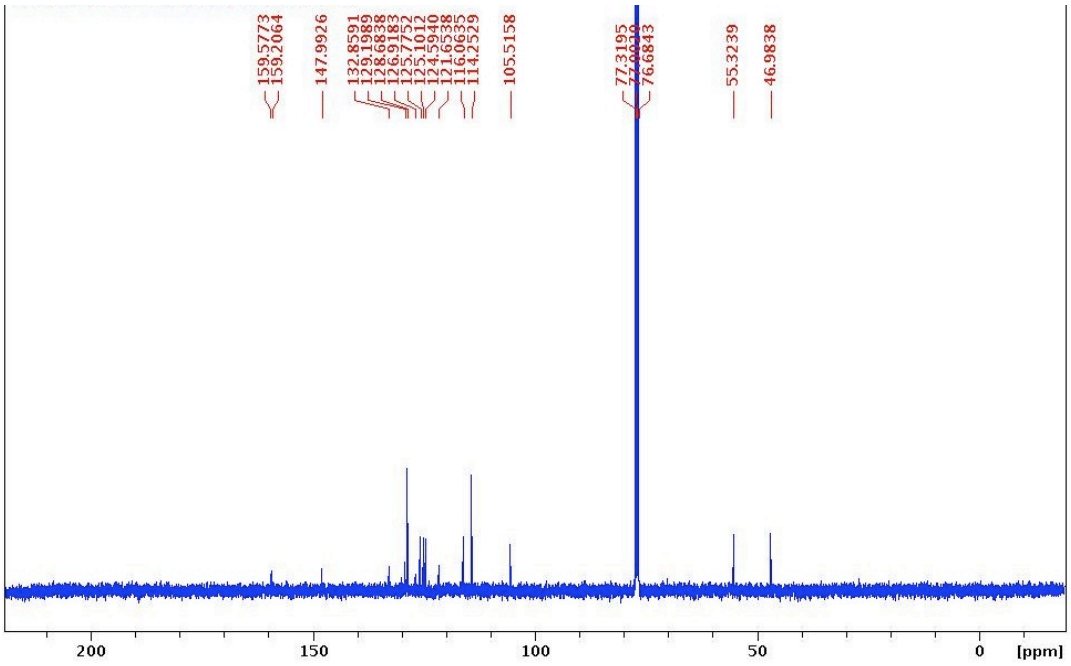
159.5773
159.2064
147.9926
132.8591
129.1989
128.6838
126.9183
125.1732
123.5941
121.6538
116.0635
114.2529
105.5158
77.3195
77.0038
76.6843
55.3239
46.9838
200
150
100
50
0
[ppm]

Compound 3-7

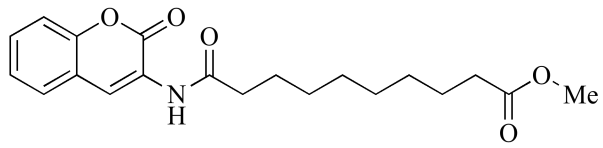
O
O
O
N
H
O
Me
O

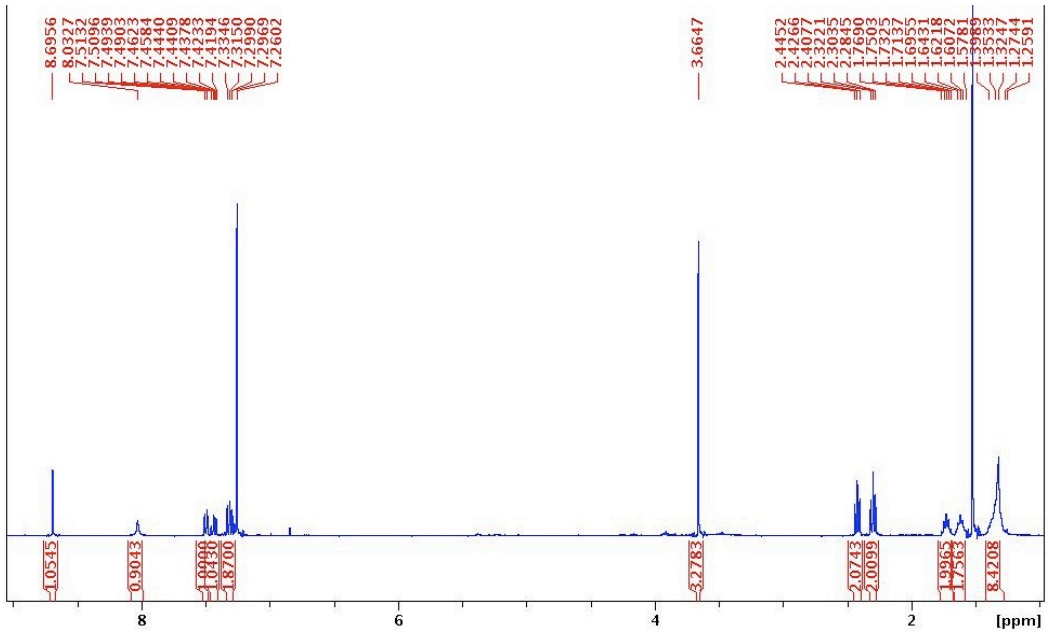
8.6956
8.0327
7.5132
7.5096
7.4939
7.4903
7.4623
7.4584
7.4440
7.4409
7.4378
7.4283
7.4184
7.3346
7.3150
7.2990
7.2969
7.2602
3.6647
2.4452
2.4266
2.4077
2.3221
2.3035
2.2845
2.1690
1.7503
1.7325
1.7137
1.6935
1.6431
1.6218
1.6072
1.5781
1.3989
1.3533
1.3247
1.2744
1.2591
1.0545
0.9043
1.0000
1.0430
1.8700
3.2783
2.0743
2.0099
1.9965
1.7563
8.4208
8
6
4
2
[ppm]

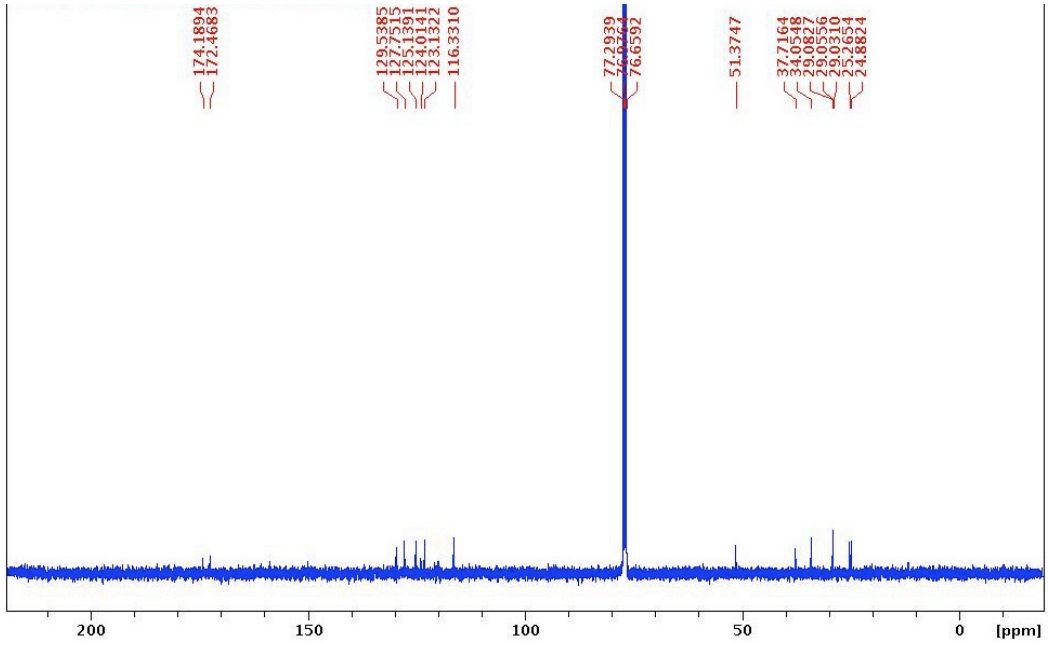
174.1894
172.4683
139.5385
127.7535
127.1515
124.0391
123.1322
116.3310
77.2939
76.8764
76.6592
51.3747
37.7164
34.0548
29.0827
29.0556
29.0310
25.2654
24.8824
200
150
100
50
0
[ppm]

Compound 3-8

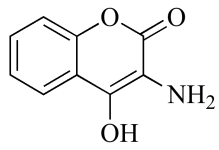
O
O
NH2
OH

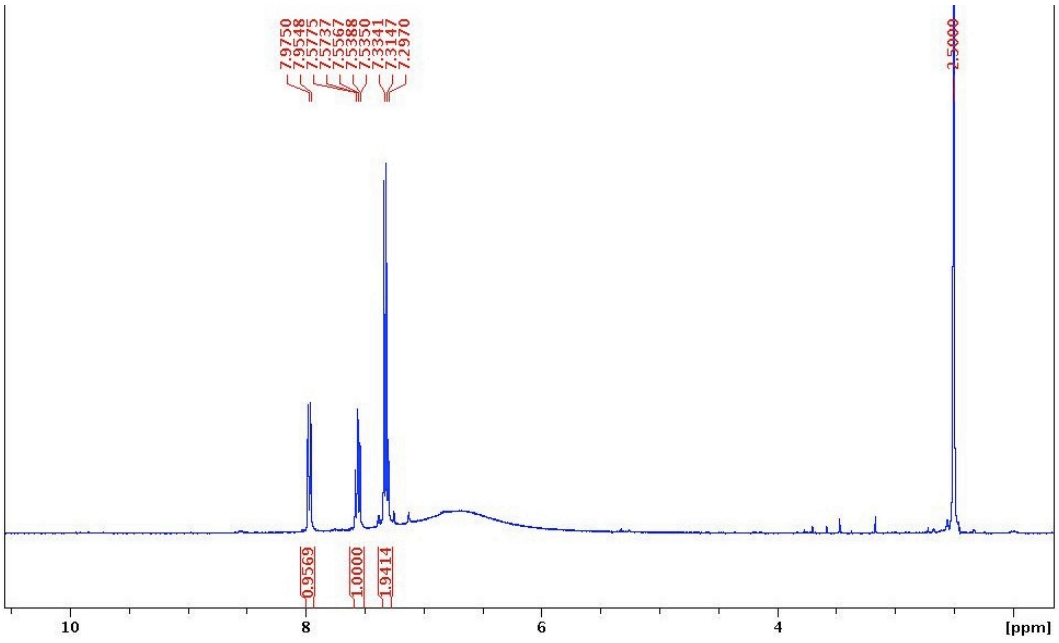
7.9750
7.9548
7.5775
7.5737
7.5567
7.5388
7.5330
7.3341
7.3147
7.2970
2.5000
0.9569
1.0000
1.9414
10
8
6
4
[ppm]

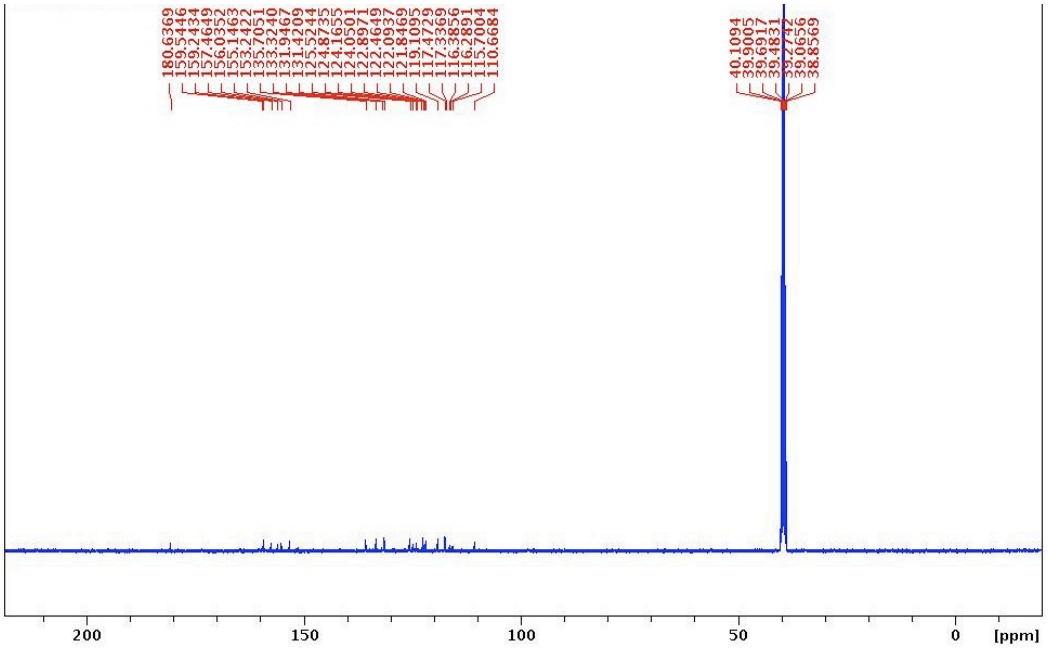
180.6369
159.5446
159.2434
157.4649
156.0352
155.1463
153.2422
135.7051
133.3240
131.9467
131.4209
125.5244
124.8735
124.1655
124.0971
122.4649
122.0837
121.8469
119.1095
117.4729
117.3369
116.3856
116.2891
115.7004
110.6684
40.1094
39.9005
39.6917
39.4831
39.2742
39.0656
38.8569
200
150
100
50
0
[ppm]

Compound 3-9

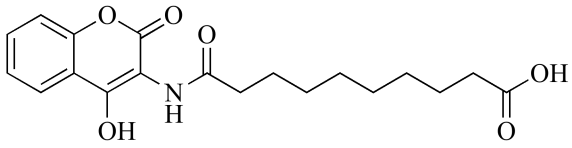
O
O
O
N
H
OH
OH
O

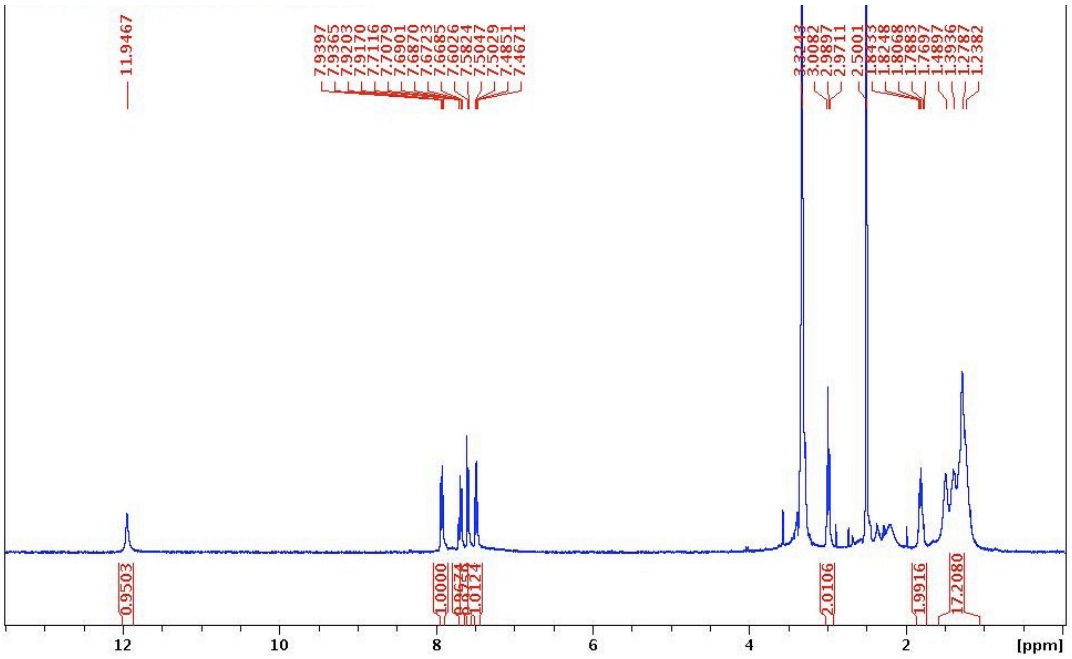
11.9467
7.9397
7.9365
7.9203
7.9170
7.7116
7.7079
7.6901
7.6870
7.6723
7.6685
7.6026
7.5824
7.5047
7.5029
7.4851
7.4671
3.3243
3.3082
2.9997
2.9711
2.5001
1.8433
1.8248
1.8068
1.7883
1.7697
1.4997
1.3936
1.3787
1.2382
0.9503
1.0000
2.0106
1.9916
17.2080
12
10
8
6
4
2
[ppm]

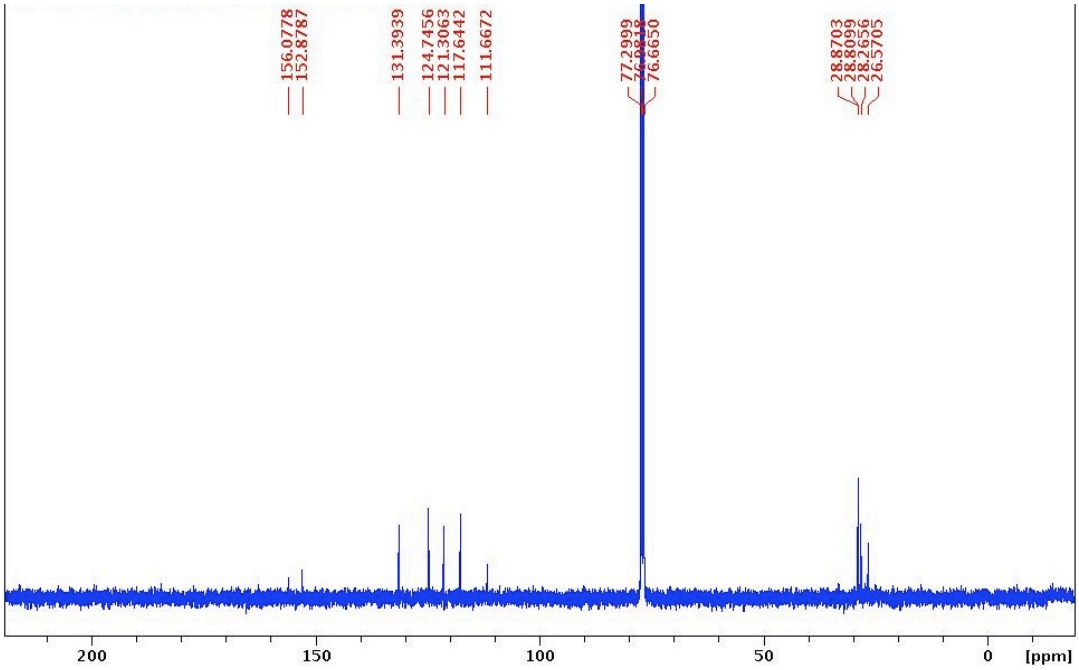
156.0778
152.8787
131.3939
124.7456
121.3063
117.6442
111.6672
77.2999
76.6650
28.8703
28.8099
28.2656
26.5705
200
150
100
50
0
[ppm]

Compound 3-11

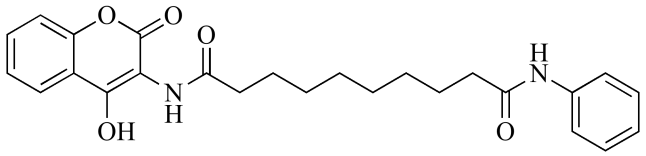

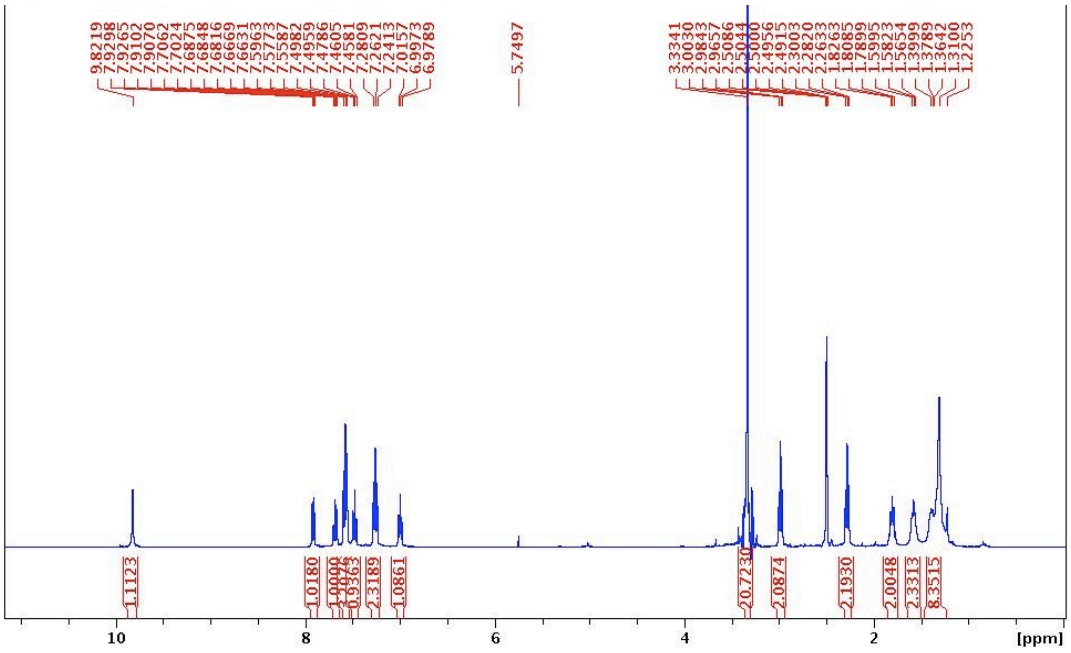

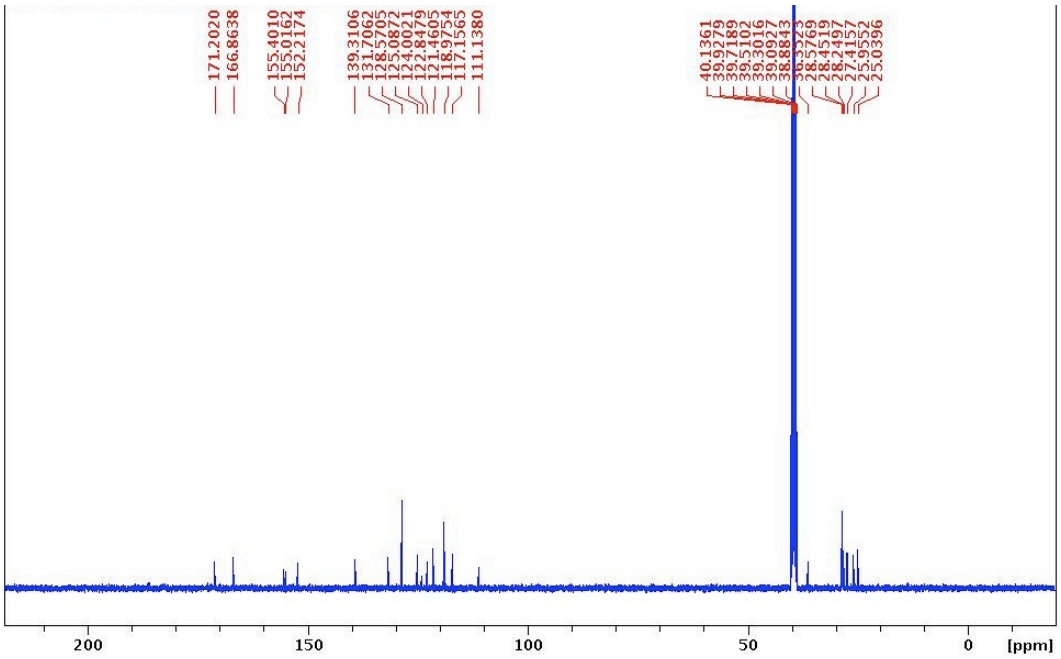

Compound 3-12

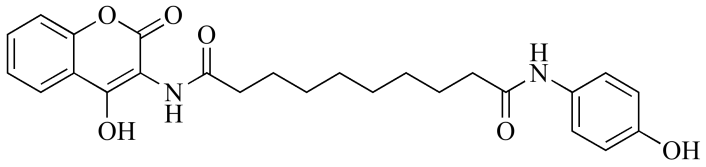

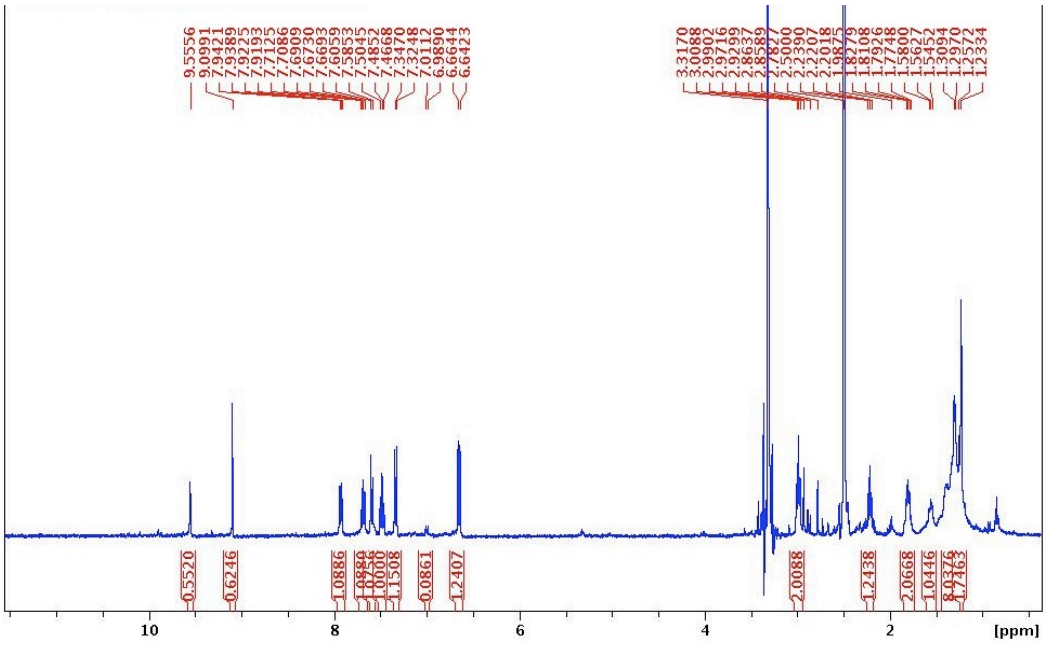

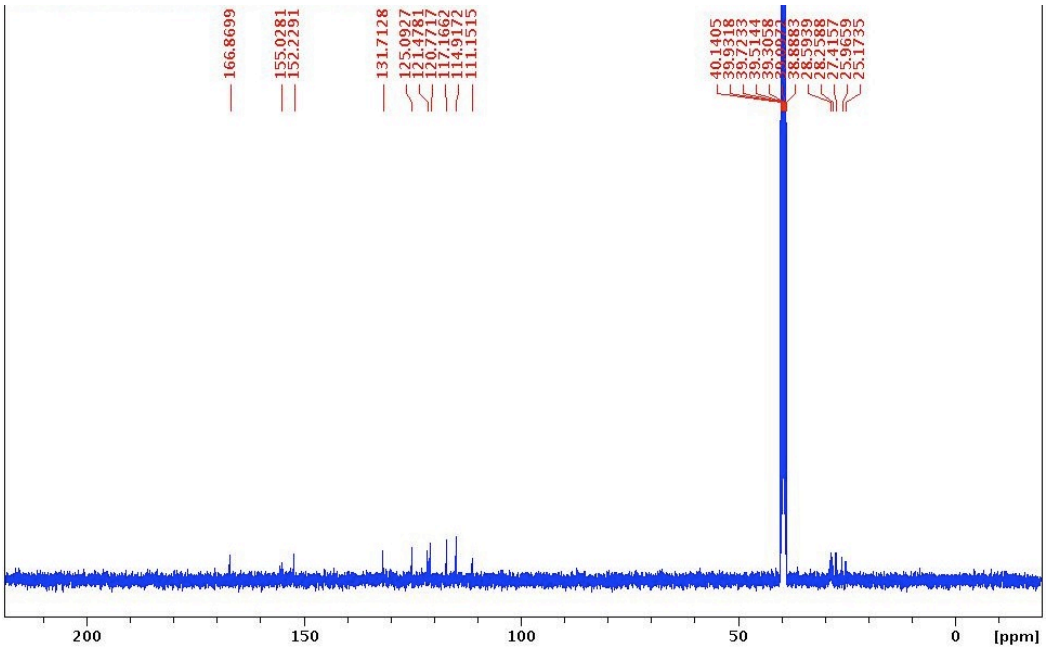

Compound 3-13

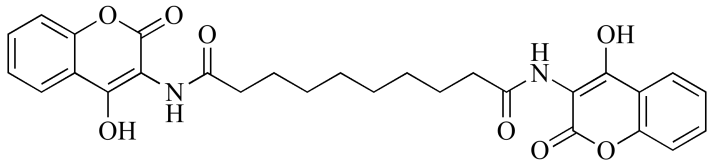

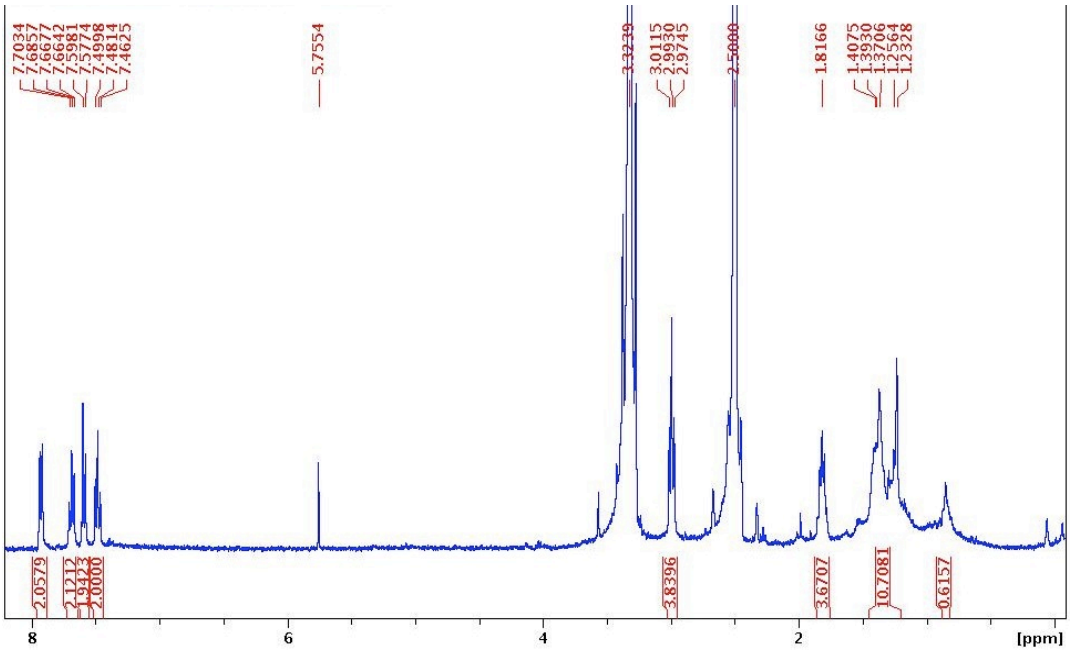

We were unable to obtain a carbon NMR spectrum for this compound.

Compound 3-19

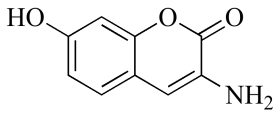

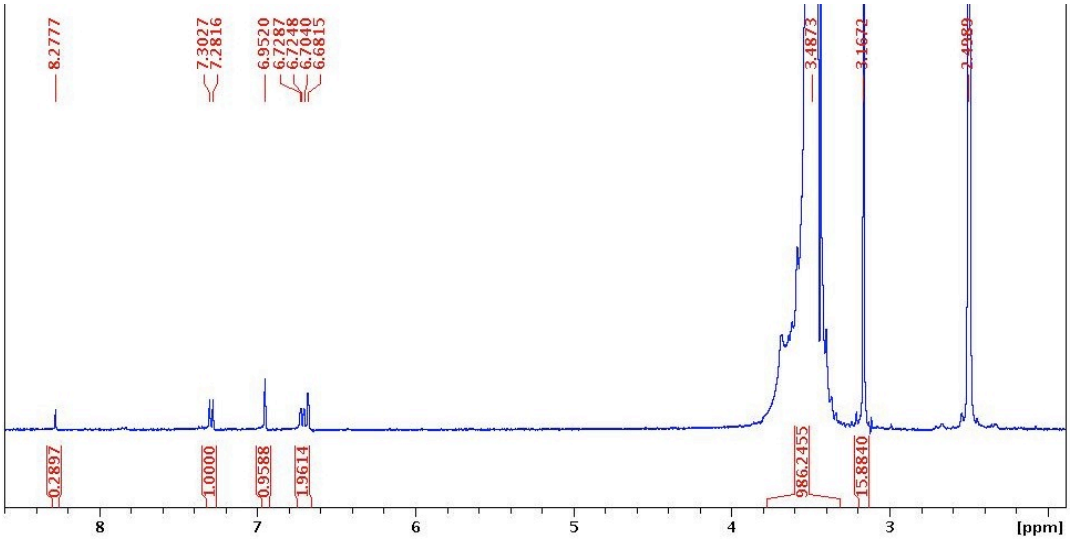

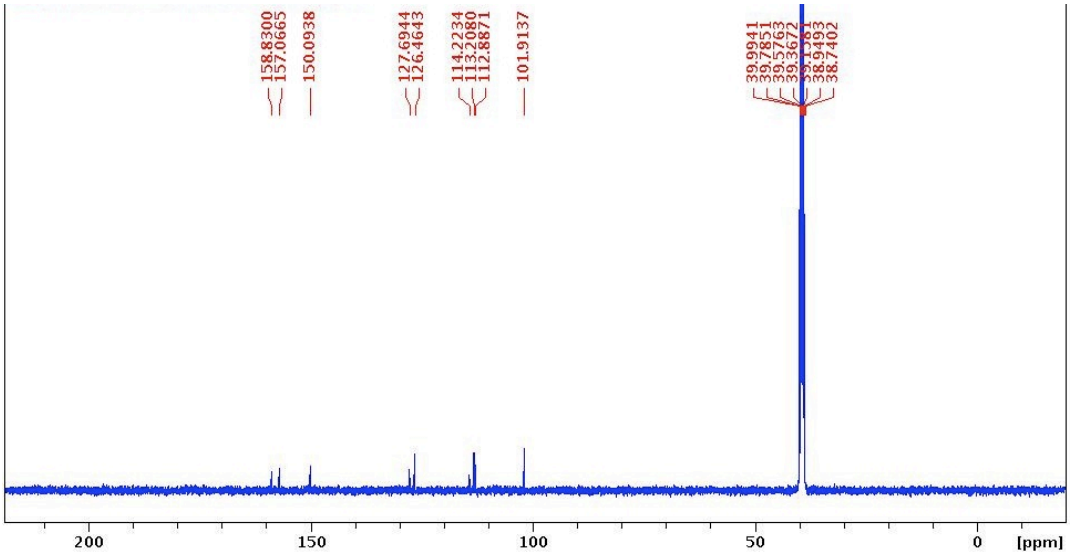

Compound 3-20

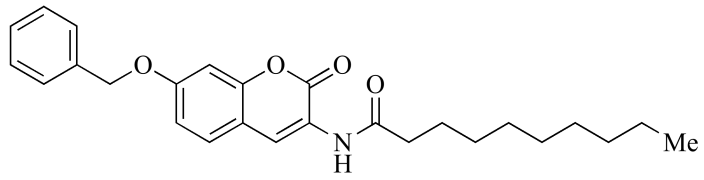

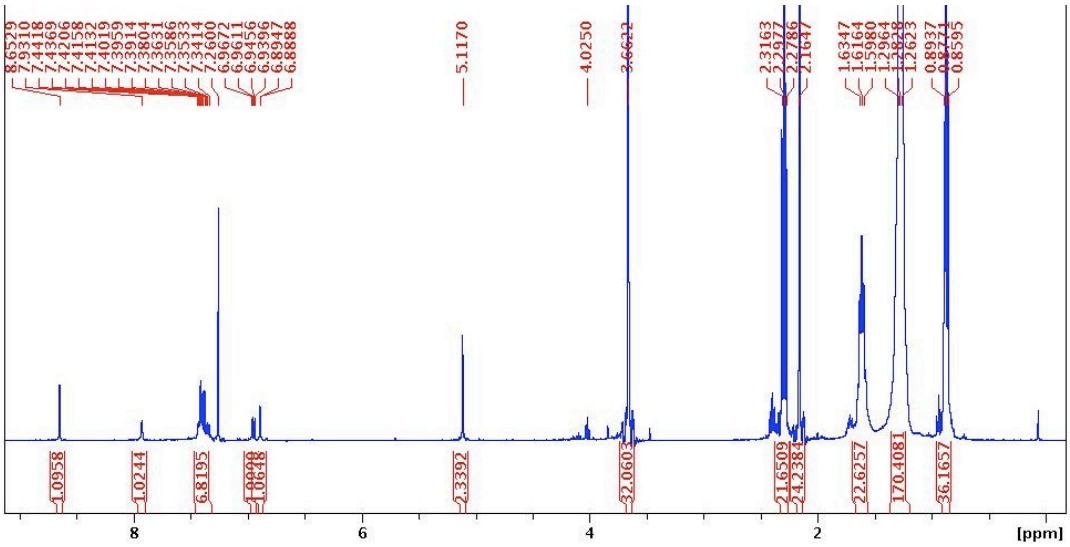

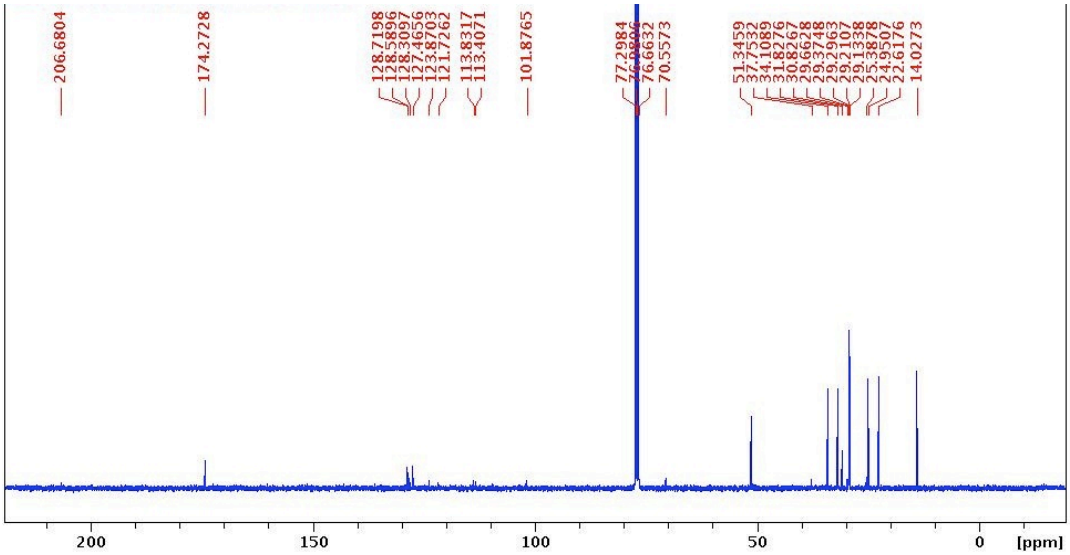

Compound 3-21

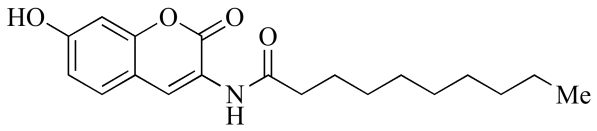

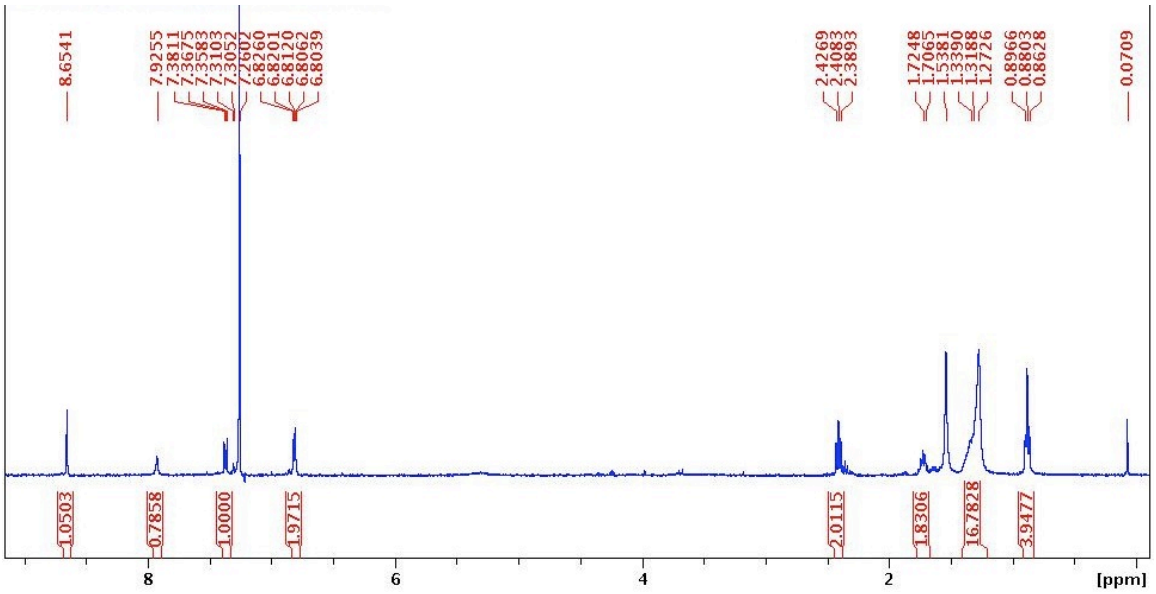

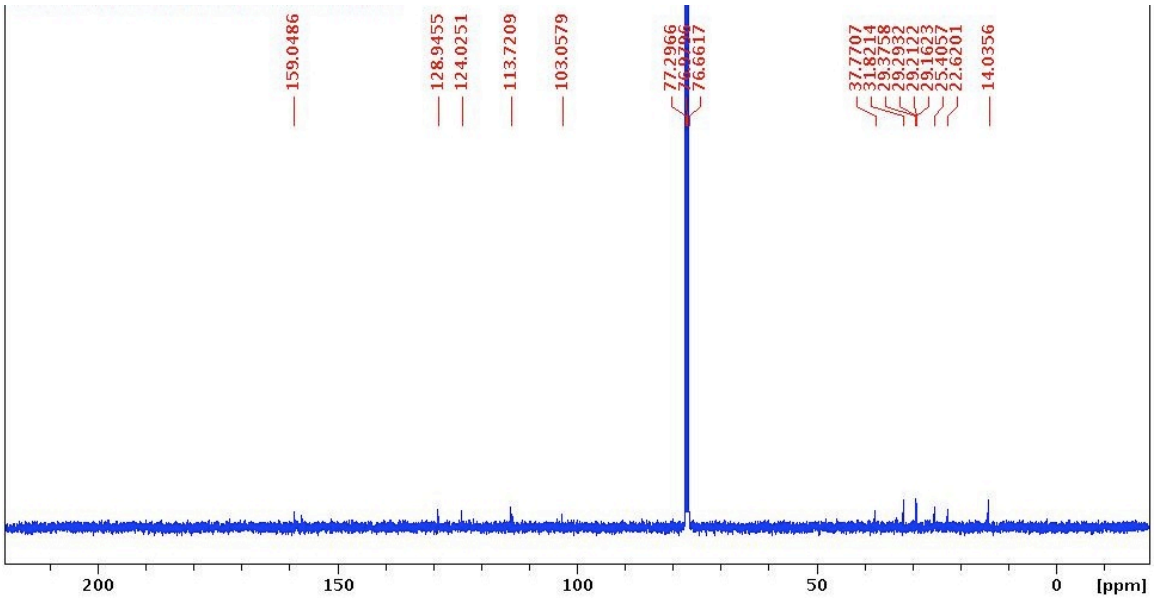

Compound 3-22

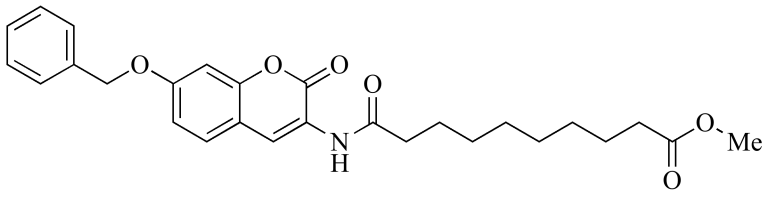

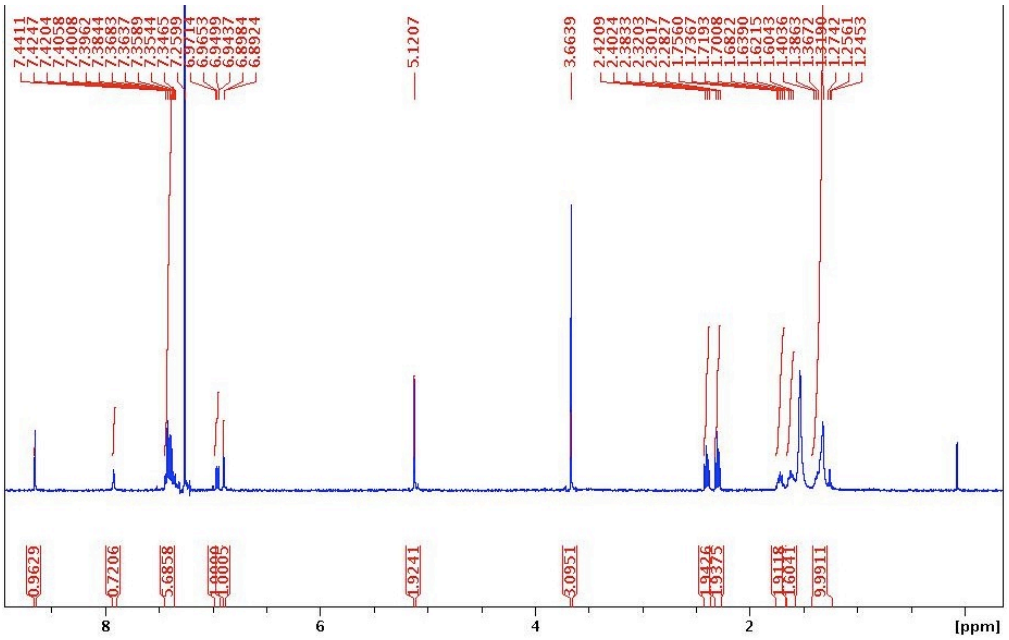

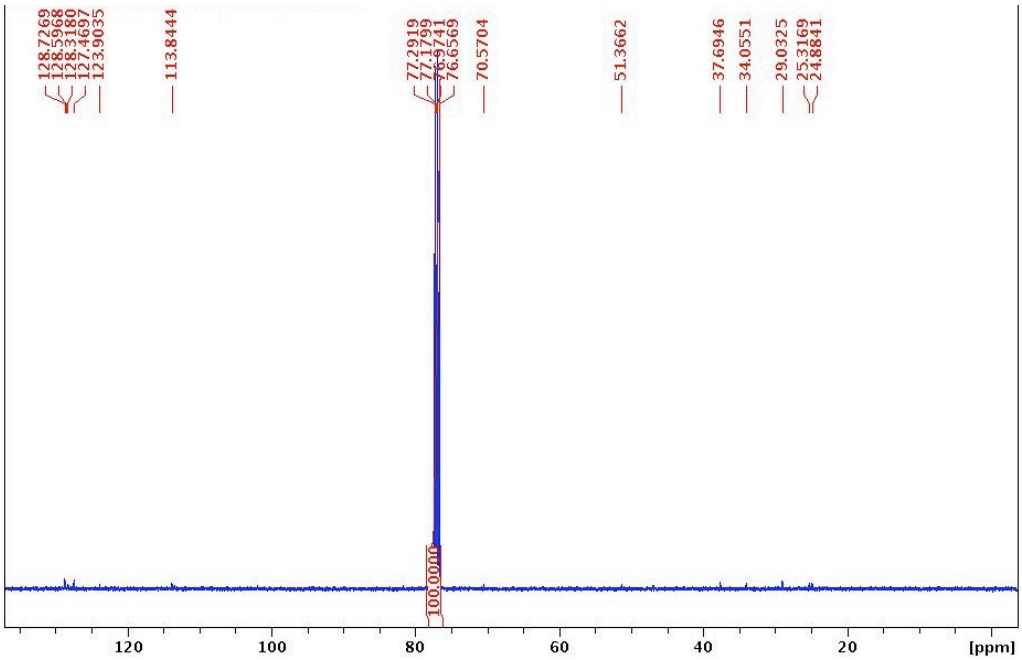

Compound 3-23

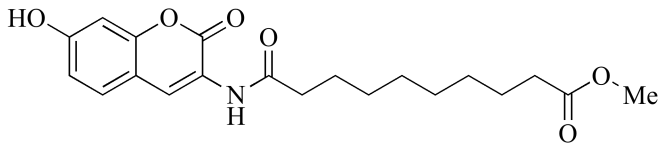

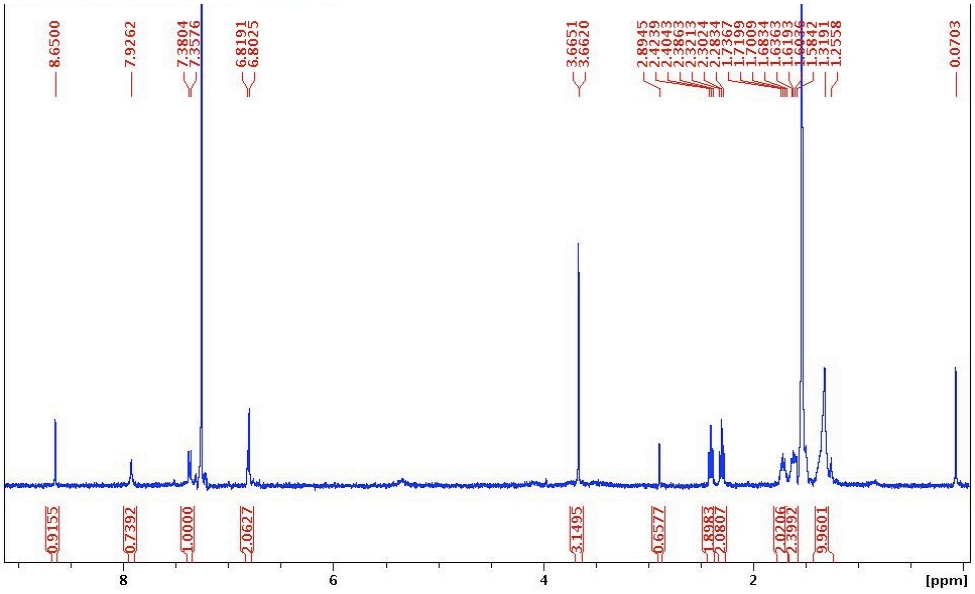

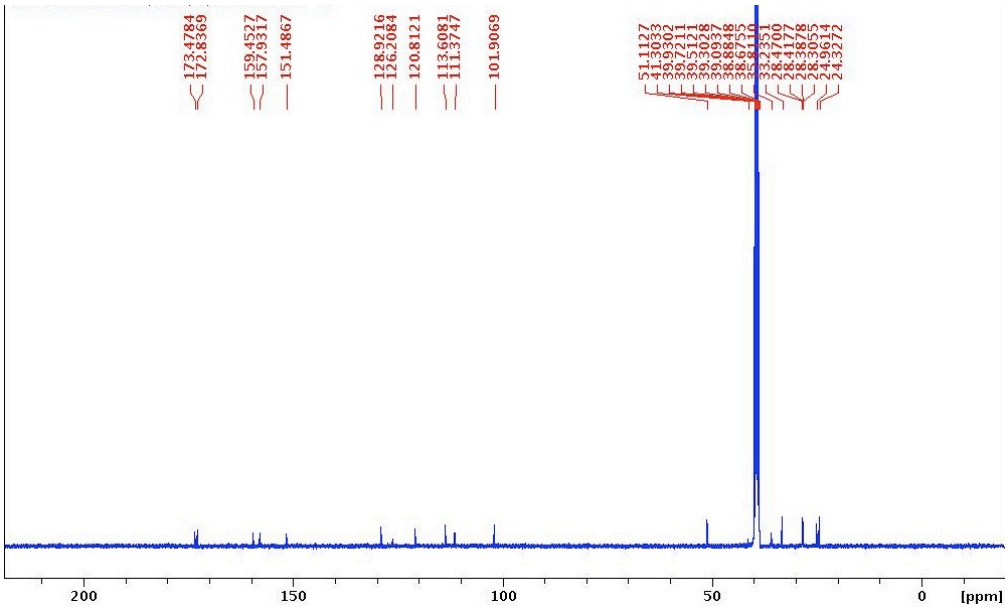

Compound 3-26

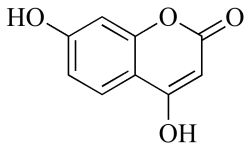

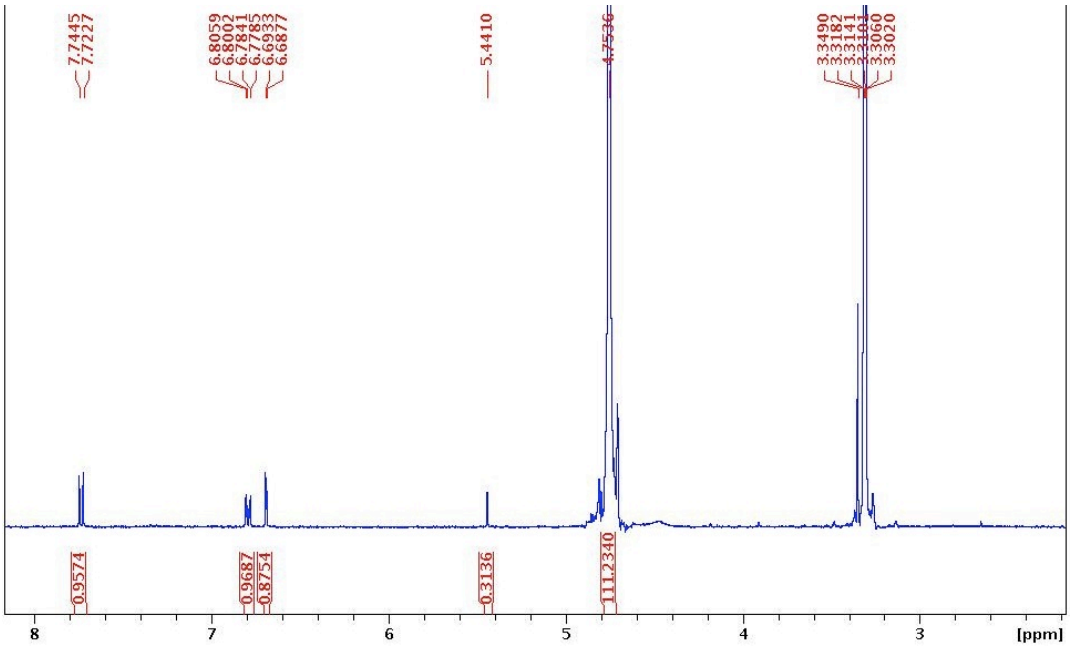

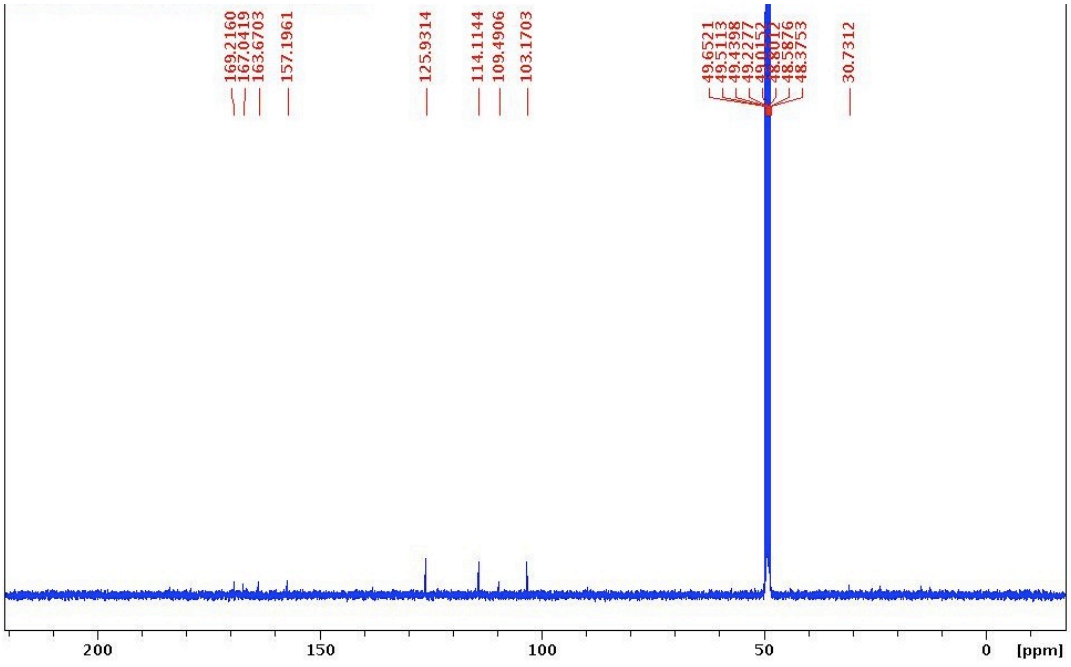

SPR Sensorgrams

3-1

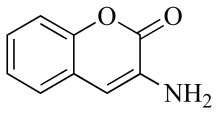

Observation: Sensorgram nearly identical to DNA gyrase control.

Conclusion: Does not inhibit DNA gyrase binding to DNA.

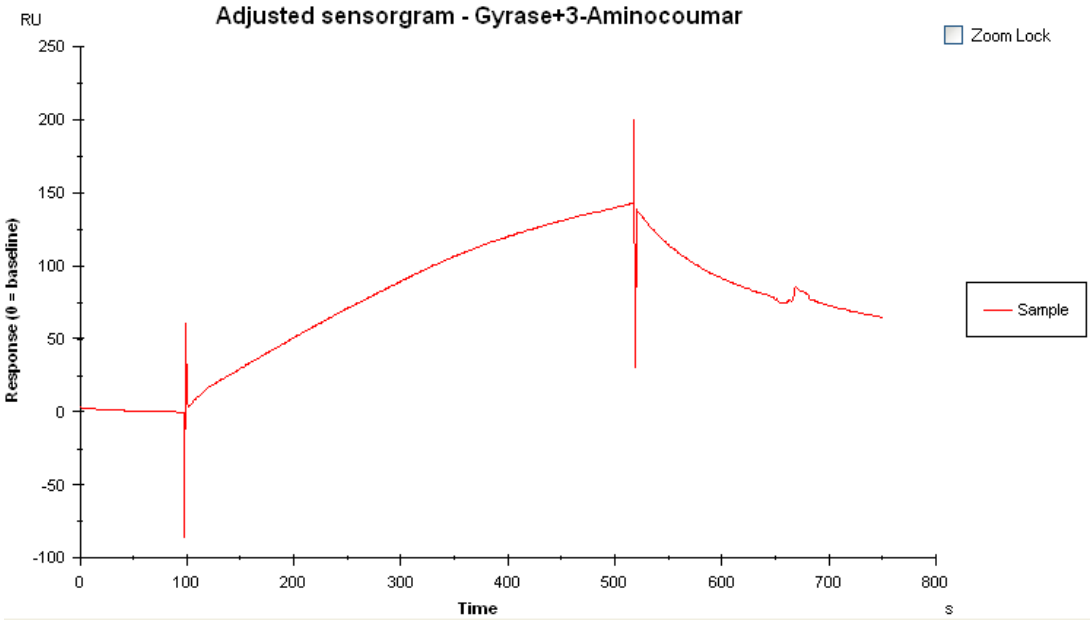

Controls:

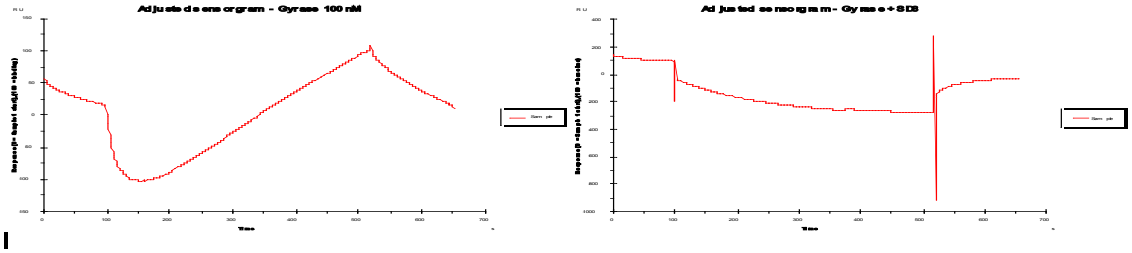

3-2

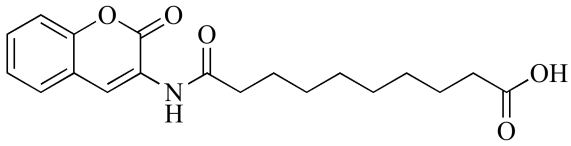

Observation: Sensorgram shows no response after addition of DNA gyrase and compound, and looks closer to that of SD8 and DNA gyrase.

Conclusion: Inhibits DNA gyrase binding to DNA.

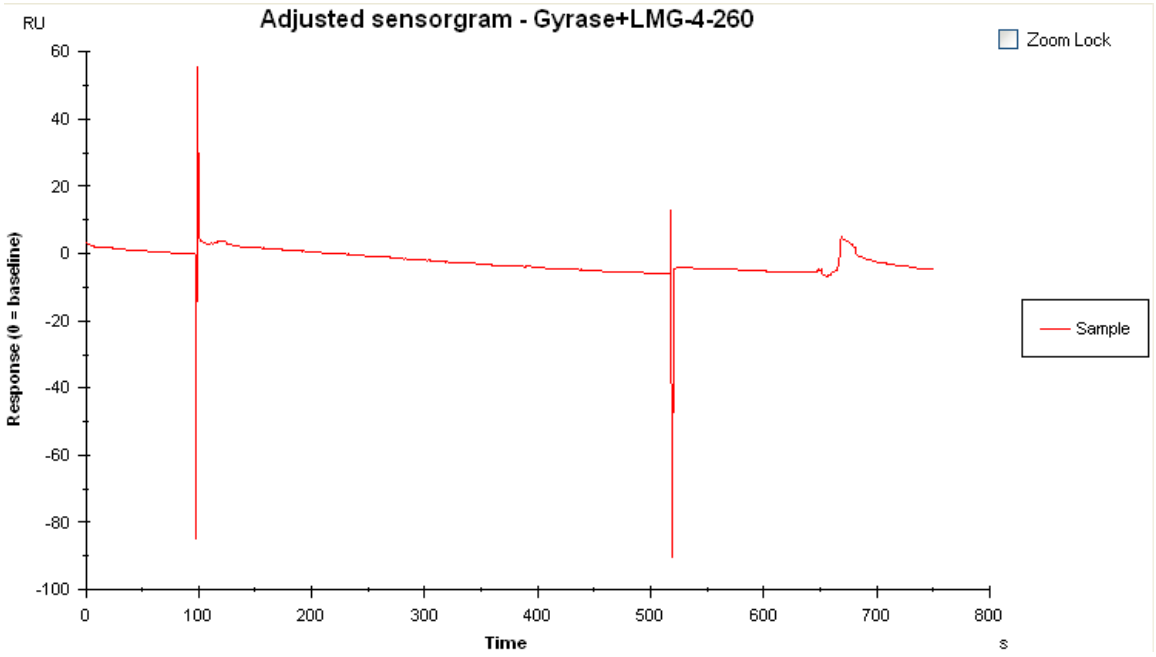

Controls:

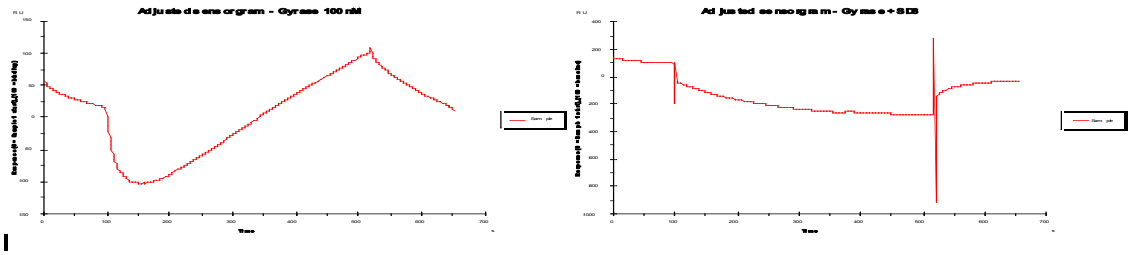

3-3

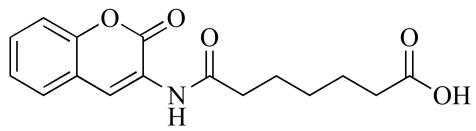

Observation: Sensorgram nearly identical to DNA gyrase control.

Conclusion: Does not inhibit DNA gyrase binding to DNA.

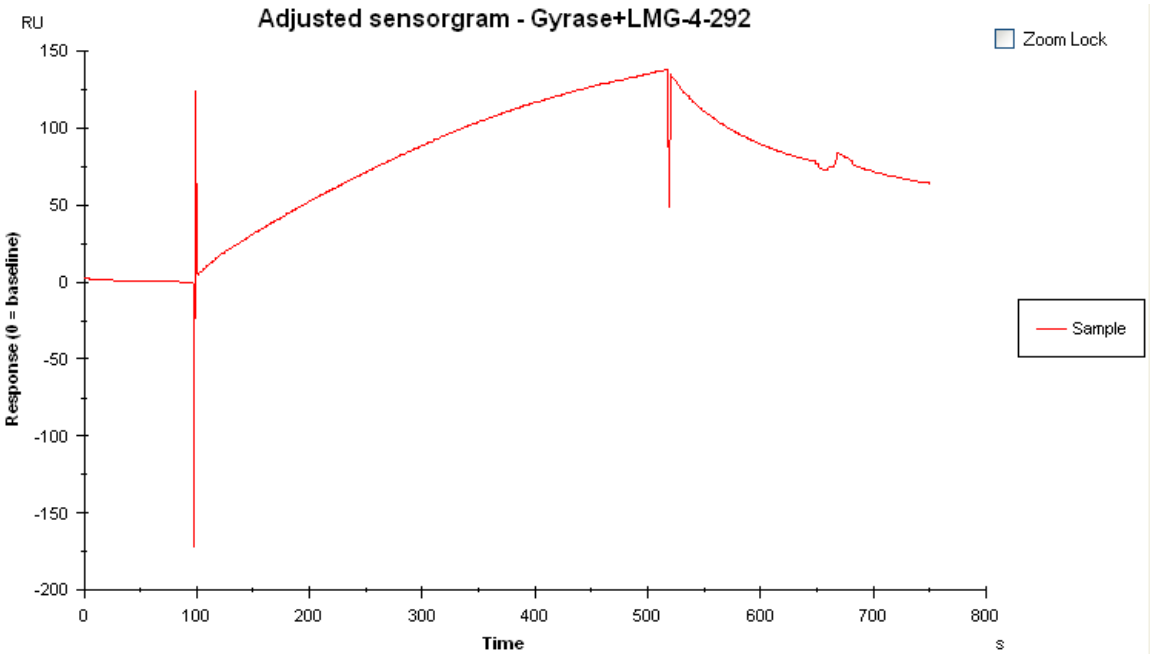

Controls:

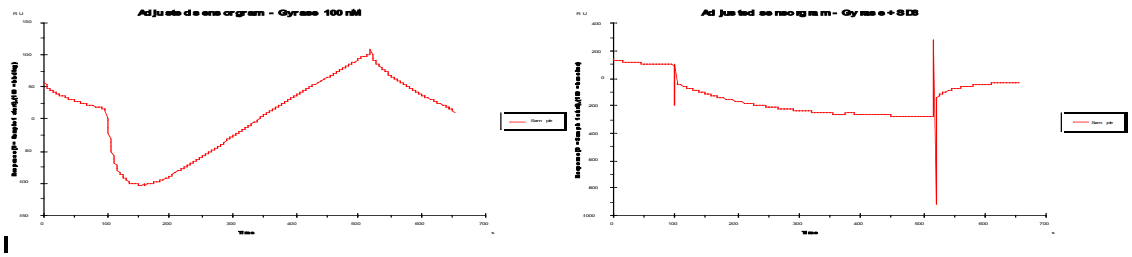

3-4

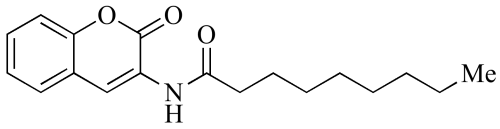

Observation: Sensorgram nearly identical to DNA gyrase control.

Conclusion: Does not inhibit DNA gyrase binding to DNA.

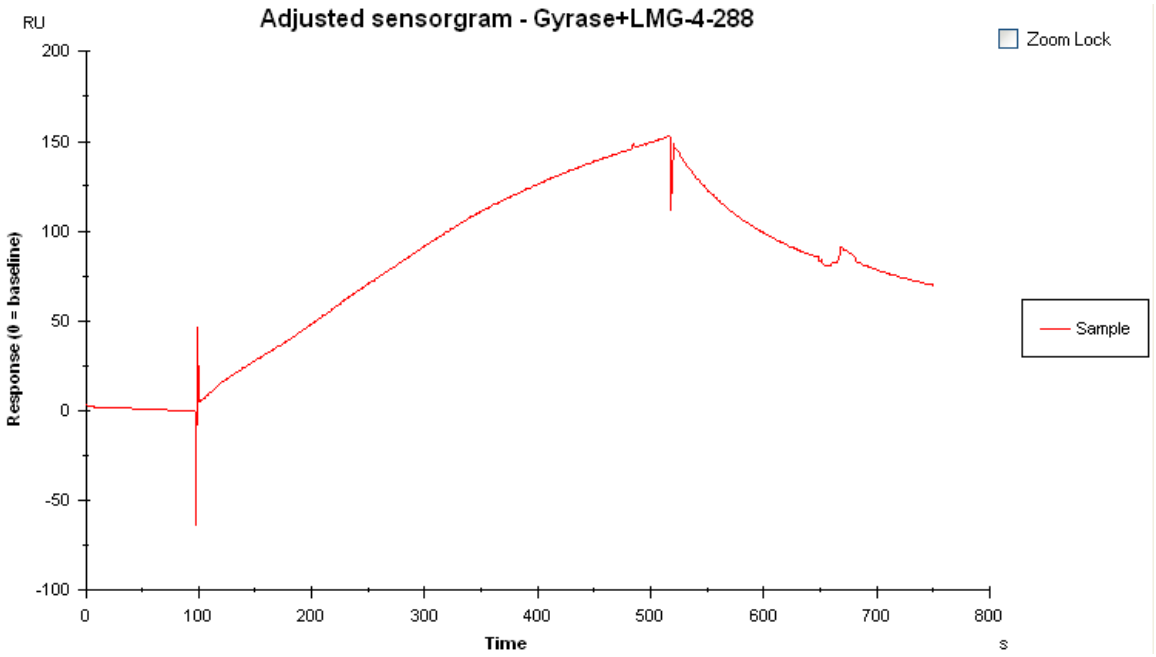

Controls:

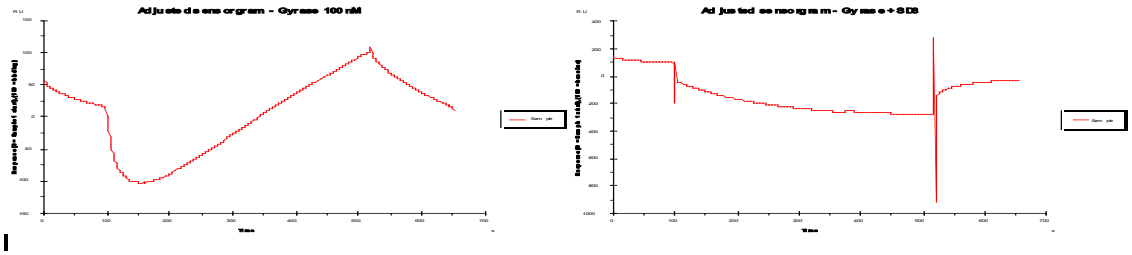

3-5

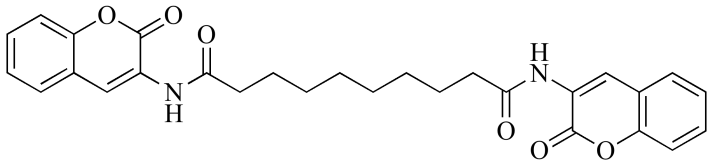

Observation: Response after addition of DNA gyrase and compound is higher than the negative control with only DNA gyrase.

Conclusion: This compound increases the binding interaction between DNA gyrase and DNA.

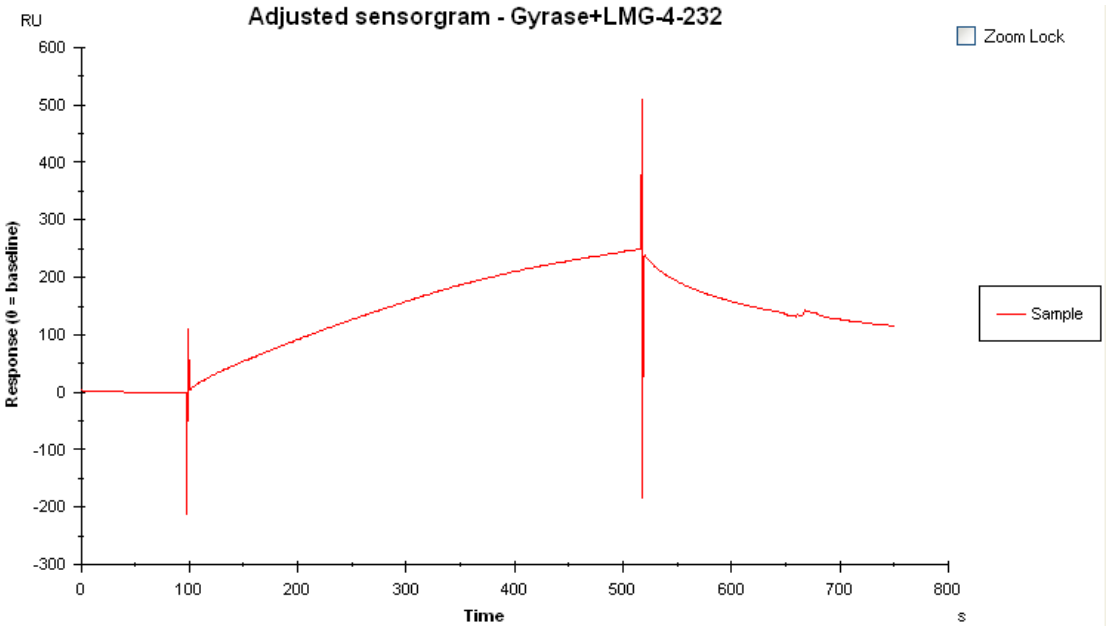

Controls:

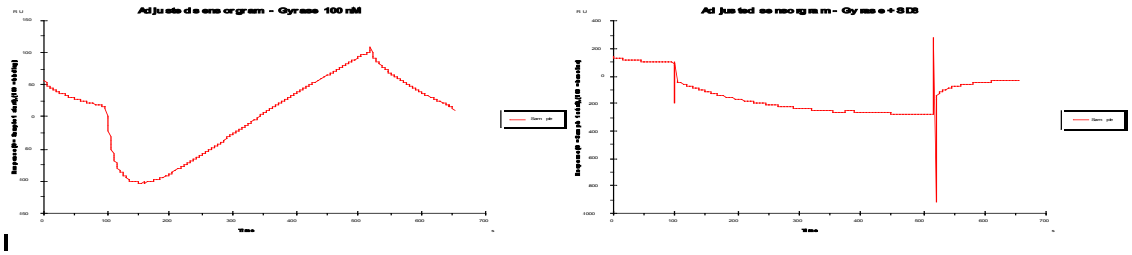

3-6

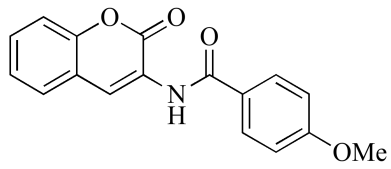

Observation: Sensorgram nearly identical to DNA gyrase control.

Conclusion: Does not inhibit DNA gyrase binding to DNA.

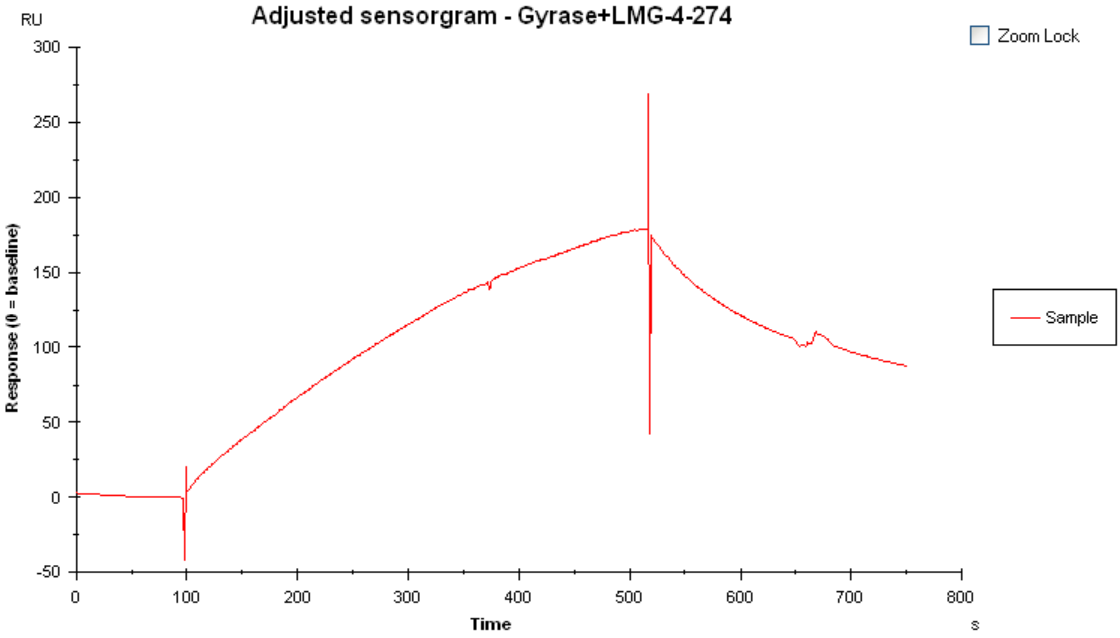

Controls:

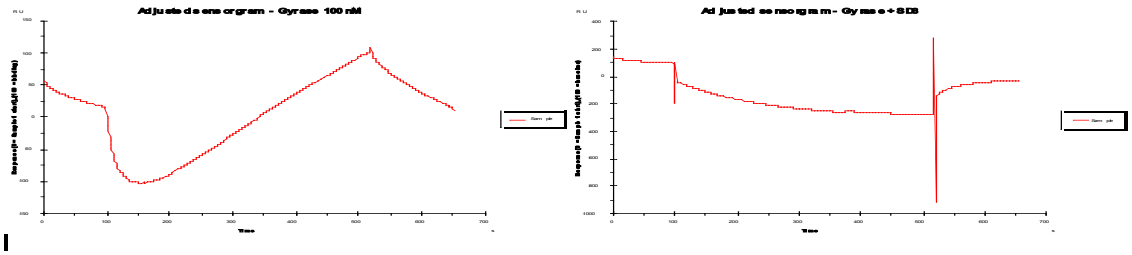

3-7

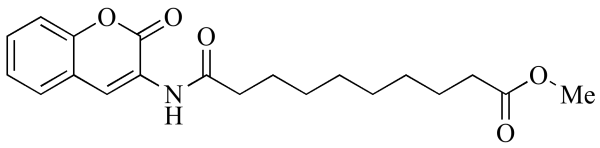

Observation: Sensorgram's response is not fully inhibited.

Conclusion: Partial inhibition of the DNA gyrase-DNA interaction

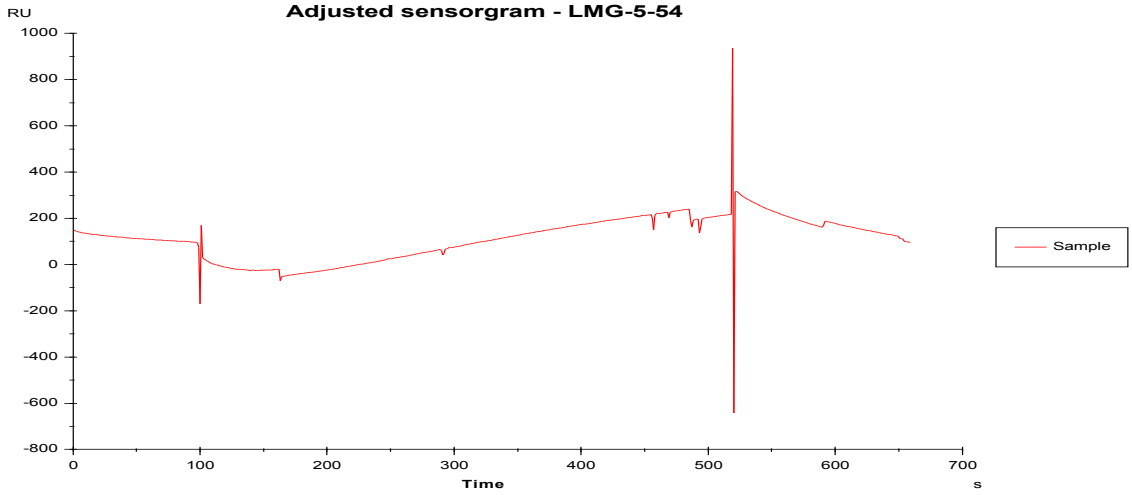

Controls:

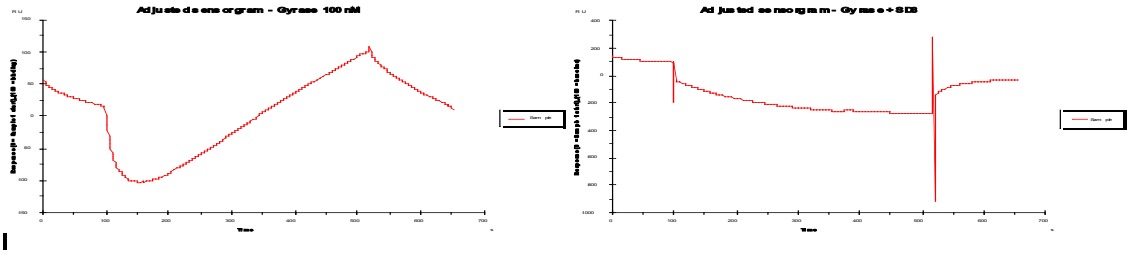

3-8

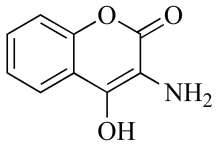

Observation: Sensorgram nearly identical to DNA gyrase control.

Conclusion: Does not inhibit DNA gyrase binding to DNA.

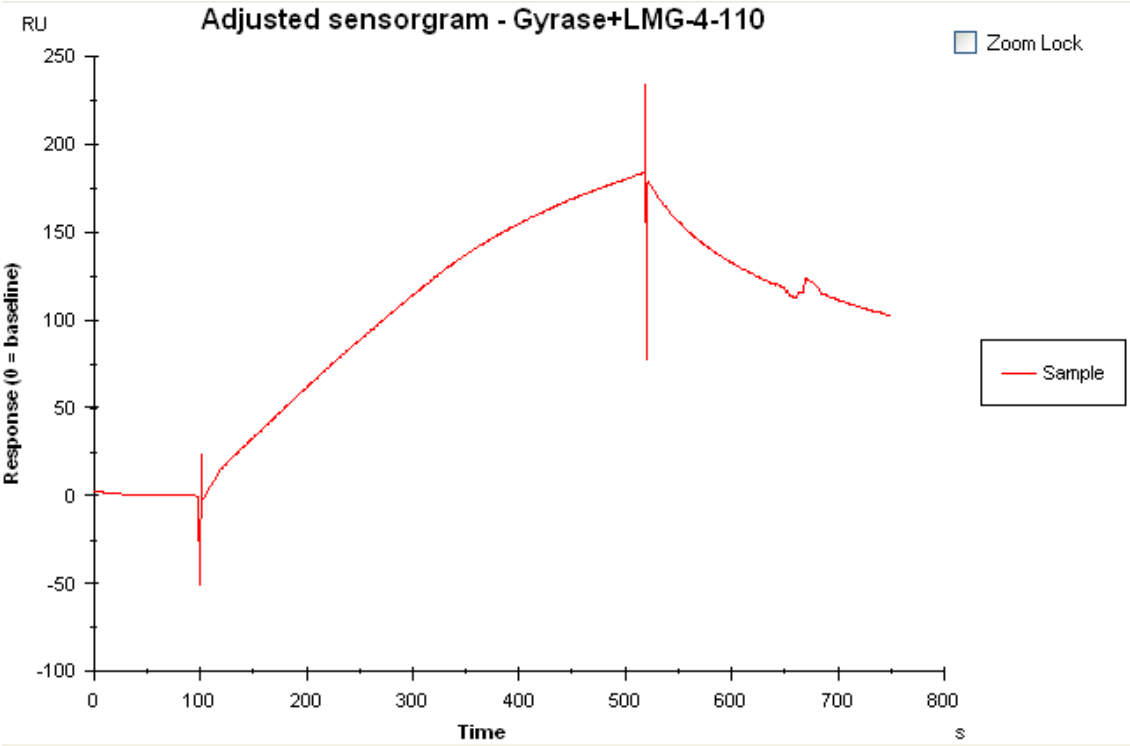

Controls:

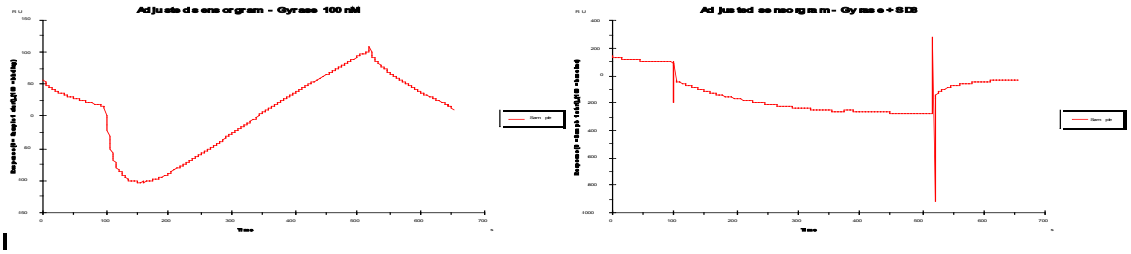

3-9

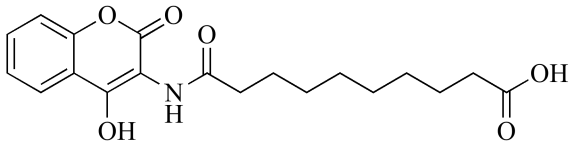

Observation: Sensorgram shows no response after addition of DNA gyrase and compound, and looks closer to that of SD8 and DNA gyrase.

Conclusion: Inhibits DNA gyrase binding to DNA.

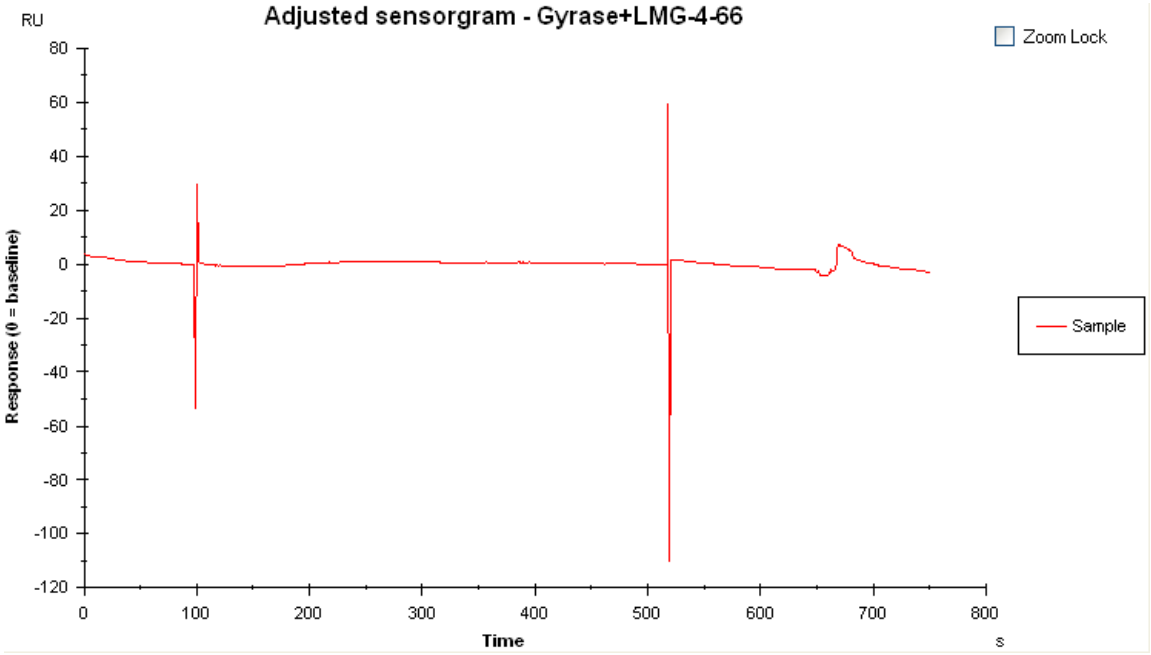

Controls:

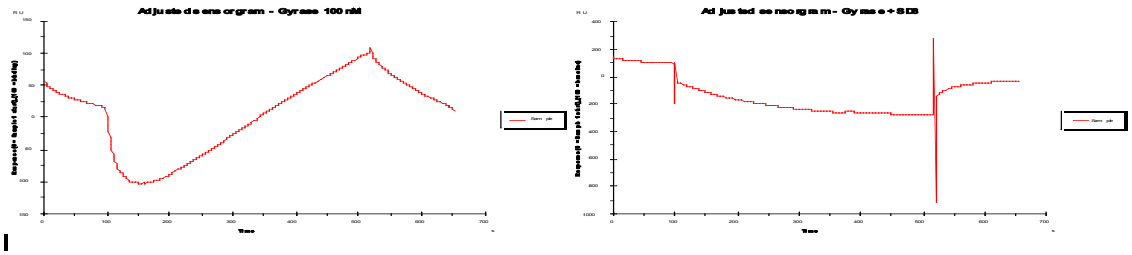

3-11

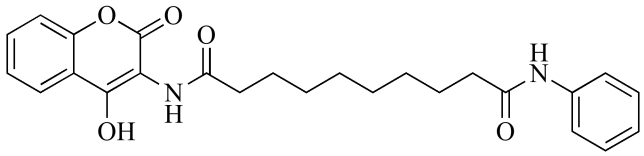

Observation: Sensorgram nearly identical to DNA gyrase control.

Conclusion: Does not inhibit DNA gyrase binding to DNA.

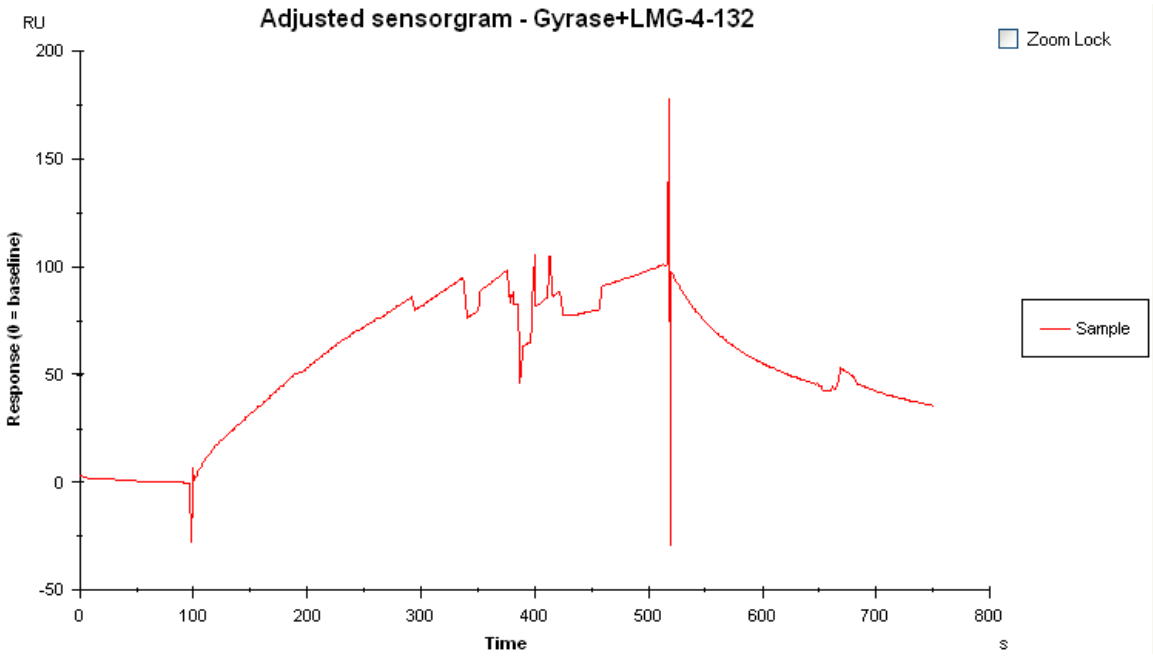

Controls:

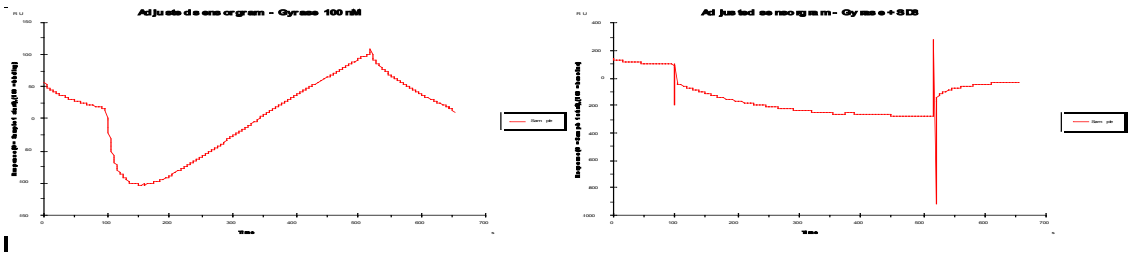

3-12

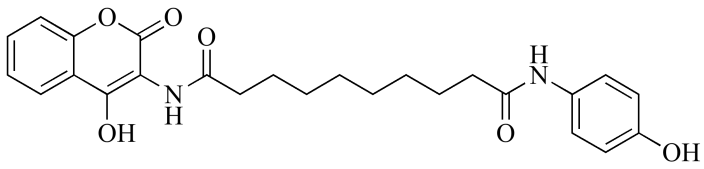

Observation: Sensorgram nearly identical to DNA gyrase control.

Conclusion: Does not inhibit DNA gyrase binding to DNA.

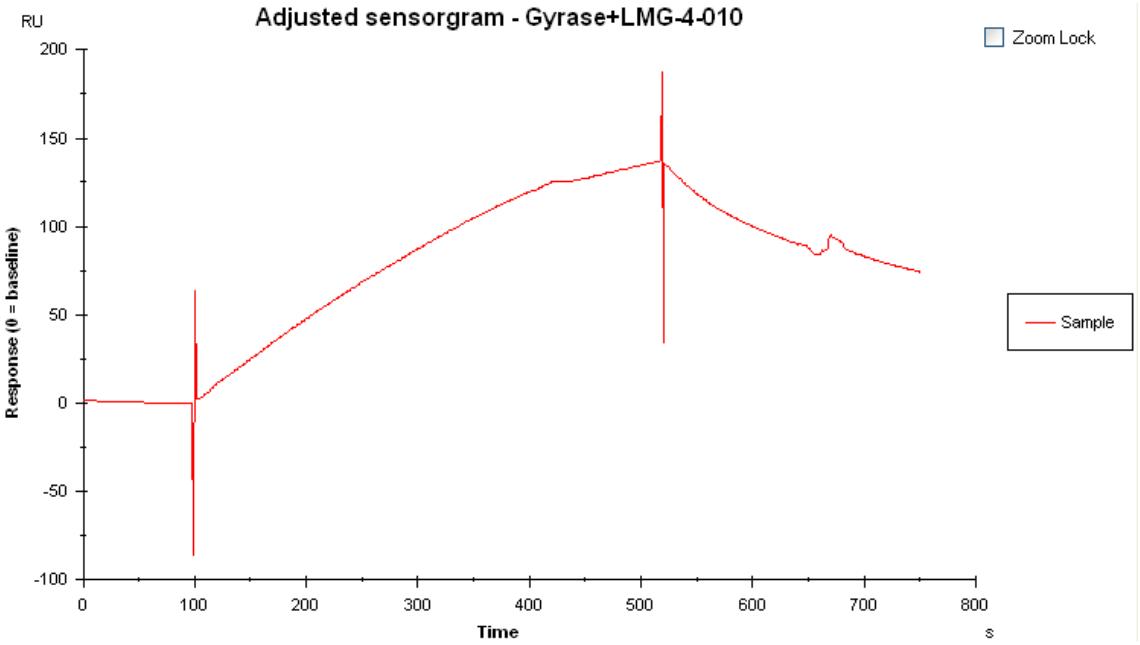

Controls:

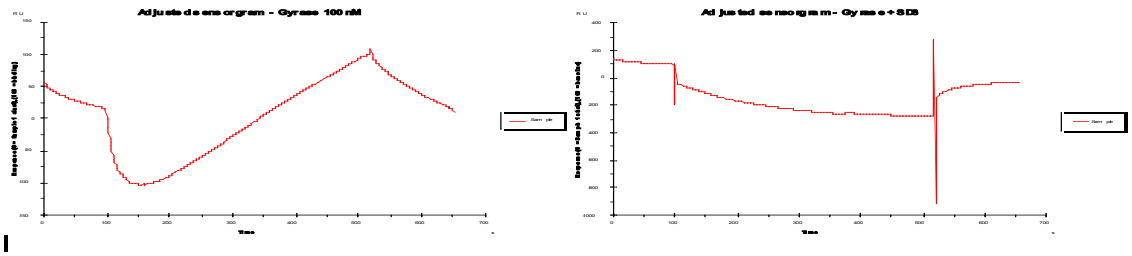

3-13

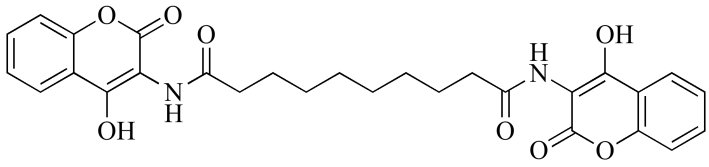

Observation: Response after addition of DNA gyrase and compound is higher than the negative control with only DNA gyrase.

Conclusion: This compound increases the binding interaction between DNA gyrase and DNA.

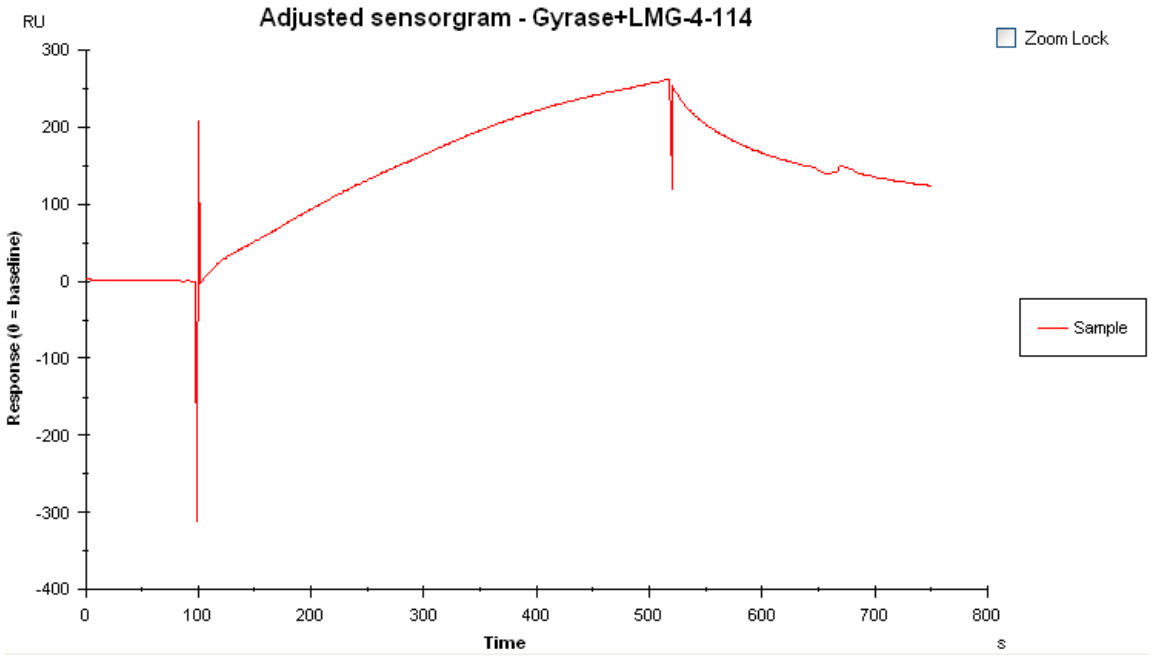

Controls:

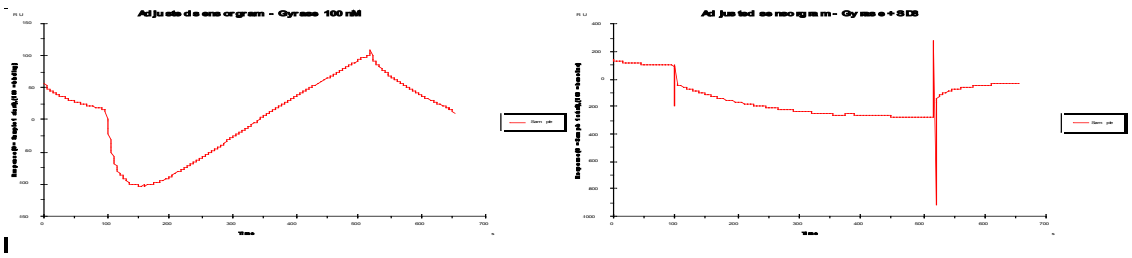

3-19

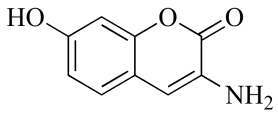

Observation: Sensorgram nearly identical to DNA gyrase control.

Conclusion: Does not inhibit DNA gyrase binding to DNA.

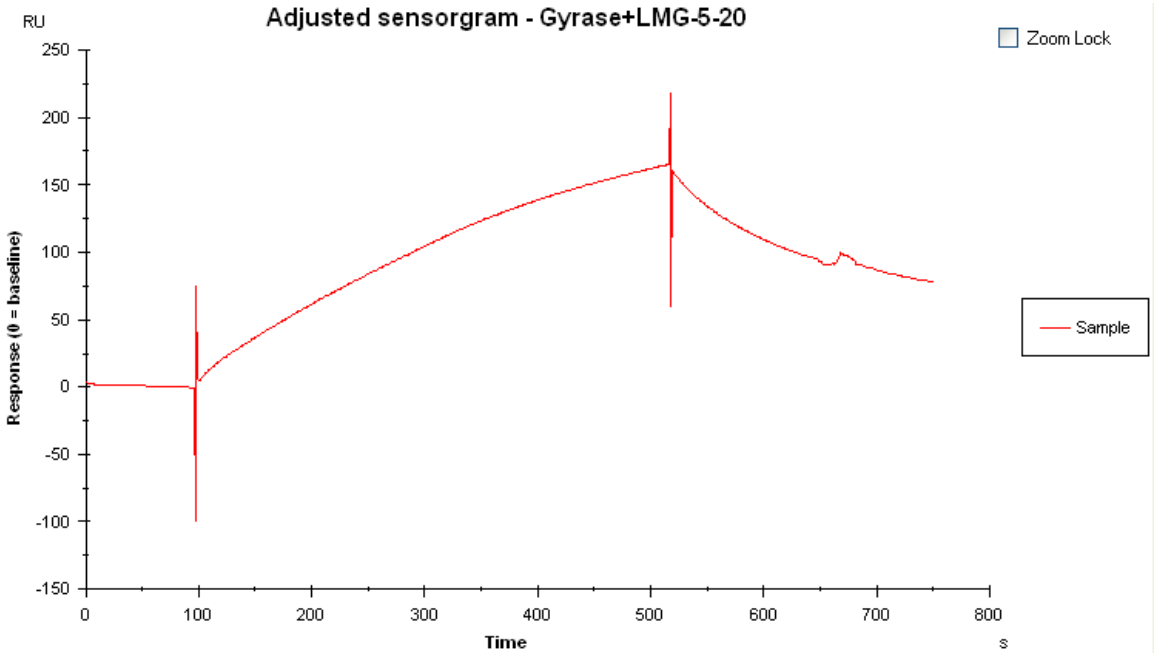

Controls:

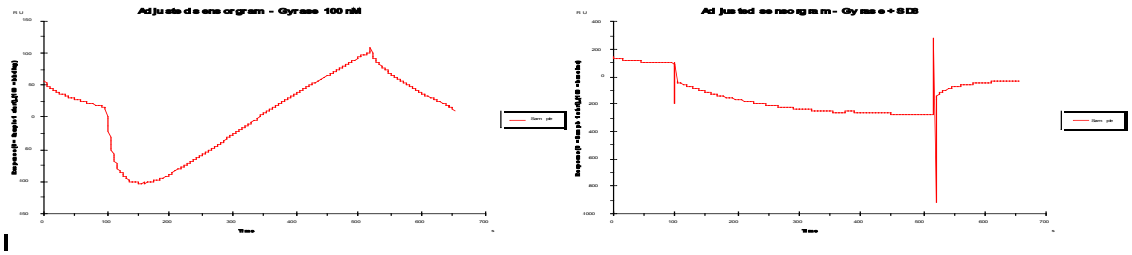

3-21

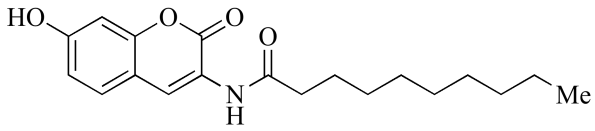

Observation: Sensorgram nearly identical to DNA gyrase control.

Conclusion: Does not inhibit DNA gyrase binding to DNA.

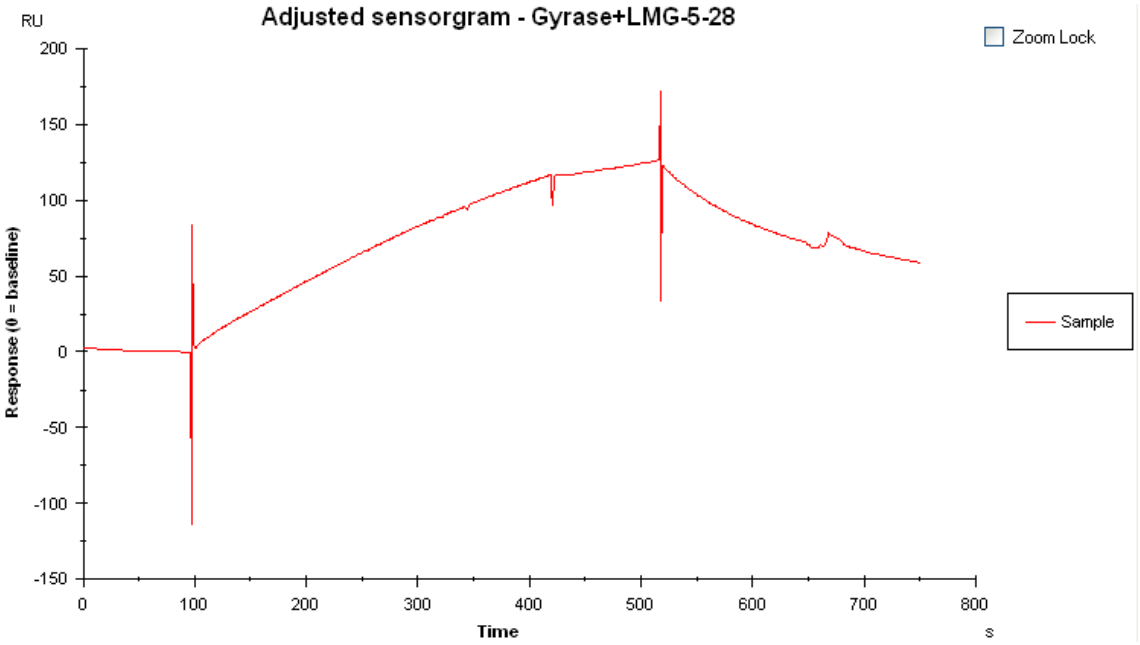

Controls:

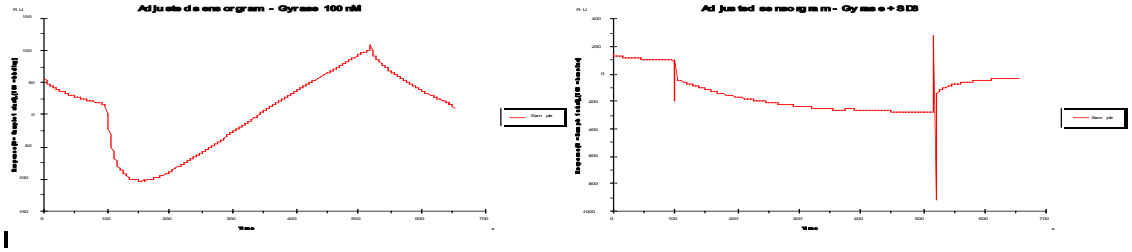

3-23

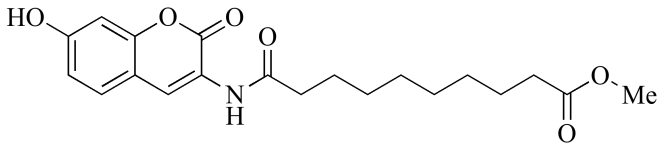

Observation: Sensorgram shows no response after addition of DNA gyrase and compound, and looks closer to that of SD8 and DNA gyrase.

Conclusion: Inhibits DNA gyrase binding to DNA.

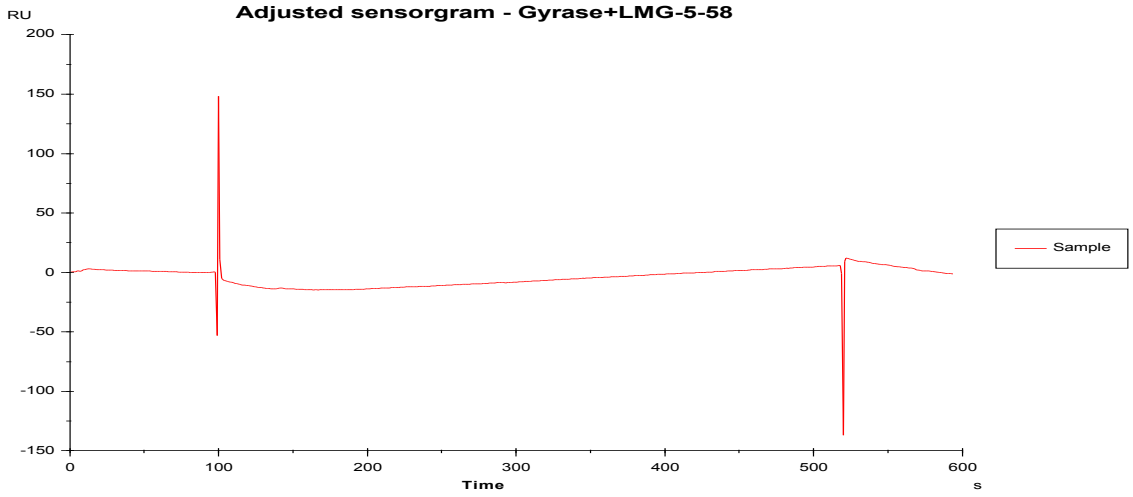

Controls:

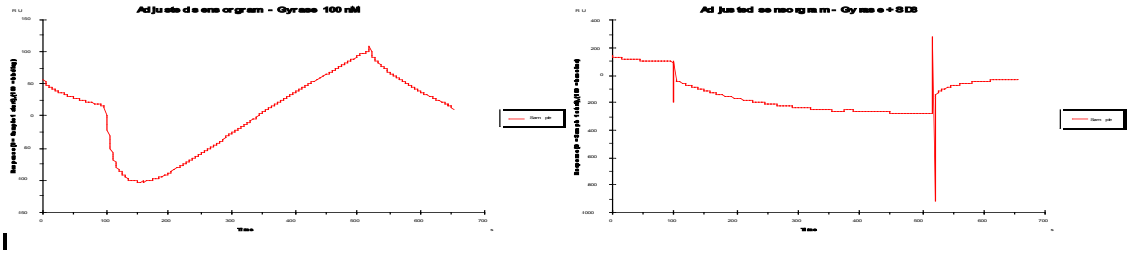

3-26

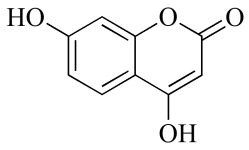

Observation: Sensorgram nearly identical to DNA gyrase control.

Conclusion: Does not inhibit DNA gyrase binding to DNA.

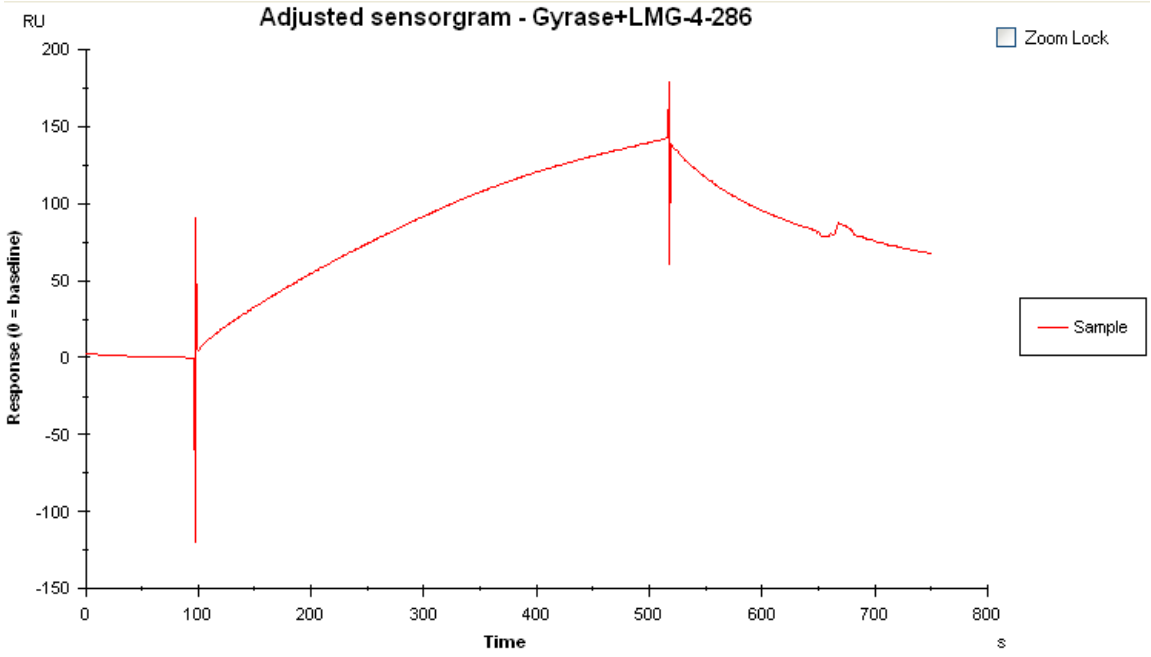

Controls: